A Study on Bucket Brigade for Cellular Production Systems with Worker Collaboration and for Order Picking Systems with Order Batching

（作業者協力を伴うセル生産システムとオーダーバッチングを伴うオーダーピッキングシステムに対するバケツリレーの研究）

Xin Zhou

D215234

Production Systems Engineering Laboratory

Graduate School of Advanced Science and Engineering

Hiroshima University

A dissertation submitted to the Graduate School of Advanced Science and Engineering, Hiroshima University for the degree of Doctor of Philosophy in Engineering

Hiroshima University, Japan

2024

Certification

This is to certify that the doctoral thesis dissertation entitled:

A Study on Bucket Brigade for Cellular Production Systems with Worker Collaboration and for Order Picking Systems with Order Batching

（作業者協力を伴うセル生産システムとオーダーバッチングを伴うオーダーピッキングシステムに対するバケツリレーの研究）

is a series of research works by Xin Zhou during his doctoral study from October 1, 2021 to September 30, 2024 in Production Systems Engineering Laboratory, Graduate School of Advanced Science and Engineering, Hiroshima University, Japan. This doctoral thesis dissertation has been accepted as a part of requirements in conferring in a Doctor of Philosophy in Engineering degree to him.

Approved by Supervisor,

Visiting Prof. Katsuhiko Takahashi

Acknowledgements

First and foremost, I would like to express my deepest gratitude and sincere appreciation to my supervisor, Visiting Prof. Katsuhiko Takahashi, for his invaluable guidance, profound understanding, and unwavering patience. This research would not have been possible without his consistent mentorship during the weekly seminars. During my doctoral study at the Production Systems Engineering Laboratory, Hiroshima University, his deep insights and commitment to academic rigor have greatly contributed to my growth, transforming me from a novice into a person has some understanding on conduct research independently. It has been a great honor to study under his esteemed guidance.

I would like to express my most heartfelt gratitude to Assoc. Prof. Morikawa Katsumi. His invaluable insights significantly aided me in building mathematical models and resolving program bugs. His constructive suggestions during the weekly seminars were tremendously beneficial and greatly contributed to the success of this research.

I would like to extend my sincere thanks to Asst. Prof. Keisuke Nagasawa for his continuous support and invaluable assistance in my research. His advice and suggestions have significantly contributed to the improvement of my research achievements. Additionally, I wish to express my deep gratitude to Assoc. Prof. Daisuke Hirotani. As my supervisor during my graduate studies at the Prefectural University of Hiroshima, he provided numerous valuable suggestions and comments, both academically and in daily life. His guidance has been instrumental in shaping my academic journey and personal development.

I would like to express my gratitude to Hiroshima University for providing me with the scholarship for my doctoral studies. The generous financial support made it possible for me to further my education in Japan, enabling me to pursue and complete this research.

Finally, and most importantly, I would like to thank my parents for their unconditional support and encouragement. I am incredibly fortunate to be surrounded by their quiet patience and unwavering love, which have accompanied me throughout my life and this academic journey.

Abstract

The concept of the bucket brigade can dynamically arrange human labor and workloads and has been widely employed in production and order picking systems. According to this concept, in a production or picking line, once the last worker or picker finishes his/her task, he/she moves to the position of the second-to-last worker or picker to take over the work of the upstream worker or picker and continue the process. Consequently, the second-to-last worker or picker moves to the position of the third-to-last worker or picker to take over his/her work, and so on, until the first worker or picker introduces new work content into the production or picking line. Previous studies have shown that the bucket brigade concept allows for the achievement of the maximum possible production rate compared to various other methods of organizing human labor and workstations.

A cellular bucket brigade production system is proposed to reduce the unproductive walk-back behavior of workers in the traditional bucket brigade production system. In a bucket brigade production system, workers often walk back to retrieve additional work content from upstream workers, which can be time-consuming as they traverse the entire production line. The idea of the cellular bucket brigade production system is to distribute work content on both sides of an aisle. Each worker assembles an item on one side of the aisle while proceeding in one direction and assembles another item on the other side while proceeding in the reverse direction. When workers need to retrieve additional work content, they only need to walk across the aisle instead of along the entire picking line. Compared to the traditional bucket brigade production system, the cellular bucket brigade production system significantly improves production efficiency.

The worker collaboration approach proves valuable in enhancing the efficiency of the cellular bucket brigade production system by reducing pickers' blocking time. A cellular bucket brigade production system is consistent with several workstations, and only one workstation is available for one worker to process item due to the space and tools limitation. When, however, a worker needs to move to the next workstation but finds it occupied by a downstream worker, the worker experiences blocking. The worker-collaboration approach facilitates collaboration among workers by enabling them to share space and tools at certain workstations. This approach effectively minimizes blocking time in the cellular bucket brigade production system, thereby enhancing production efficiency.

The order batching method addresses the challenge of small-sized orders in the bucket brigade order picking system. Small-sized orders significantly impair the system's efficiency, as pickers must make multiple trips to fulfill these orders, resulting in inefficiencies. The order batching method resolves this issue by grouping small-sized orders into batches, allowing multiple orders to be fulfilled in a single trip. This approach improves the efficiency of the order picking system.

The conveyor system reduces the walk time of pickers in the bucket brigade order picking system by assisting them in transporting totes. After picking all items in an order, pickers still need to walk to the unloading station to unload the totes associated with that order. Additionally, after handing over the tote to the second picker, the first picker must traverse a considerable distance back to introduce a new tote, resulting in unproductive walking behavior during the loading and unloading processes, which affects the overall efficiency of the system. Introducing a conveyor system to transport totes from the loading station to the first picker and from the last picker to the unloading station significantly reduces the pickers' walk time, thereby improving the efficiency of the order picking system.

This dissertation proposes two collaboration models for the cellular bucket brigade production system from different perspectives to enhance production efficiency. One problem addressed is the underperformance of existing collaborative models in achieving higher throughput in some cases due to design limitations. Another issue is the complexity of worker operation principles and the occurrence of many unproductive movements. A comparison between the proposed and existing models demonstrates significant improvements in the throughput figures achieved by the proposed models.

In this dissertation, an order batching model is proposed to enhance the productivity of bucket brigade order picking systems when encountering small-sized orders. The previous model batched orders by minimizing batch completion time, but this approach proved challenging due to the complexity of the bucket brigade order picking system, especially when dealing with non-identical pickers. Consequently, the previous model relied on estimated completion time formulas, leading to errors and blocking issues in the order picking system. To address these challenges, this study proposes the Balanced Batching Model for Bucket Brigade (BBMB). Previous research indicates that bucket brigade order picking systems achieve maximum productivity when they are balanced, with balanced work content directly contributing to system balance. Building on these concepts, the BBMB model batches orders by balancing work content in the order picking system. The BBMB model demonstrates increased productivity in bucket brigade order picking systems when handling many small-sized orders. Compared to the previous model, the BBMB model reduces the blocking time percentage from 4.46–12.5% to 0.26–5.66% in various simulation experiment scenarios.

In this dissertation, an enhanced bucket brigade order picking system with a conveyor is proposed to mitigate the unnecessary walking behaviors of pickers in bucket brigade order picking system. The proposed order picking system incorporates a conveyor system to assist pickers by transporting totes with completed orders to the unloading station and introducing new empty totes from the loading station. By doing so, the proposed order picking system reduces the average total walking time cost by 36.64% and increases productivity by 9.65%.

Keywords: Bucket brigade, production system, worker collaboration, order picking system, order batching, conveyor

Table of Contents

List of Figures

List of Tables

Chapter 1 Introduction

1.1 Background

A production system is any method used in industry to create goods and services from various resources (Holstein & Tanenbaum, 2024). An order picking system (OPS) is the process of retrieving goods from specific storage locations to fulfill customer orders (Casella et al., 2023). Humans play an important role in both systems, especially when a significant amount of human labor is required. Typically, workers refers to people who produce products in a production system, while pickers refers to individuals who pick items in an OPS. When the size of a production or order picking system is large, multiple workers or pickers are necessary. At this point, appropriately assigning human labor and workload becomes crucial, as this assignment is directly related to the efficiency of the systems.

One traditional method is static assignment. Static assignment involves allocating tasks to workers based on predefined roles and responsibilities. This method is simple to implement and manage, providing clear expectations for each worker. It can, however, lead to inefficiencies if workloads vary significantly, potentially resulting in some workers' being overburdened while others are underused.

In a production system that employs static assignment, workers are typically assigned to workstations to complete specific tasks, as shown in Figure 1-1. After a worker finishes the tasks at a workstation, the item is handed to the next worker for further processing. If, however, the workloads at different workstations vary significantly, some workers may be busy completing tasks, while others remain idle after finishing tasks.

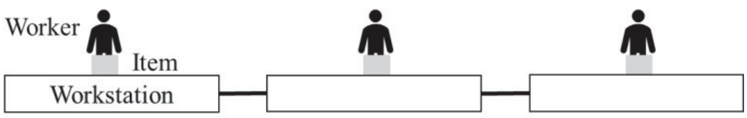

Figure 1-1 An example of static assignment in a production system.

Zone picking is an example of static assignment in the OPS, where pickers are assigned to specific zones and each picks items only in his/her designated area, as shown in Figure 1-2. After a picker collects all the items for an order and places them in a tote in the zone, the tote is transported to the next zone by a conveyor, and the next picker continues picking items for the order. This method reduces travel time, increases picking efficiency, and simplifies training since pickers only need to know their specific zones. It can, however, lead to imbalances if some zones have more items to pick than others. Therefore, exploring more flexible methods to dynamically assign human labor and workload becomes necessary.

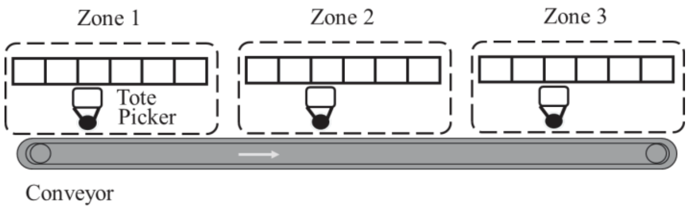

Figure 1-2 An example of static assignment in a zone-picking system.

The bucket brigade method, proposed by Bartholdi and Eisenstein (1996a), aims to dynamically and efficiently arrange human labor and workload in production lines. The idea of the bucket brigade is inspired by the Toyota Sewn Products Management System (TSS). Figure 1-3 shows the movement of workers in a bucket brigade production line. Each worker carries an item from station to station and processes it at each station, as shown in Figure 1-3(a), until the last worker completes the item at the end of the line, as shown in Figure 1-3(b). The last worker then walks back to take the item from the second-to-last worker and continues processing it, as shown in Figure 1-3(c). Consequently, the second-to-last worker walks back to the position of the third-to-last worker to take over the item, and so on, until the first worker walks back to the start of the line to begin processing a new item, as shown in Figure 1-3(d).

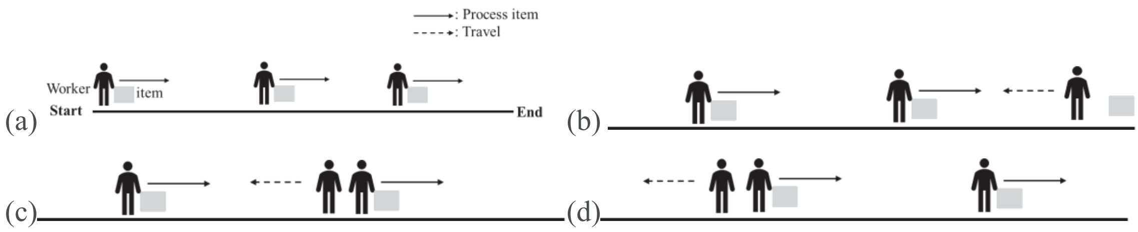

Figure 1-3 Movement of workers in a bucket brigade production line.

The bucket brigade method is widely applied in production systems and OPSs. Several examples demonstrate the improvements companies have achieved by implementing the bucket brigade concept (Bartholdi & Eisenstein, 2006a). Revco Drug Stores (now CVS) increased pick rates by 34% in their national distribution center. At Anderson Merchandisers, pickers increased production rates by 20% and reduced variance in pick rates by 90% during a two-week trial. In the Ford Customer Service Division, the most popular products were moved out of carousels and into flow racks, where they were picked by a bucket brigade, resulting in a pick rate increase of over 50%.

The bucket brigade shows several advantages compared to other ways of organizing production lines. Firstly, it can dynamically arrange human labor and work content without requiring management intervention. On the contrary, it assigns a specific amount of work content to each worker. In a bucket brigade production line, the amount of work content assigned to workers depend on their capability. High-skill workers have the chance to process more work content, as they can carry items to more stations and process them before the items are taken by other workers. Secondly, the bucket brigade shows high efficiency. Bartholdi and Eisenstein (1996a) claim that the maximum possible production rate can be achieved by applying this concept compared to various other methods of organizing workers and workstations. The dynamic allocation of tasks ensures that no worker is idle and the line keeps moving, leading to higher overall productivity.

The bucket brigade method is a self-balancing line. When workers in a bucket brigade production line are ordered from slowest to fastest in processing items, the system will spontaneously converge to a balance status. *Balance status* refers to a condition where downstream workers consistently walk backward to the same position to take over items from upstream workers. According to Bartholdi and Eisenstein (1996a), in this status, the arrangement of labor and work content is optimal, leading to the shortest cycle time for the system.

Figure 1-4 is a time chart showing the self-balancing characteristics of a bucket brigade production system. The horizontal axis represents the position of workers in the production line, and the vertical axis represents time. The length of the production line is normalized to one unit, and three workers work on the line. The different colored lines in the figure represent the movement trajectories of the workers as time increases: blue for worker 1, red for worker 2, and yellow for worker 3. The work velocities (forward velocities) of the three workers are $\mathrm{V1} = 1$, $\mathrm{V2} = 2$, and $\mathrm{V3} = 3$, and the backward walk time is considered instantaneous since it is insignificant compared to work time (Bartholdi & Eisenstein, 1996a). The points where an upstream worker hands the item to the downstream worker are marked. The hand-off points before the balance status are black, and those in the balance status are red. The initial positions of the workers are 0, 0.5, and 0.75, respectively. The workers walk forward, complete their workloads, then walk backward to start new workloads. The workloads are evenly distributed along the production line, and the distance a worker has traveled reflects the amount of work he/she has completed.

From Figure 1-4 we observe that, after a certain period, the workers always walk backward to the same positions to take over items from the upstream workers. This phenomenon is known as the self-balance characteristic of the bucket brigade. The fixed point where worker i hands the item to worker $i+1$ is related to the work velocity of the workers and can be calculated as $\frac{\sum_1^i v_j}{\sum_1^n v_j}$ (Bartholdi & Eisenstein, 1996a), where n is the total number of workers. In this balance status, the production system achieves its maximum production rate, and this balance status can be spontaneously achieved. Therefore, a bucket brigade is useful for organizing labor and workloads.

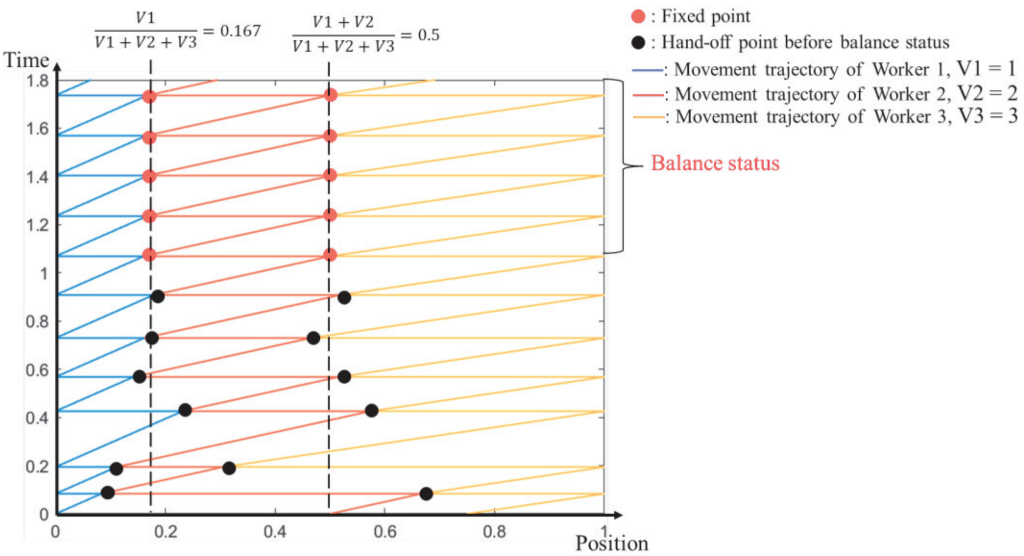

Figure 1-4 Self-balance characteristics of a bucket brigade production line.

Although the bucket brigade is a useful method for organizing production and order picking systems, problems still exist in systems applying this concept due to the gap between the assumed and real conditions. For example, in a bucket brigade production line, the work content is usually assumed to be evenly distributed, workers' velocities are consistent, and the walk-back time cost is ignored. Such conditions are difficult to satisfy in real life, however. The gap between the ideal and real conditions can cause the bucket brigade production system to yield unsatisfactory results. Improving the effectiveness of systems that have adapted the bucket brigade concept is the main topic of this dissertation.

1.2 Literature Review

1.2.1 Bucket Brigade Production System

Bartholdi and Eisenstein (1996a) first introduced the bucket brigade concept and applied it to the production system. They demonstrated that, under certain conditions, such as constant worker velocities, which arrange workers from slowest to fastest, bucket brigades could achieve optimal throughput and balance workload among workers. Furthermore, the allocation of workload is spontaneous because it is self-adjusting without management intervention.

Bartholdi et al. (1999) expanded on their initial work by developing mathematical models to analyze the performance of two- and three-worker bucket brigade production lines and discussed the types of worker asymptotic behavior under the different speeds. For a two-worker bucket brigade production line, there are only two types of worker asymptotic behavior: the line achieves either the one-cycle optimal production rate or the two-cycle suboptimal production rate. The one-cycle asymptotic worker behavior indicates the position of a worker handing off items to a downstream worker, which spontaneously converge to a fixed point. Two-cycle means two different fixed points appear cyclically. For a three-cycle bucket brigade production line, they summarized different worker asymptotic behavior in four regions divided by the ratios of the velocities of each worker to the last worker. In region 1, where workers are sequenced from slowest to fastest, the movements of the workers spontaneously converge to a fixed point, and the line is perfectly balanced, with an optimal production rate. In regions 2 and 3, where workers are sequenced other than slowest-to-fastest, faster workers tend to be blocked by slower ones, and the line achieves a two-cycle and three-cycle suboptimal production rate. In region k, where the first worker is fastest and the second is slowest, the cycle of the line is larger than 3.

Bartholdi et al. (2001) indicated that bucket brigades can be effective even in the presence of variability in the work content. In addition, they reported confirmation at the national distribution center of a major chain retailer, which experienced a 34% increase in productivity after the workers began picking orders by bucket brigade. Bartholdi and Eisenstein (2005) studied how one firm used bucket brigades as an intermediate strategy to migrate from craft assembly to assembly lines. To understand the trade-offs in migrating from craft to assembly lines, Bartholdi et al. (2006b) adapted bucket brigades to a network of subassembly lines. By applying bucket brigades, the system converged to a status in which every worker repeated the same portion of work-content to process the product. Furthermore, the system achieved the maximum possible throughput.

Hirotani et al. (2006) examined less-restrictive conditions that can make bucket brigades achieve the same self-balancing effect. The blocking condition and convergence condition are formulated for the production line with n workers. From the formulation, conditions can be obtained mathematically except in cases where workers are sequenced from slowest to fastest. Bratcu and Dolgui (2009) studied the normative model of bucket brigades without the restrictive assumption of workers' infinite backward velocity. A common finite backward velocity for all workers was assumed. The study showed that the sufficient condition to obtain a self-balancing behavior in the finite backward velocity model is the same as for the normative model in which workers have infinite backward velocities.

De Carlo et al. (2013) applied bucket brigades to an assembly line for luxury handbags. They performed a testing activity in a company producing fashion handbags to compare the self-made design with the bucket brigades and with a simple assembly line balancing-problem algorithm. The results show that the assembly line with bucket brigades significantly increased the production rate because of the advantages of bucket brigades in terms of flexibility, the reduction of work in the process, and the ability to handle small anomalies.

Bukchin et al. (2018) studied the bucket brigade production systems under the assumption of stochastic worker speeds. They claimed that a fastest-to-slowest order with respect to expected speeds may be optimal as long as the standard deviation of the fastest worker is large enough. In addition, in a stochastic environment, the bucket brigade can improve the throughput rate compared to parallel workers even though no blockage or starvation may occur in the latter.

Wang et al. (2022) studied the bucket brigade production system with discrete workstations under the assumption that the time duration for each worker to serve a job at a station is exponentially distributed with a rate that depends on the station's expected work content and the worker's work speed. They proved that, if the work speeds of the workers are independent of the jobs, then the probability distribution of the hand-off station vector will converge to a unique stationary distribution as the number of jobs approaches infinity. Furthermore, the average throughput and of the inter-completion time converge to a constant that depends on stationary distribution.

By reviewing the literature related to the bucket brigade production systems, several conclusions can be drawn. Applying the bucket brigade method to production systems to organize human labor and workloads significantly increases the production rate because it balances workloads among workers. It does, however, have a weakness in terms of blocking. *Blocking* occurs when workers have stochastic speeds or when the sequence of workers is not arranged from slowest to fastest.

1.2.2 Cellular Bucket Brigade Production System

The cellular bucket brigade production system was first proposed by Lim (2011). It is a design aimed at reducing unproductive travel distances. In traditional bucket brigade production systems, a worker walks backward along the production line to retrieve items from the upstream worker. When the upstream worker is far from the worker walking backward, significant time is spent on this unproductive travel. To mitigate the time cost of walking backward, the cellular bucket brigade production system was proposed.

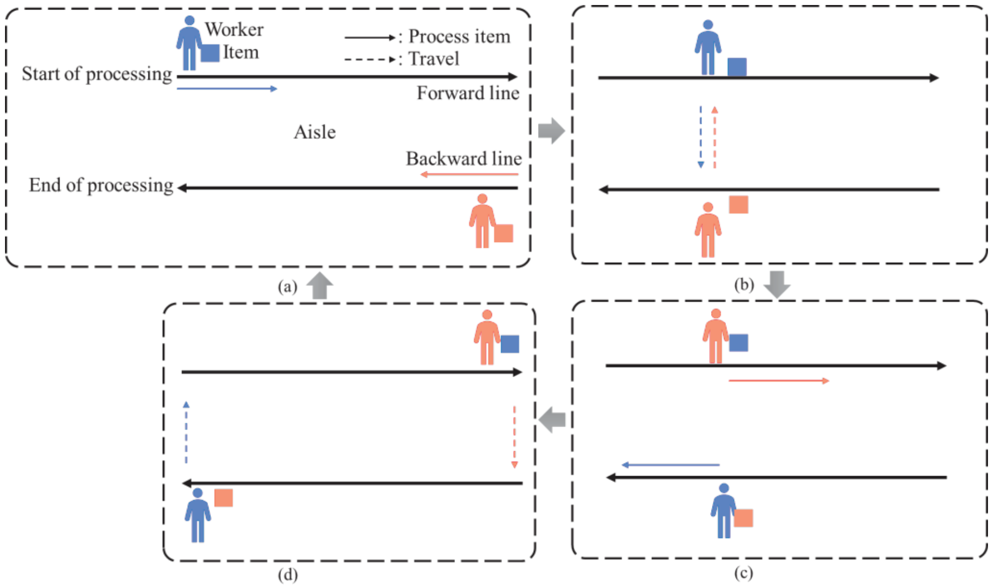

Figure 1-5 Movement of workers in a cellular bucket brigade production system.

Figure 1-5 illustrates the movement of workers in a cellular bucket brigade production system. Unlike the single-line layout of traditional bucket brigade systems, the production line in a cellular bucket brigade system is divided into two parallel lines on both sides of an aisle. The starting point for processing a new item is on the left side of the forward line, and the point where processing is completed is on the left side of the backward line. Workers process items in opposite directions on the two lines, as shown in Figure 1-5(a). When two workers align horizontally, as seen in Figure 1-5(b), they exchange their work by relinquishing their items, crossing to the aisle, then taking over each other's items to continue work, as depicted in Figure 1-5(b) and Figure 1-5(c). When the last worker completes processing on the backward line (left side of the backward line), they cross the aisle to the starting point of the forward line (left side of the forward line) to initiate a new item. When a worker reaches the end of the forward line, they cross the aisle with the item to the backward line to continue processing the item, as shown in Figure 1-5(d).

In a cellular bucket--brigade production system, the distance workers must walk backward depends on the spacing between the two lines. Properly setting the distance between the lines can reduce the time cost associated with walking backward compared to traditional bucket brigade production systems.

Lim and Wu (2014) extended cellular bucket brigades to consider discrete workstations. They proposed an operating protocol to coordinate workers on the U-line. In this protocol, the system can be configured to maximize productivity. The experiment showed that the system always converges to a fixed point or a period-2 orbit and that the operating protocol significantly outperforms static work-allocation policies when there is high variability in worker velocity. Lim (2017) evaluated the performance of cellular bucket brigades with hand-off times. Although cellular bucket brigades reduce unproductive backward-walking time, they require more hand-offs to assemble a product than traditional bucket brigades. These hand-offs may waste significant production capacity, as each requires an exchange of work, which can be complicated and time-consuming in practice. Therefore, they investigated the effect of hand-off times on the performance of cellular bucket brigades. Comparison experiments showed that, even with significant hand-off times, cellular bucket brigades remain substantially more productive than traditional bucket brigades, especially if the team size is small and workers' work velocities are close to their walk velocities.

By reviewing the literature related to cellular bucket brigade production systems, several conclusions can be drawn. Compared to traditional bucket brigade production systems, the unproductive walk-back time is reduced because workers need only walk to another line in the opposite direction to take items rather than walking along the same line. The blocking problem, however, still exists in cellular bucket brigade production systems, particularly when lines are divided into discrete workstations and workloads are arranged inappropriately.

1.2.3 Bucket Brigade Order Picking Systems

Bartholdi and Eisenstein were the first to propose the concept of the bucket brigade and apply it to OPSs (Bartholdi & Eisenstein, 1996b). In a bucket brigade OPS, items are typically stored in linearly arranged flow racks. Pickers keep their designated sequence because this arrangement, where pickers are ordered from the slowest to the fastest, is recognized as the most efficient for achieving maximum productivity (Bartholdi & Eisenstein, 1996b). Pickers walk forward to pick items for their orders along linearly arranged flow racks. When the last picker completes order picking and arrives at the end of the picking line, he/she walks backward to get another order from the upstream picker. Then the upstream picker walks backward to do the same. This process continues until the first picker walks backward to the start of the picking line to introduce a new order. According to these operation principles, each picker has a dynamic zone for picking items for different orders. The study by Bartholdi and Eisenstein (1996b) shows that a bucket brigade OPS can spontaneously achieve a balance status when the distribution of work content is balanced and pickers are arranged from slowest to fastest in the system, resulting in the highest efficiency.

Blocking delays are a major cause of efficiency loss in the bucket brigade OPS. Parikh (2006) designed OPSs for distribution centers by referring to the bucket brigade concept. The author indicated that imbalanced workloads in the bucket brigade OPS led to blocking delays among pickers, where an upstream picker is blocked behind a downstream picker. Hong et al. (2015) proposed closed-form solutions to quantify the level of blocking in the bucket brigade OPSs, considering the time costs of walking forward and backward, as well as hand-off delays. They found that throughput was improved and variability was reduced in the OPSs that applied the bucket brigade concept. The number of items in each order is random, however, which causes workload variation per order. In addition, bucket brigade order picking experiences picker blocking when there is a workload imbalance per pick face. Hong et al. (2015) suggested that aggregating orders into batches smoothed the workload variation by pooling the randomness of picks in each order and that slowest-to-fastest picker sequencing modulates picker blocking between two pickers.

Granotto et al. (2019) investigated the effect of worker fatigue on the throughput of a two-worker bucket brigade OPS to obtain more realistic results. Fatigue reduces the throughput of the OPS due to the slowdown of the pickers. Furthermore, the hand-off position along the picking line over time is affected by the changing of the ratio of the workers' speeds. To enable managers to better predict the behavior of a bucket brigade OPS, Granotto et al. (2019) proposed a function to model the slowdown of the order pickers during the work shift over time.

By reviewing the literature related to bucket brigade OPSs, several conclusions can be drawn. The efficiency of OPSs is significantly improved by applying the bucket brigade method. The problem of blocking, however, decreases the system's efficiency. In an OPS, the number of items in orders is uncontrollable, and pickers' speeds vary due to fatigue. These factors cause imbalanced workloads among pickers, which eventually leads to blocking. Reducing the effect of blocking in bucket brigade OPSs remains a challenge.

1.2.4 Order Batching in Order Picking Systems

Order batching is a method of allocating a group of orders into several batches. By applying order batching, the workload among pickers can be rearranged and the number of trips needed to fulfill orders is reduced. Hong et al. (2012) developed an order batching formulation and heuristic-solution procedure to solve large-scale order batching problems in parallel narrow-aisle OPSs. In a narrow-aisle OPS, items are placed on parallel shelves. One order is assigned to one picker, and the picker must travel through the entire OPS to pick items for the order. Hong et al. (2012) pointed out that order batching can decrease the pickers' total travel distance not only by reducing the number of trips but also by shortening the length of each trip.

Pan et al. (2015) proposed an order batching approach based on a group genetic algorithm to balance the workload of each picking zone and minimize the number of batches in a pick-and-pass OPS in an effort to improve system performance. In a pick-and-pass OPS, items are stored in pick zones connected by a conveyor. Each picker is responsible for picking items in a fixed zone. After a picker collects all the items for an order and places them in a tote in the zone, the tote is transported to the next zone by a conveyor, and the next picker continues picking items for the order. Pickers may be idle if no orders are transported by the conveyor from the upstream pick zone. The authors claim that minimizing idle time can be achieved by balancing workloads in each pick zone and that the minimum total operation time can be reached by forming the smallest number of batches at the same time.

Matusiak et al. (2014) introduced a joint order batching and picker-routing method to solve precedence-constrained routing and order batching problems in a picker-to-parts OPS. In a picker-to-parts OPS, items are placed on parallel shelves, and one order is assigned to one picker. The picker travels through the entire OPS to pick items for orders. Their study showed a similar conclusion that batching customer orders in a warehouse can result in considerable savings in order-pickers' travel distances. Scholz and Wäscher (2017) developed an iterated local search approach for batching orders to demonstrate the benefits of solving the order batching and picker-routing problem in a more integrated way. Muter and Öncan (2022) investigated the integration of the order batching and picker-scheduling problem to minimize both the total travel time to collect all items and the makespan of the pickers in picker-to-parts OPS.

Hong et al. (2016) applied order batching to minimize batch-completion time in the bucket brigade OPS. Their model calculated batch-completion time based on pick time, walk time, and blocking-delay time. They assumed uniform picking and walking velocities for all pickers, essentially treating pick time and walk time as constants. This assumption simplifies completion-time minimization, which becomes equivalent to minimizing blocking-delay time.

Fibrianto and Hong (2019) extended the model to scenarios with non-identical pickers, proposing the DIBMB model. Still, considering non-identical pickers makes quantifying the pick time of the pickers more challenging. Although they introduced methods to estimate pick-time costs, estimation errors prevent the OPS from achieving the theoretical minimum blocking delay and completion time.

By reviewing the literature related to order batching in OPSs, several conclusions can be drawn. Applying order batching to OPSs can decrease the pickers' total travel distance by reducing the number of trips and shortening the length of each trip. Additionally, order batching helps balance workloads among pickers. Blocking occurs in bucket brigade OPSs due to imbalanced work content. Therefore, implementing order batching can be useful in reducing the effect of blocking on the efficiency of bucket brigade OPSs.

1.3 Issues with Applying the Bucket Brigade

Considerable research found in the literature review has focused on applying the bucket brigade to production and OPSs to improve efficiency. Issues arise, however, when implementing the bucket brigade concept in these systems, primarily involving blocking, halting, and unproductive travel. This section explains the causes of these issues and their effect on system efficiency.

The blocking problem is usually caused by uneven distribution of work content in a bucket brigade production system. In such a system, the production line consists of several workstations where workers use tools to process items. A worker needs more time to complete complex tasks at a station and less time for simpler tasks. When a worker finishes a simple task quickly, the next station with more complex tasks may still be occupied by another worker. At this point, blocking occurs because the next station has tools and space for only one worker. Therefore, the worker is blocked at the current station until the next worker leaves the next station.

The halting problem usually occurs in cellular bucket brigade production systems when work content is not evenly distributed between the two lines. A cellular bucket brigade production system consists of two parallel lines, each with several workstations. Two workers on different lines exchange work content when their horizontal positions coincide. *Halting* occurs when a worker finishes a task at a station while another worker is still processing an item at the opposite station. At this point, halting occurs because the other worker has not finished his/her work and cannot move to the end of the station to coincide with the first worker's horizontal position.

The halting problem shares some similarities but also has some differences with the blocking problem. Both halting and blocking problems occur when worker finishes work at a station and wishes to move to another station. The difference is that blocking occurs when a worker cannot move to the next station in the same line, while halting occurs when a worker cannot move to a station on the opposite line.

The unproductive travel problem is usually discussed in bucket brigade OPSs. In these systems, items are stored in a linear arrangement of pick faces. Pickers travel along these pick faces to retrieve items according to orders. The travel behavior of pickers among the items is considered unproductive compared to the act of picking items. Efficiency is significantly affected if the travel distance is long.

It is worth noting that, although blocking, halting, and unproductive-travel problems are mentioned in different systems, it does not mean that these problems exist only in specific systems. These problems may occur in any system that applies the bucket brigade concept. For example, in a bucket brigade production line, the unproductive-travel problem occurs when workers walk backward long distances to take items from upstream workers.

Blocking, halting, and unproductive-travel problems are the main reasons that systems that adopt the bucket brigade concept lose efficiency. Therefore, the primary research objective of the dissertation is to reduce the influence of these problems. The details of the research objectives are introduced in the following section.

1.4 Research Objectives

This dissertation studied the application of the bucket brigade concept in production systems and OPSs. A review of the previous literature reveals that the bucket brigade is the most common concept in these two systems. When these systems adopt bucket brigade, blocking, halting, and unproductive travel are the main factors affecting system efficiency. Therefore, the primary objective of this study is to reduce the effect of these three issues on efficiency.

For production systems, the cellular bucket brigade production system is the subject of research. Compared to the traditional bucket brigade production system, it reduces the effect of unproductive travel. Blocking and halting issues, however, still exist within the system. To address these two problems, worker collaboration is introduced. Therefore, the first specific research objective is:

1. Analyze the effect of worker collaboration on the cellular bucket brigade production system.

For this research objective, this dissertation will compare the performance of the cellular bucket brigade production system with worker collaboration and the traditional cellular bucket brigade in terms of production time, blocking rate, and throughput. It will also identify factors contributing to further optimizing the system’s efficiency.

Upon completing the first research objective, factors that help improve system efficiency will be identified. Based on these factors, the second specific research objective is:

2. Develop optimization models for the cellular bucket brigade production system.

For the second specific research objective, this study will propose models to optimize worker sequence, worker allocation, and the allocation of work content in a cellular bucket brigade production system.

For OPSs, this dissertation discusses the bucket brigade OPS. In the bucket brigade OPS, blocking and unproductive travel are issues. Order batching can effectively solve the blocking problem, as it can balance the distribution of workloads within the system. The third specific research objective is:

3. Study the effect of order batching on the bucket brigade OPS.

For the third research objective, this study will examine the effect of order batching on system efficiency and propose an efficient order batching model.

To address the unproductive travel issue, introducing a conveyor system is a useful method, as it can assist pickers in transporting items. The fourth specific research objective is:

4. Introduce a conveyor system to assist pickers in a bucket brigade order picking system.

For the fourth research objective, this study will propose an enhanced bucket brigade OPS with a conveyor to reduce the walking distance of pickers.

According to these research objectives, this dissertation studied the cellular bucket brigade production system in Chapter 2 and the bucket brigade OPS in Chapters 3 and 4. The study identified several issues that affect the performance of these systems. To mitigate the effect of these issues, Chapters 2, 3, and 4 propose several models, as described in the next section.

1.5 Dissertation Outline

This dissertation comprises five chapters, with the research topics distributed among them as follows:

- Chapter 1 introduces the background of the dissertation, literature review, issues of applying the bucket brigade, and research objectives.
- Chapter 2 proposes two models aimed at improving the efficiency of the cellular bucket brigade production system with worker collaboration.

- Chapter 3 develops an algorithm to simulate the operation of the bucket brigade order picking system, along with an order batching model designed to reduce blocking time in the system.
- Chapter 4 proposes an enhanced bucket brigade order picking system with a conveyor to reduce the walking distance of pickers during the order-loading and -unloading processes.
- Chapter 5 summarizes the results of this dissertation and discusses future research directions related to it.

Chapter 2 Bucket Brigade for Cellular Production System with Worker Collaboration

2.1 Introduction

Production lines are required to fulfill the need for improved throughput. Bucket brigades have been spotlighted due to their self-balancing and self-organizing capabilities, which achieve a production rate that, for typical production lines, is the maximum possible among all the different ways of organizing workers and workstations (Bartholdi & Eisenstein, 1996a). If the sequence of workers in bucket brigades is ordered from slowest to fastest (Bartholdi et al., 1999) or satisfies specific conditions (Hirotani et al., 2006), the production line will converge to a fixed point. This means that a downstream worker always goes back and takes over an item from an upstream worker at the same position. Furthermore, this production line will provide the maximum throughput. Despite these considerable advantages, achieving and maintaining the ideal maximum throughput is still a remote possibility due to limitations of the conditions. The assumptions of bucket brigades restrict the production line to a consecutive line in which the workers maintain the same speed. Additionally, the time cost of workers' unproductive behaviors (e.g., going back and taking over) is considered zero. The more typical situation, however, is that the production line is divided into several workstations (Lim & Yang, 2009), workers operate at different speeds at the different positions on the production line (Armbruster & Gel, 2006), and the time cost of unproductive behavior is not zero (Hong, 2018; Hong & Kim, 2018; Lim, 2017). To date, considerable research has been conducted on easing the constraints of both production lines and workers.

To improve the efficiency of bucket brigades, worker collaboration is used to accelerate the workers' speed (Pratama et al., 2018a), and cellular bucket brigades have been proposed to reduce the unproductive time cost (Lim & Wu, 2014) and eliminate the effect of speed variability (Lim, 2011). Blocking and halting disappear in cellular bucket brigades by using worker collaboration (Pratama et al., 2018b).

In this study, we propose two production models from different perspectives. One model focuses on the details of the existing model. The previous collaborative production model presented by Pratama et al. (2018b) has improved the production efficiency considerably when blocking and/or halting occurs in cellular bucket brigades. In some cases, however, the maximum throughput that can be achieved is not available due to the unsuitable arrangement of workers at certain stages. Therefore, we have revised the previous model to improve the throughput in such cases and obtained the specific conditions that make the proposed model better than the existing model.

The other model comes from a more macro-perspective. Two problems should be solved to improve the throughput further. First, the existing model is too complex. Second, it includes many unproductive behaviors. This complexity makes using the model confusing for management. Unproductive behavior leads directly to the decline of production efficiency.

Based on the above points, we revised the previous model to a simpler one. To understand the features of the new model, a comprehensive analysis was carried out. Additionally, the unproductive behaviors were reduced. Compared to cellular bucket brigades, the revised model achieves considerable improvements in some cases.

2.2 Model Definitions and Previous Models

2.2.1 Model Definition

We adopt the definitions of U-lines with three stations given by Lim and Wu (2014). A U-line consists of three stages: Stages 1 and 3 are parallel to each other, as if on either side of an aisle, and Stage 2 is between Stages 1 and 3, as shown in Figure 2-1. A stage can be further divided into several workstations. Workers process items with tools in the workstations. Unbalanced distribution of the work content among workstations may reduce the throughput of the production line. Lim and Wu's study showed that increasing the number of workstations can reduce the effect of unbalanced work content distribution on the throughput (Lim, 2011). If, however, each stage is separated into many workstations, this gives rise to a continuous line instead of a production line with discrete workstations.

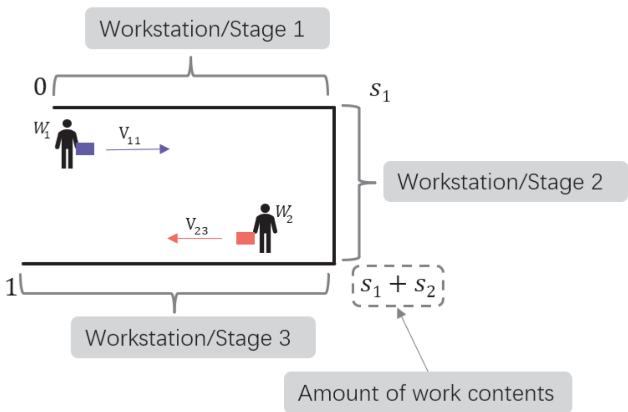

Figure 2-1 Stages and workstations in the U-line.

As in Pratama et al. (2018b), the number of workstations in this study is three, which indicates that every stage contains a workstation, as shown in Figure 2-1. S_j denotes the workstation j, where the value of S_j is the work content assigned to workstation j. The work content is evenly distributed in the workstations, and the total work content is normalized to 1 (i.e., $\sum_{j=1}^{3} S_j = 1$). Therefore, we use "1" at the end point of the U-line in Figure 2-1 to describe the total amount of work content rather than $S_1 + S_2 + S_3$. There are two workers in the U-line, denoted as W_1 and W_2. Both workers are cross-trained, so they can work in any stage of the U-line. The velocity of W_i at S_j is defined as V_{ij} for $i = 1, 2$ and $j = 1, 2, 3$. One workstation only is available for one worker for each CBB. We also assume that the time cost of travel among the stages and of the hand-off for workers is zero, as in Pratama et al. (2018b), since these are much shorter than the time worker spends on producing.

For worker collaboration in the production model, three new concepts were introduced by Pratama et al. (2018b). The first is *worker collaboration*, a behavior that allows W_1 and W_2 to process the same item together. Unlike cellular bucket brigades, two workers in a collaborative model can work in the same workstation. The second new concept is a buffer in which the worker can drop an item temporarily. The third is a collaborative coefficient, α, that reflects the collaborative efficiency of workers, which is a constant ranging from 0 to 1 ($0 < \alpha \leq 1$), where a bigger collaborative coefficient indicates more efficient collaboration. The collaborative velocity of W_1 and W_2 at workstation j can be described as $\alpha(V_{1j} + V_{2j})$, for j = 1, 2, 3.

All the variables used in this paper are summarized in the following list. Note that, although some of them do not appear in this section because they relate to special and specific situations of the production line, they are still included in the list for convenient checking.

Variables.

- S_j: At workstation j where $j = 1, 2,$ and 3, S_j equals the amount of work contents assigned to workstation j.
- W_i: Worker number i where $i = 1, 2$.
- V_{ij}: The velocity of worker i at workstation j.
- α: Collaborative coefficient ranging from 0 to 1, reflecting the collaborative efficiency of workers.
- h_i: The position that is determined by projecting W_i's position on the horizontal axis.
- X_i: The place where two workers meet and start the ith collaboration.
- CT: Cycle time of production model.
- TH: Throughput of production model.
- $D_{i,j}$:The numerator of the partial differential of TH in $Region\ i$ to S_j.
- RD: Relative difference in throughput.

2.2.2 Previous Models

Cellular Bucket Brigades

The velocity of workers is assumed as a constant for bucket brigades with discrete workstations. In this situation, a solution of worker and task assignment is derived to achieve and maintain maximum throughput. Lim and Wu (2014) released the limitation of the velocities, so variable velocity appears in the production line. The previous solution is no longer suitable for this kind of production line. To overcome the effect of variability, the use of cellular bucket brigades was proposed, which perform better than bucket brigades under random worker velocities.

Figure 2-2 shows the movement rules of workers for cellular bucket brigades, where the horizontal position h_i is determined by projecting W_i's location on the horizontal axis. W_1starts to process an item at S_1 and W_2 starts at another stage; when their horizontal positions coincide, they exchange their items.

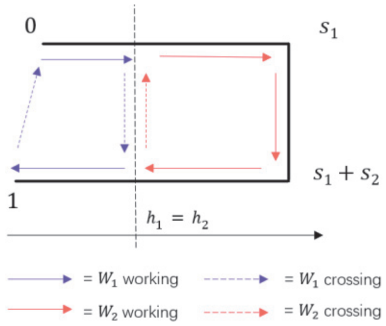

Figure 2-2 Operating principle of cellular bucket brigades.

Blocking and Halting Problem

Although cellular bucket brigades have a higher throughput compared to bucket brigades under the influence of variability, blocking and halting remain problems that cause decreased throughput. Figure 2-3(a) and 2-3(b) show an example. In Figure 2-3(a), when W_1 arrives at the end of S_1, he/she cannot move on since W_2 is working in S_2 and a workstation is only available for one worker. Therefore, blocking occurs at the end of S_1 (red circle). In Figure 2-3(b), when W_1 arrives at the end of S_3, he/she cannot introduce a new item from the start of S_1. Hence, halting occurs at the end of S_3 (red circle).

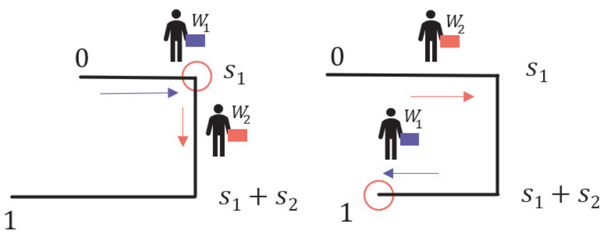

(a) (b)

Figure 2-3 Blocking and halting occurrence in cellular bucket brigades.

Worker Collaboration Type 1

To eliminate the blocking and halting in U-lines, Pratama et al. (2018b) proposed two types of collaborative models, called Worker Collaboration Type 1 and Worker Collaboration Type 2. After comparing the two models, they claimed that Worker Collaboration Type 1 is better than Type 2. Therefore, we focus on Worker Collaboration Type 1 in this study.

Figure 2-4 shows the worker movement behavior of Worker Collaboration Type 1. X_i is the meeting point for workers, where they start the ith collaboration. Workers follow a similar collaboration rule: when one worker arrives at the end point of a stage, he/she puts the item into a buffer or sets down the finished item and goes to the meeting point to collaborate with the co-worker.

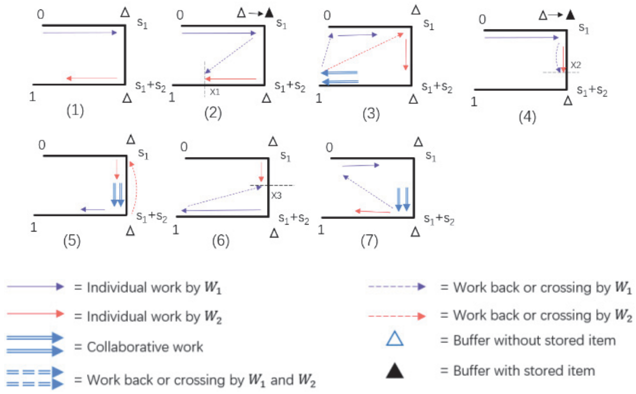

Figure 2-4 Operational principle of Worker Collaboration Type 1.

2.3 Collaborative Model with More Collaboration and Multiple Buffers

2.3.1 Worker Arrangement and Buffer-Use Problem

One of the keys to increasing the capacity of a production line is to get faster workers to do more work. For example, the fastest worker should be arranged as the last one in the BB. In Worker Collaboration Type 1, however, there are two different workers who start separately to process the item in S_3 at Steps 1 and 5. This indicates that, whether the two workers are fast or slow in S_3, most of the work content in S_3 must be done individually. In some cases, this is against the principle of worker arrangement in a production line. For example, when both workers can process an item quickly in S_3 compared with working in other stages, it is a loss to let only one of them do most of the work in S_3.

The second buffer is usually idle in Worker Collaboration Type 1. If we take advantage of the collaboration properly and improve the use of the second buffer, the throughput of the existing model will be further increased.

2.3.2 Proposed Model 1 and Worker Behavior Analysis

Model 1

Model 1 has made some changes to Worker Collaboration Type 1. Figure 2-5 shows the worker movement behavior of Model 1, in which workers start by collaborating in S_3, instead of starting separately. One benefit of the collaboration is that it allows both workers to process the item at the stage where they have fast velocities. Therefore, Model 1 will perform better than Worker Collaboration Type 1 in this situation. Also, compared with Worker Collaboration Type 1, Model 1 includes more balanced use of the two buffers' collaborative work contents in S_2 and S_3.

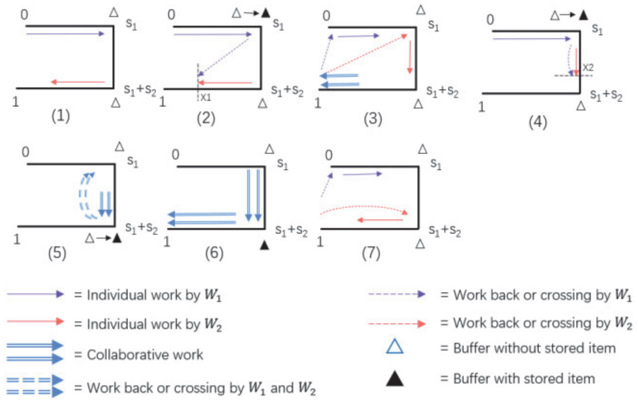

Figure 2-5 Operational principle of Model 1.

Analysis of Worker Behavior in Model 1

$\boldsymbol{Case\ 1}$: $\frac{S_1}{V_{11}} < \frac{S_3}{V_{23}}, \frac{S_1}{V_{11}} < \frac{S_2}{V_{22}}$

As Figure 2-5 shows, W_1 starts to process an item at S_1, and W_2 starts at S_3 in Step 1. In Step 2, W_1 finishes the work content of S_1 before W_2 at S_3, which can be expressed as $\frac{S_1}{V_{11}} < \frac{S_3}{V_{23}}$, so W_1 should put the item into Buffer 1, go to the position where W_2 is still working, and collaborate with him/her. Note that, when W_1 is crossing the U-line, W_2 continues his/her work. Since the crossing time is ignored, the meeting point X_1 can be expressed as $X_1 = V_{23} * \frac{S_1}{V_{11}} + S_1 + S_2$. In Step 3, after collaboration, W_1 goes to the start of S_1 and introduces a new item into the production line, and W_2 takes an item from Buffer 1 to continue the process. In Step 4, W_1 reaches the end of S_1 before W_2 at S_2, which can be expressed as $\frac{S_1}{V_{11}} < \frac{S_2}{V_{22}}$, and W_1 behaves similarly to Step 2. The meeting point X_2 can be expressed as $X_2 = V_{22} * \frac{S_1}{V_{11}} + S_1$. In Step 5, after the collaboration has finished at S_2, they put the item into Buffer 2 and go back to take an incomplete item from Buffer 1. In Step 6, this time the two workers collaborate with each other throughout the whole of S_2 and S_3. In Step 7, W_1 introduces a new item into the production line again, while W_2 continues to process the item at S_3.

Table 2-1 Formulas for $Case$ 1

	Formulas
Condition	$\frac{S_1}{V_{11}} < \frac{S_3}{V_{23}}, \frac{S_1}{V_{11}} < \frac{S_2}{V_{22}}$
Meeting point	$X_1 = V_{23} * \frac{S_1}{V_{11}} + S_1 + S_2$ $X_2 = V_{22} * \frac{S_1}{V_{11}} + S_1$
Cycle time	$CT = 2\frac{S_1}{V_{11}} + \frac{1-X_1}{\alpha*(V_{13}+V_{23})} + \frac{S_1+S_2-X_2}{\alpha*(V_{12}+V_{22})} + \frac{S_2}{\alpha*(V_{12}+V_{22})} + \frac{S_3}{\alpha*(V_{13}+V_{23})}$

Table 2-1 summarizes the formulas for calculating the meeting point and the cycle time and the conditions that Model 1 must satisfy for applying the formulas. If the conditions are changed, the formulas should also be modified. Four groups of formulas need to be proposed for four different cases since there are two conditions in the table; Table 2-1 shows the formulas for $Case$ 1.

The first condition in Table 2-1 corresponds to the first collaboration in Figure 2-5 at Step 2, where W_1 finishes the work content of S_1 before W_2 at S_3 $(i.e., \frac{S_1}{V_{11}} < \frac{S_3}{V_{23}})$. The second condition corresponds to the second collaboration in Figure 2-5 at Step 4, where W_1 reaches the end of S_1 before W_2 at S_2 $(i.e., \frac{S_1}{V_{11}} < \frac{S_2}{V_{22}})$. The following three cases are variations of $Case$ 1 with different conditions.

$Case$ 2: $\frac{S_1}{V_{11}} \geq \frac{S_3}{V_{23}}, \frac{S_1}{V_{11}} < \frac{S_2}{V_{22}}$

Figure 2-6 shows the workers' behavior in the first collaboration, where W_2 arrives at the end of S_3 before W_1 at S_1 in Step 2 (i. e., $\frac{S_1}{V_{11}} \geq \frac{S_3}{V_{23}}$). For the second collaboration, it remains as shown in
Figure 2-6 at Step 4.

In this case, W_2 should go to the meeting point X_1 and collaborate with W_1. The meeting point X_1 can be expressed as $X_1 = V_{11} * \frac{S_3}{V_{23}}$. Table 2-2 shows the formulas corresponding to the case in
Figure 2-6.

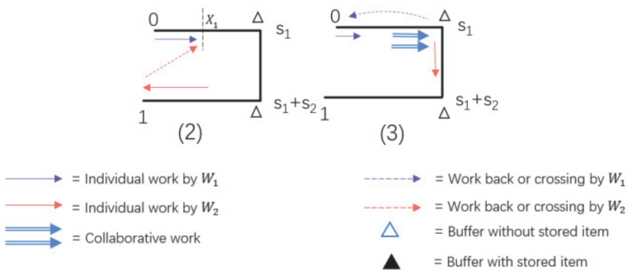

Figure 2-6 Behavior of workers in $Case$ 2.

Table 2-2 Formulas for $Case$ 2.

	Formulas
Condition	$\frac{S_1}{V_{11}} \geq \frac{S_3}{V_{23}}, \frac{S_1}{V_{11}} < \frac{S_2}{V_{22}}$
Meeting point	$X_1 = V_{11} * \frac{S_3}{V_{23}}$ $X_2 = V_{22} * \frac{S_1}{V_{11}} + S_1$
Cycle time	$CT = \frac{S_3}{V_{23}} + \frac{S_1 - X_1}{\alpha * (V_{11} + V_{21})} + \frac{S_1}{V_{11}} + \frac{S_1 + S_2 - X_2}{\alpha * (V_{12} + V_{22})} + \frac{S_2}{\alpha * (V_{12} + V_{22})} + \frac{S_3}{\alpha * (V_{13} + V_{23})}$

$\boldsymbol{Case\ 3}$: $\frac{S_1}{V_{11}} < \frac{S_3}{V_{23}}, \frac{S_1}{V_{11}} \geq \frac{S_2}{V_{22}}$

The behavior of workers in the second collaboration is shown in Figure 2-7. The second collaboration stays the same as in
Figure 2-6.

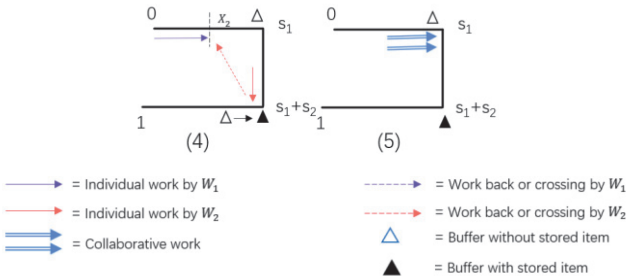

Figure 2-7 Behavior of workers in $Case$ 3.

In Figure 2-7, W_2 reaches the end of S_2 before W_1 at S_1 in Step 4, which can be expressed as $\frac{S_1}{V_{11}} \geq \frac{S_2}{V_{22}}$. The meeting point X_2 in this situation can be expressed as $X_2 = V_{11} * \frac{S_2}{V_{22}}$. Table 2-3 shows the formulas that correspond to Figure 2-7.

Table 2-3 Formulas for $Case$ 3.

	Formulas
Condition	$\frac{S_1}{V_{11}} < \frac{S_3}{V_{23}}, \frac{S_1}{V_{11}} \geq \frac{S_2}{V_{22}}$
Meeting point	$X_1 = V_{23} * \frac{S_1}{V_{11}} + S_1 + S_2$ $X_2 = V_{11} * \frac{S_2}{V_{22}}$
Cycle time	$CT = \frac{S_1}{V_{11}} + \frac{1 - X_1}{\alpha * (V_{13} + V_{23})} + \frac{S_2}{V_{22}} + \frac{S_1 - X_2}{\alpha * (V_{11} + V_{21})} + \frac{S_2}{\alpha * (V_{12} + V_{22})} + \frac{S_3}{\alpha * (V_{13} + V_{23})}$

$\boldsymbol{Case\ 4}$: $\frac{S_1}{V_{11}} \geq \frac{S_3}{V_{23}}, \frac{S_1}{V_{11}} \geq \frac{S_2}{V_{22}}$

In Figure 2-8, the behavior of workers in Steps 2–5 is the same as in Figuress 2-5 and 2-6, which contain two collaborations. Table 2-4 shows the formulas corresponding to Figure 2-8.

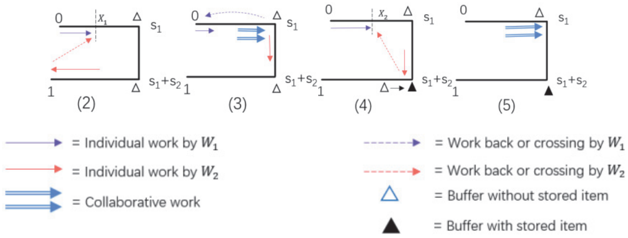

Figure 2-8 Behavior of workers in $Case$ 4.

After the cycle time of Model 1 is obtained, we transfer the cycle time to the average throughput by means of Eq. (1), where the numerator of the formula equals 2 because two products are completed in one production cycle for Model 1 in Steps 3 and 6.

$$TH = \frac{2}{CT} \tag{2-1}$$

Table 2-4 Formulas for $Case$ 4.

	Formulas
Condition	$\frac{S_1}{V_{11}} \geq \frac{S_3}{V_{23}}, \frac{S_1}{V_{11}} \geq \frac{S_2}{V_{22}}$
Meeting point	$X_1 = V_{11} * \frac{S_3}{V_{23}}$ $X_2 = V_{11} * \frac{S_2}{V_{22}}$
Cycle time	$CT = \frac{S_3}{V_{23}} + \frac{S_1 - X_1}{\alpha*(V_{11}+V_{21})} + \frac{S_2}{V_{22}} + \frac{S_1 - X_2}{\alpha*(V_{11}+V_{21})} + \frac{S_2}{\alpha*(V_{12}+V_{22})} + \frac{S_3}{\alpha*(V_{13}+V_{23})}$

2.3.3 Throughput Figure Analysis for Model 1

Figure 2-9(a) shows the throughput figure of Model 1 with $V_{11} = 1.2$, $V_{12} = 1, V_{13} = 0.8$, $V_{21} = 0.8, V_{22} = 1$, $V_{23} = 1.2$ and $\alpha = 1.0$. The S_j axis in Figure 2-9 is the amount of work content assigned to workstation S_j $(j = 1, 3)$, and the TH axis is the throughput. Figure 2-9(b) is the top view of Figure 2-9(a), which is separated into $Regions$ $1, 2,$ 3 and 4 by $Solid\ boundary$ $S_1 = V_{11}\frac{S_3}{V_{23}}$ and $dashed\ boundary$ $S_3 = \left(-\frac{V_{22}}{V_{11}} - 1\right) * S_1 + 1$. The workers' behavior of Model 1 in $Region\ i$ corresponds to the above Table i.

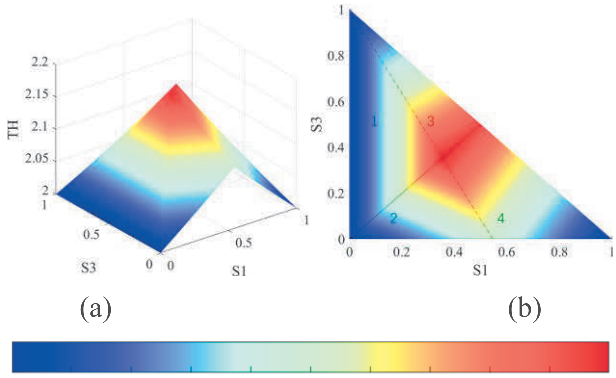

(a) (b)

Figure 2-9 Throughput figure of Model 1.

Figure 2-10 is the draft figure of Figure 2-10(b) with two boundaries and three arrows. Points A–F mark the crossing point of the boundaries and axes. Arrows indicate the trend of the throughput function; the throughput increases along the arrows. There is no vertical arrow in $Region$ 1 since the throughput maintains the same value in the vertical direction in $Region$ 1. For Model 1, the maximum throughput point only appears at one of the crossing points (Appendix A.1).

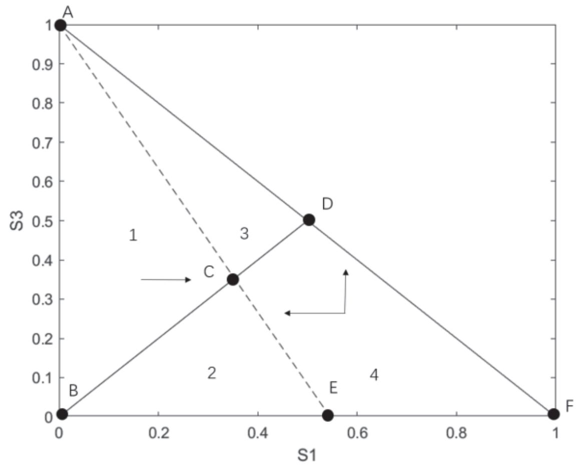

Figure 2-10 Draft throughput figure of Model 1.

The throughput functions of Model 1 in the four regions are monotonic to S_1 and S_3 (Appendix A.1). Therefore, a method capable of finding the location of the maximum throughput can be developed. This method will give managers the details of the throughput figures to arrange the work content at the workstations instead of drawing a true throughput figure using professional software.

Although the work content assigned to workstations at the maximum throughput point is sometimes illogical, since some workstations contain too much work content while others have little, this still provides guidance that lets managers know the relationship between the throughput and the work content at the workstations. Moreover, they can arrange the distribution of the work content as closely as possible to the maximum throughput point to make sure the production line achieves its best performance.

$Method$ 1 is a method that can find the location of the maximum throughput point in a draft throughput figure.

$Method$ 1: Find the location of the maximum throughput point in a draft throughput figure.

(1) Draw a draft throughput figure with two boundaries.

$Solid\ boundary$: $S_1 = V_{11}\frac{S_3}{V_{23}}$

$Dashed\ boundary$: $S_3 = \left(-\frac{V_{22}}{V_{11}} - 1\right) * S_1 + 1$

(2) Judge the relationship between 0 and the differentiations of the throughput functions in $Regions$ 1 and 4. Arrows are used to indicate the trend of the throughput function. The throughput increases along the arrow.

(3) Based on the directions of the arrows, some candidate points can be obtained, and the maximum throughput point is determined by comparing the throughput values of the candidate points.

It is worth noting that, when we judge the relationship between 0 and the differentiations of the throughput functions, in fact, only the numerators of the differentiations are necessary because the denominators are always larger than 0. Here, $Regions$ 2 and 3 are ignored to simplify the method.

Define $D_{i,j}$ as the numerator of the partial differential of the throughput in $Region$ 1 to S_j.

$Region$ 1:

$$D_{1,1} = \frac{1}{\alpha*(V_{12}+V_{22})} - \frac{2}{V_{11}} + \frac{\frac{V_{22}}{V_{11}}+1}{\alpha*(V_{12}+V_{22})} + \frac{V_{23}}{\alpha*V_{11}(V_{13}+V_{23})}$$

$$D_{1,3} = \frac{2}{\alpha*(V_{12}+V_{22})} - \frac{2}{\alpha*(V_{13}+V_{23})}$$

$Region$ 4:

$$D_{4,1} = -\frac{1}{\alpha*(V_{11}+v21)} + \frac{1}{\alpha*(V_{12}+V_{22})} + \frac{1}{V_{22}} - \frac{\frac{V_{11}}{V_{22}}+1}{\alpha*(V_{11}+V_{21})}$$

$$D_{4,3} = \frac{1}{\alpha*(V_{12}+V_{22})} - \frac{1}{\alpha*(V_{13}+V_{23})} + \frac{1}{V_{22}} - \frac{1}{V_{23}} - \frac{v11}{\alpha*V_{22}(V_{11}+V_{21})} + \frac{V_{11}}{\alpha*V_{23}(V_{11}+v21)}$$

Example. The velocities and collaborative coefficient of workers are given as $V_{11} = 1, V_{12} = 3, V_{13} = 2, V_{21} = 2, V_{22} = 3, V_{23} = 1$, and $\alpha = 1$. Find the maximum throughput point.

$Solid\ boundary$: $S_3 = \mathrm{S}_1$

$Dashed\ boundary$: $S_3 = -4 * \mathrm{S}_1 + 1$

$Region$ 1: $D_{1,1} = -0.833, D_{1,3} = -0.33$

$Region\ 2$: $D_{2,1} = -0.278$, $D_{2,3} = -0.61$

Based on the value of $D_{i,j}$ and the two boundaries, we can draw a draft throughput figure of the example as shown in Figure 2-11. According to the directions of the arrows, Points B and E are candidate points.
$TH_B = 6, TH_E = 4.36.$

After calculating and comparing the throughput of the candidate points, Point B is the maximum throughput point. According to the position of the maximum throughput point in the figure, we can infer that the throughput increases with more work content assigned to S_2. Therefore, when a manager manages the distribution of work contents in the production line, he/she should take advantage of S_2 and assign more work content to it. Note that, although this production line will achieve its best performance when workers only work in S_2, it is impossible to satisfy this condition. Otherwise, the production line becomes a continuous linear line and has only one kind of work content.

It is worth noting that, except for $Method\ 1$, the maximum throughput point can also be obtained by comparing the throughput of these crossing points directly.

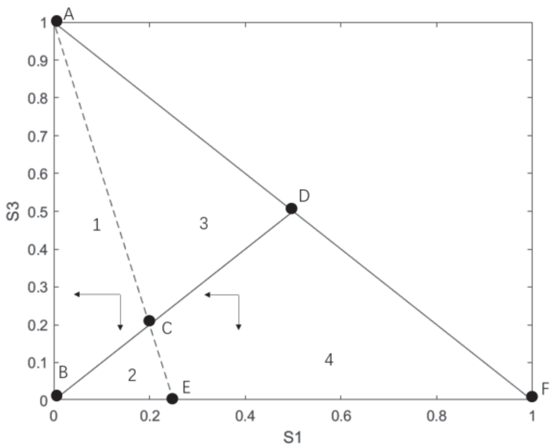

Figure 2-11 Example draft throughput for Model 1.

2.4 Collaborative Model with Simpler Rules

2.4.1 Model Complexity and Unproductive Behavior Problem

Model 1 improves the throughput of the production line further under certain conditions compared to the previous model, but Model 1 still has disadvantages in some cases.

First, it is a complex production system consisting of seven steps and four different cases. The complexity not only confuses the manager when using the model but also increases the learning cost of workers and the probability of operational errors. If we simplify the production model to one with fewer production steps and cases, this problem can be solved.

Second, workers cross the U-line very frequently in Model 1. They drop off the item and go to the meeting point for collaboration many times. Although the time cost of a worker's unproductive movements (crossing the U-line and putting the item into the buffer) is assumed to be 0, in the real world, this sort of time cost still exists. Especially for a long U-line, the effect of unproductive behavior on the throughput becomes more obvious. Therefore, revising Model 1 to a collaborative model with simpler worker movements (fewer production steps and cases) and less-frequent crossing of the U-line can further improve its efficiency.

2.4.2 *Proposed Model 2 and Worker Behavior Analysis*

Model 2

Model 2 is a new design of a collaborative production system in which the worker-movement rules are simplified and the frequency of workers crossing the U-line decreases significantly. Figure 2-12 shows the worker-movement rules of Model 2, which has two different cases depending on whether W_1 reaches the end of S_1 earlier than W_2 at S_2.

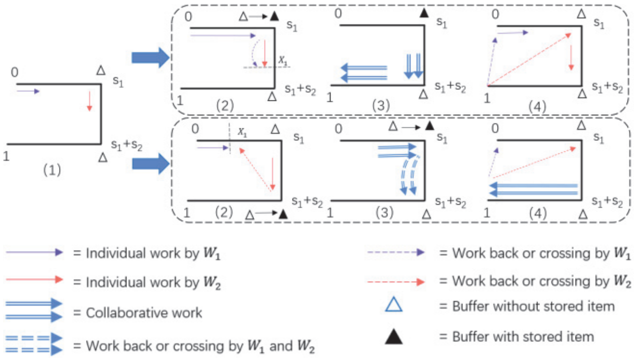

Figure 2-12 Operational principle of Model 2.

Analysis of Worker Behavior in Model 2

In Model 2, there are two different cases. In $Case$ 1, W_1 reaches the endpoint of S_1 before W_2 arrives at S_2's endpoint at Step 2, while the situation is reversed in $Case$ 2. Therefore, the distinctive conditions of $Case$ 1 and $Case$ 2 can be derived. If $Condition$ 3 is satisfied, workers should follow the operating principle of $Case$ 1; otherwise, they follow $Case$ 2.

$Condition$ 3: $\frac{S_1}{V_{11}} < \frac{S_2}{V_{22}}$

$Case$ 1: $\frac{S_1}{V_{11}} < \frac{S_2}{V_{22}}$

For $Case$ 1, in Step 1, W_1 starts to process an item at S_1, and W_2 starts at S_2. In Step 2, when W_1 reaches the end of S_1, he/she should put the item into Buffer 1, go to meeting point X_1, and collaborate with W_2. The meeting point X_1 can be expressed as $X_1 = V_{22} * \frac{S_1}{V_{11}} + S_1$. In Step 3, two workers collaborate with each other until they complete the item at the end of the production line. In Step 4, W_1 goes to the start of S_1 and introduces a new item into the production line, and W_2 takes an item from Buffer 1 to continue the process.

Table 2-5 Parameter Calculation of $Case$ 1.

	Formulas
Condition	$\frac{S_1}{V_{11}} < \frac{S_2}{V_{22}}$
Meeting point	$X_1 = V_{22} * \frac{S_1}{V_{11}} + S_1$
Cycle time	$CT = \frac{S_1}{V_{11}} + \frac{S_1+S_2-X_1}{\alpha*(V_{12}+V_{22})} + \frac{S_3}{\alpha*(V_{13}+V_{23})}$

$\boldsymbol{Case\ 2}$: $\frac{S_1}{V_{11}} \geq \frac{S_2}{V_{22}}$

For $Case$ 2, Step 1 is the same as in $Case$ 1. In Step 2, this time W_2 reaches the end of S_2 before W_1; therefore, he/she should put the item into Buffer 2 and go to meeting point X_1 to collaborate with W_1. The meeting point X_1 can be defined as $X_1 = V_{11} * \frac{S_2}{V_{22}}$. In Step 3, since an item already exists in Buffer 2, after the two workers put their items into Buffer 1, they should directly pick up the item from Buffer 2 and continue to process it at S_3. Step 4 is the same as in $Case$ 1.

Table 2-5 and Table 2-6 show each parameter's calculation for Model 2. With the different conditions, the formulas for calculating the meeting point and cycle time are different. Table 2-5 and Table 2-6 correspond to $Case$ 1 and $Case$ 2, respectively.

Table 2-6 Parameter Calculation of $Case$ 2.

	Formulas
Condition	$\frac{S_1}{V_{11}} \geq \frac{S_2}{V_{22}}$
Meeting point	$X_1 = V_{11} * \frac{S_2}{V_{22}}$
Cycle time	$CT = \frac{S_2}{V_{22}} + \frac{S_1-X_2}{\alpha*(V_{11}+V_{21})} + \frac{S_3}{\alpha*(V_{13}+V_{23})}$

After the cycle time of $Case$ 1 or 2 is obtained, we transfer the cycle time to throughput by means of Eq. 2-2. Unlike Eq. 2-1, the numerator of Eq. 2-2 equals 1 because Model 2 completes only one product in one production cycle.

$$TH = \frac{1}{CT} \qquad 2-2$$

2.4.3 *Throughput Figure Analysis for Model 2*

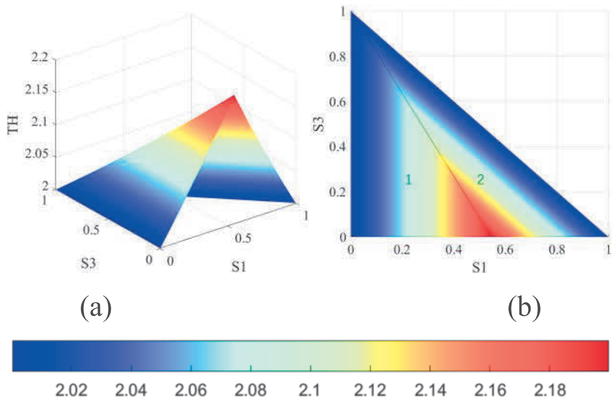

Figure 2-13 Throughput figure of Model 2.

Figure 2-13(a) shows the throughput figure of Model 2 with $V_{11} = 1.2$, $V_{12} = 1$, $V_{13} = 0.8$, $V_{21} = 0.8$, $V_{22} = 1$, $V_{23} = 1.2$, $and\ \alpha = 1.0$. The S_j axis in Figure 2-13 is the work content assigned to workstation S_j $(j = 1, 3)$, and the TH axis is the throughput. Figure 2-13(b) is the top view of Figure 2-13(a), which is divided into $Regions\ 1\ and\ 2$ by boundary $S_3 = \left(-\frac{V_{22}}{V_{11}} - 1\right) * S_1 + 1$. In $Region\ i$, workers follow the operating principle of $Case\ i$.

Figure 2-14 is the draft figure of Figure 2-13(b) with $Boundary\ AC$ and arrows. Points A–D mark the crossing points of the boundaries and axes. For a similar reason, the value of the throughput remains unchanged in the vertical direction in $Region\ 1$, so no vertical arrow appears. As in Model 1, the maximum throughput point of Model 2 only appears at one of the crossing points (Appendix A.3).

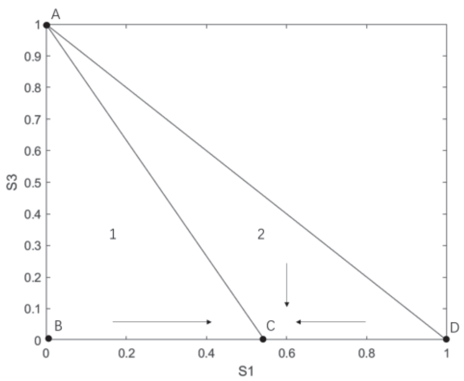

Figure 2-14 Draft throughput figure of Model 2.

$Method\ 2$ is like $Method\ 1$ in that it can find the location of the maximum throughput point in a draft throughput figure.

$Method$ 2: Find the location of the maximum throughput point in a draft throughput figure.

(1) Draw a draft throughput figure with $Boundary\ AC$.
(2) Judge the relationship between 0 and the differentiations of throughput functions. Arrows are utilized to indicate the trend of the throughput function. The throughput increases along the arrow.
(3) Based on the directions of the arrows, some candidate points can be obtained, and the maximum throughput point is decided by comparing the throughput values of the candidate points.

Define $D_{i,j}$ as the numerator of the partial differential to S_j in $Region$ 1.

$Region$ 1:

$$D_{1,1} = \frac{\frac{V_{22}}{V_{11}} + 1}{\alpha * (V_{12} + V_{22})} - \frac{1}{V_{11}}$$

$$D_{1,3} = \frac{1}{\alpha * (V_{12} + V_{22})} - \frac{1}{\alpha * (V_{13} + V_{23})}$$

$Region$ 2:

$$D_{2,1} = \frac{1}{V_{22}} - \frac{\frac{V_{11}}{V_{22}} + 1}{\alpha * (V_{11} + V_{21})}$$

$$D_{2,3} = \frac{1}{V_{22}} - \frac{1}{\alpha * (V_{13} + V_{23})} - \frac{V_{11}}{\alpha * V_{22} * (V_{11} + V_{21})}$$

Example. The velocities and collaborative coefficients of the workers are given as $V_{11} = 1.2$, $V_{12} = 1$, $V_{13} = 0.8$, $V_{21} = 0.8$, $V_{22} = 1, V_{23} = 1.2\ and\ \alpha = 1.$ Find the maximum throughput point.

$Boundary\ AC$: $S_3 = -1.83 * \mathrm{s}1 + 1$
$Region$ 1: $D_{1,1} = 0.083, D_{1,3} = 0$
$Region$ 2: $D_{2,1} = -0.1$, $D_{2,3} = -0.1$

Based on the value of $D_{i,j}$ and $Boundary\ AC$, we can draw a draft throughput figure of the example as shown in Figure 2-15. According to Figure 2-15, Point C is the maximum throughput point. As in the example for Model 1, although Model 2 achieves the maximum throughput at Point C, this does not indicate that managers must assign the work content to the production line strictly according to the position of the maximum throughput point. This method attempts to provide some information on the increasing throughput trend to help managers to make decisions when assigning work content.

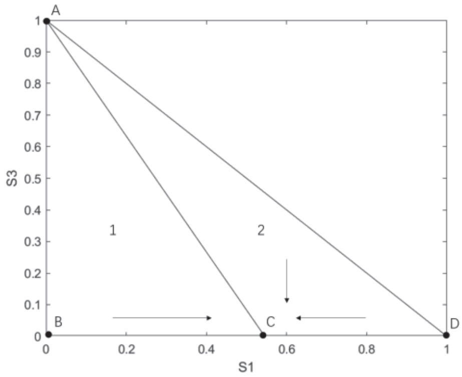

Figure 2-15 Example draft throughput figure of Model 2.

2.5 Numerical Experiment

2.5.1 Best Worker Sequence

We define the best worker sequence as the sequence that makes Model 2 achieve the highest throughput. $Sequence\ AB/BA$ indicates that Workers A/B start at Stage 1 and Workers B/A start at Stage 2, as shown in Figure 2-16. The best worker sequence is either $Sequence\ AB\ or\ BA$ since there are only two possible combinations. The best worker sequence, however, does not always remain the same, and it varies between $Sequence\ AB$ and BA under the different work-content assignments. In a relative difference figure, such variation is reflected in the fact that AB is the best worker sequence in some regions, while in others the best worker sequence is BA. In this section we analyze the relationships among the work content assignment, worker velocity, and the best worker sequence and develop a method to confirm the best work sequence in each region of the relative difference figure. We discuss the best worker sequence in the cases where the collaborative coefficient α is equal to 1 or not, separately, since the case $\alpha \neq 1$ is more complex than the case $\alpha = 1$.

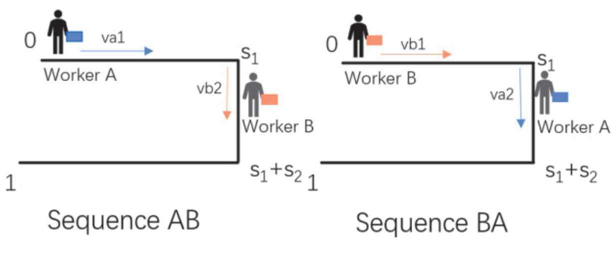

Figure 2-16 Sequences AB and BA.

Case $\alpha = 1$

The best worker sequence remains the same in the entire relative difference figure when the collaborative coefficient α is 1. $Condition$ 4 is the condition where the best worker sequence is $Sequence\ AB$ ($\alpha = 1$). If $\frac{V_{a1}}{V_{a2}} < \frac{V_{b1}}{V_{b2}}$, the best worker sequence is $Sequence\ BA$, and the worker sequence has no effect on the throughput of the production model if $\frac{V_{a1}}{V_{a2}} = \frac{V_{b1}}{V_{b2}}$.

$Condition\ 4$: $\frac{V_{a1}}{V_{a2}} > \frac{V_{b1}}{V_{b2}}$

(See Appendix A.5).

Figure 2-17 shows the relative difference in throughput between $Sequences\ AB\ and\ BA$, where the horizontal axis is the work content assigned to S_1 and the vertical axis is the work content assigned to S_3. With different work content assignment policies, workers may need to follow different operational principles ($Case\ 1\ or\ Case\ 2$).

Define the situation in which workers of $Sequence\ AB$ follow $Case\ i$ and workers of $Sequence\ BA$ follow $Case\ j$ as $CiCj$. There are two kinds of boundaries in Figure 2-17 that divide the figure into $Regions\ C1C1, C1C2/C2C1, and\ C2C2$. The expressions for these boundaries are:

$Solid\ boundary$: $S_3 = \left(-\frac{V_{a2}}{V_{b1}} - 1\right) S_1 + 1$

$Dashed\ boundary$: $S_3 = \left(-\frac{V_{b2}}{V_{a1}} - 1\right) S_1 + 1$

If $\frac{V_{a1}}{V_{b2}} > \frac{V_{b1}}{V_{a2}}$, the $Solid\ boundary$ is located before the $Dotted\ boundary$, and $Region\ C1C2$ appears in the relative difference figure. If $\frac{V_{a1}}{V_{b2}} < \frac{V_{b1}}{V_{a2}}$, the $Dashed\ boundary$ is located before the $Solid\ boundary$, and $Region\ C2C1$ appears (Appendix A.4).

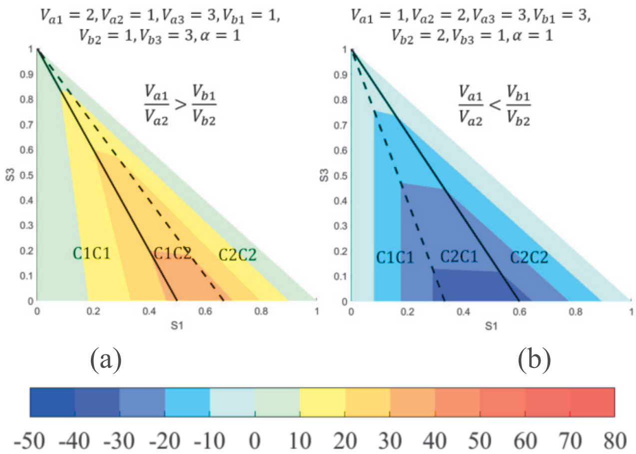

Figure 2-17 Relative difference in throughput between sequences AB and BA (%).

In Figure 2-17(a), the best worker sequence is AB because $Condition\ 4$ is satisfied. Therefore, all the relative differences are positive values. In Figure 2-17(b), all the relative differences are negative values since $\frac{V_{a1}}{V_{a2}} < \frac{V_{b1}}{V_{b2}}$.

Case $\alpha \neq 1$

When collaborative coefficient $\alpha \neq 1$, the best worker sequence is not unique in the relative difference figure. Figure 2-18 shows an example with $V_{a1} = 1, V_{a2} = 2, V_{a3} = 3,\ V_{b1} = 3, V_{b2} = 2, V_{b3} = 1, and\ \alpha = 0.4$. An additional boundary ($Red\ boundary$) appears in Figure 2-18. The $Red\ boundary$ distinguishes the positive and negative value of the relative difference. It has different expressions with different orders of $Solid\ and\ Dashed\ boundaries$.

To discuss the best worker sequence in the relative difference figures, we divided the figure into several regions ($Region\ CiCj$) according to the different operating principles and confirmed the best worker sequence for each region. $Method$ 3 helps us decide the boundaries of the regions and judge the best worker sequence in each region.

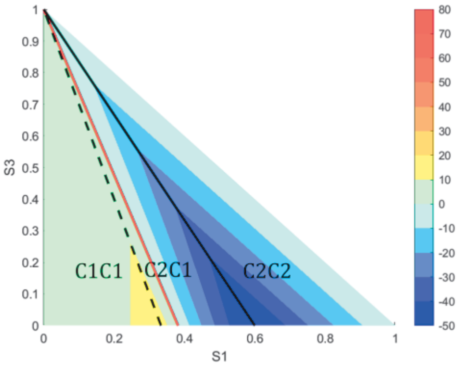

Figure 2-18 Relative difference in throughput between sequences AB and BA (%).

$Method$ 3: Getting the distribution of the best worker sequence in a relative difference figure.

(1) Draw a figure with two/three boundaries.

$Solid\ boundary$: $S_3 = \left(-\frac{V_{a2}}{V_{b1}} - 1\right) S_1 + 1$, $Dashed\ boundary$: $S_3 = \left(-\frac{V_{b2}}{V_{a1}} - 1\right) S_1 + 1$.

a) if $\frac{V_{b1}}{V_{a2}} < \frac{V_{a1}}{V_{b2}}$ ($Region\ C1C2\ appears$) $Red\ boundary$ 1

b) if $\frac{V_{b1}}{V_{a2}} > \frac{V_{a1}}{V_{b2}}$ ($Region\ C2C1\ appears$). $Red\ boundary$ 2

c) if $\frac{V_{b1}}{V_{a2}} = \frac{V_{a1}}{V_{b2}}$. No $Red\ boundary$ and no $Region\ C1C2/C2C1$.

(2) Judge $Regions\ C1C1\ and\ C2C2$

If $Condition$ 5 is satisfied, $Region\ C1C1$ increases in area ($Sequence\ AB$ is the best sequence).

a) If $\frac{V_{b1}}{V_{a2}} = \frac{V_{a1}}{V_{b2}}$ $Conclusion$ 1, End.

b) If $\frac{V_{b1}}{V_{a2}} \neq \frac{V_{a1}}{V_{b2}}$

If $Condition\ 6$ is satisfied, $Region\ C2C2$ increases in area.

(3) Judge $Region\ C1C2/C2C1$

a) $Red\ boundary$ is located in $Region \frac{C1C2}{C2C1}$. $Conclusion\ 2$

b) $Red\ boundary$ is beyond $Region \frac{C1C2}{C2C1}$. $Conclusion\ 3$. End.

$Red\ boundary\ 1$:

$$S_3 = \left(-\frac{\frac{1}{V_{a1}}-\frac{1}{(V_{a1}+V_{b1})\alpha}-\frac{V_{b2}}{V_{a1}(V_{a2}+V_{b2})\alpha}}{\frac{1}{V_{a2}}-\frac{1}{(V_{a2}+V_{b2})\alpha}-\frac{V_{b1}}{V_{a2}(V_{a1}+V_{b1})\alpha}}-1\right)S_1+1.$$

$Red\ boundary\ 2$:

$$S_3 = \left(-\frac{\frac{1}{(V_{a1}+V_{b1})\alpha}-\frac{-V_{a2}+V_{a2}\alpha+V_{b2}\alpha}{V_{b1}(V_{a2}+V_{b2})\alpha}}{\frac{1}{(V_{a2}+V_{b2})\alpha}-\frac{-V_{a1}+V_{a1}\alpha+V_{b1}\alpha}{V_{b2}(V_{a1}+V_{b1})\alpha}}-1\right)S_1+1.$$

$Condition\ 5$: $\frac{\alpha(V_{a2}+V_{b2})-V_{b2}}{V_{a1}} < \frac{\alpha(V_{a2}+V_{b2})-V_{a2}}{V_{b1}}$

$Condition\ 6$: $\frac{\alpha(V_{a1}+V_{b1})-V_{a1}}{V_{b2}} < \frac{\alpha(V_{a1}+V_{b1})-V_{b1}}{V_{a2}}$

(Please check the Appendix A.6–A.11 for the proof process)

$Conclusion\ 1$: When the $Solid\ boundary$ and the $Dashed\ boundary$ coincide with each other, the entire relative difference figure shows one kind of area, as shown in Figure 2-19(a).

$Conclusion\ 2$: When the $Red\ boundary$ is located in $Region\ C1C2/C2C1$, the increased/decreased part of $Region\ C1C2/C2C1$ is adjacent to the other region's increased/decreased part, as shown in Figure 2-19(b).

$Conclusion\ 3$: When the $Red\ boundary$ is beyond $Region\ C1C2/C2C1$, if $Regions\ C1C1\ and\ C2C2$ are the same type of area, $Region\ C1C2/C2C1$ is the same as the other regions, as shown in Figure 2-19(c). Otherwise, $Region\ C1C2/C2C1$ is the same as the non-zero region, as Figure 2-19(d) shows.

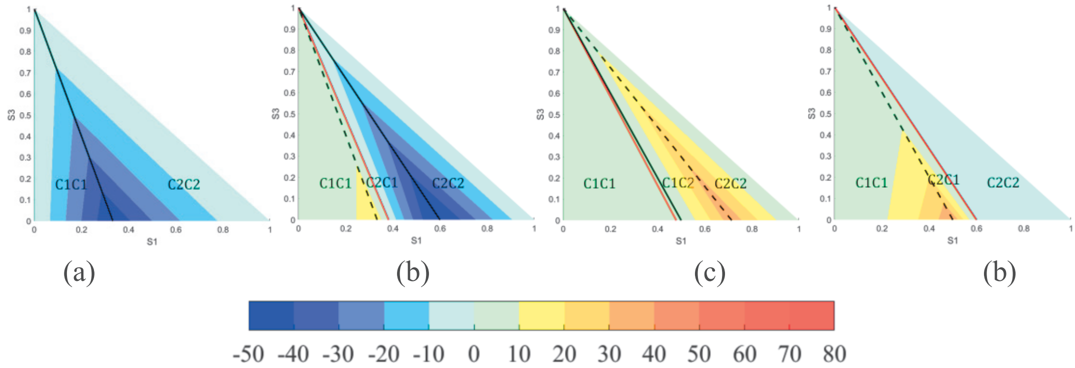

Figure 2-19 Cases corresponding to $Conclusions\ 1,\ 2, and\ 3$.

Example. Suppose $V_{a1} = 1.2, V_{a2} = 1, V_{a3} = 0.8, V_{b1} = 0.8,\ V_{b2} = 1, V_{b3} = 1.2, and\ \alpha = 0.4$. Draw the distribution figure of the best worker sequence.

(1) $Solid\ boundary: S_3 = -2.25 * S_1 + 1$
$Dashed\ boundary: S_3 = -1.83 * S_1 + 1$
$Red\ boundary: S_3 = -2.17 * S_1 + 1$

(2) $Region\ C1C1: -0.17 > -0.25$, decrease in area. $Region\ C2C2: -0.4 < 0$, increase in area.

(3) According to $Conclusion\ 1$, the left part of $Region\ C1C2$ is decreased in area, and the right part is increased in area.

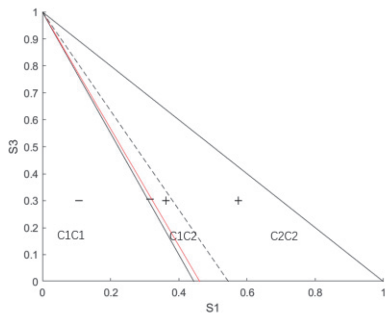

Figure 2-20 Example result of draft figure.

2.5.2 *Throughput Comparison Between Model 1 and Previous Model*

$Condition\ 1$ is the condition of Model 1 better than Worker Collaboration Type 1. If $\alpha = 1$, $Condition\ 1$ can be simplified as $Condition\ 2$ (see Appendix A.2).

$$Condition\ 1: \frac{V_{22}}{V_{12}+V_{22}} + \frac{V_{13}}{V_{13}+V_{23}} < \alpha$$

$Condition\ 2: \frac{V_{13}*V_{22}}{V_{12}*V_{23}} < 1$

Figure 2-21 shows the relative difference figures in the throughput between Model 1 and Worker Collaboration Type 1. The horizontal axis is the work content assigned to S_1, the vertical axis is the work contents assigned to S_3, and the value is the relative difference, which is calculated by Eq. 2-3.

$$RD = \frac{TH_{Model\,1} - TH_{WCT1}}{TH_{WCT1}} * 100 \qquad 2-3$$

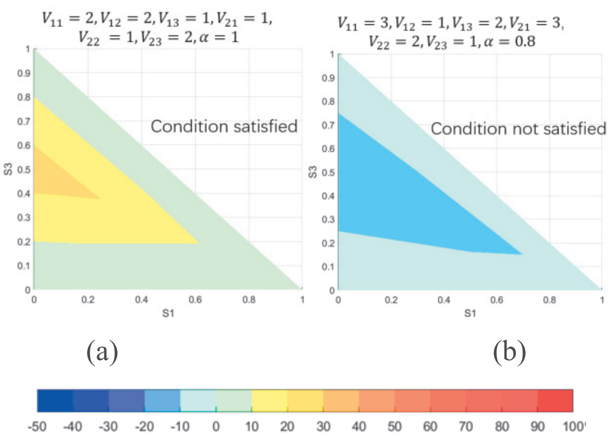

Figure 2-21 Relative difference in throughput between Model 1 and Worker Collaboration Type 1 (WCT1).

For Figure 2-21(a), $Condition\ 2$ is satisfied. Therefore, in the entire figure, Model 1 gives higher throughput, while for Figure 2-21(b), $Condition\ 1$ is not satisfied. Hence, Worker Collaboration Type 1 performs better than Model 1.

2.5.3 Throughput Comparison Between Model 2 and Previous Model

Figure 2-22 shows the relative difference in throughput between Model 2 and cellular bucket brigades. The conditions of the workers in Figure 2-22(a) are given as $V_{11} = 1.2$, $V_{12} = 1$, $V_{13} = 0.8$, $V_{21} = 0.8$, $V_{22} = 1$, $V_{23} = 1.2, and\ \alpha = 1$. In Figure 2-22(b), the velocities are the same, while the collaborative coefficient α decreases to 0.8.

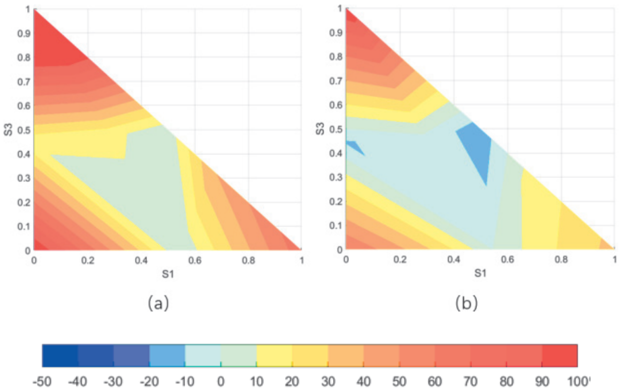

Figure 2-22 Relative difference in throughput between Model 2 and cellular bucket brigades.

Model 2 performs better in the whole of Figure 2-22(a), especially in the three corners of the figure, where it achieves significant improvement over cellular bucket brigades. A similar comparison was made by Pratama et al. (2018b). Worker Collaboration Type 1 also reveals an outstanding improvement in the three corners of the figure. It performs badly on throughput, however, compared with cellular bucket brigades when the cellular bucket brigades' converge condition is satisfied (central part of the figure). Unlike Worker Collaboration Type 1, Model 2 shows its potential to be a superior alternative to cellular bucket brigades regardless of the condition of the stages. In the central part of Figure 2-22(b), the cellular bucket brigade achieves higher throughput than Model 2 due to the reduced collaborative coefficient, but Model 2 still outperforms cellular bucket brigades on the figure's three angles.

2.6 Summary

In this chapter, we discussed the Worker Collaboration Type 1 proposed by Pratama et al. (2018b) from two perspectives. One focused on the details of the model; Model 1 was proposed to deal with the worker arrangement and buffer-use rate problem for certain steps in Worker Collaboration Type 1. The other one came from a more macro-perspective; Model 2 was presented to mitigate the time wasted on unproductive behavior in the whole of Worker Collaboration Type 1. Both proposed models exhibit considerably improved throughput compared to the existing models when the conditions are satisfied.

Based on our analysis, managers can use these results directly to improve productivity in real implementations. If $Conditions\ 1\ or\ 2$ are satisfied, Model 1 shows a higher priority as a replacement for cellular bucket brigades compared to Worker Collaboration Type 1. Model 2 is a better alternative to cellular bucket brigades than Worker Collaboration Type 1 when the time cost of unproductive behaviors includes non-negligible parts of the cycle time. Moreover, if managers select Model 1 or 2 as a production line, $Methods\ 1\ and\ 2$ can help them assign the work content among the workstations. Additionally, $Method\ 3$ provides an area distribution figure of the best worker sequence for Model 2. According to this figure, managers can arrange the worker sequence quickly.

Ideally, we want a condition in which the collaborative coefficient α has a large value—in other words, where the job is suitable to be handled individually and collaboratively. This kind of job should be flexible enough to be processed by one or two workers at the different production steps. The work zone for the workers in the production line needs to be spacious enough for two workers to work at the same position and time.

Models 1 and 2 are both designed for a two-worker and three-workstation U-shaped production line. If the number of workstations is more than three, which indicates that some stages may contain two or more workstations, Models 1 and 2 cannot eliminate the blocking and halting within a stage. This is because the collaborative behavior capable of eliminating the blocking and halting starts only after one worker gets to the end of a stage. To reduce the effect of the blocking and halting, we can refer to the collaborative model proposed by Pratama et al. (2018b), where workers start collaboration when one worker arrives at the end of a workstation in a straight production line. The straight production line could be thought of as a stage for Models 1 and 2. If the number of workers is more than two, two or more workers could start with collaboration to separate them into two groups; then, Models 1 and 2 can be applied. This tentative ideal, however, is not appropriate for some situations because it leads to too many workers collaborating with each other after one group of workers finishes their item at the end of a stage. Revising Models 1 and 2 for cases of more than two workers and three workstations would be an interesting topic for future research.

Appendix

The Appendix includes the proofs for all the conclusions that appear in the main body of the chapter. In this section, the assumptions for the proofs are limited by Section 2.1: Model Definitions.

A.1 Location of Maximum Throughput Point for Model 1

The maximum throughput only appears at one of the crossing points.

Proof:

For Region 1:

$$X_1 = V_{23} * \frac{S_1}{V_{11}} + S_1 + S_2, X_2 = V_{22} * \frac{S_1}{V_{11}} + S_1$$

$$CT = 2\frac{S_1}{V_{11}} + \frac{1-X_1}{\alpha*(V_{13}+V_{23})} + + \frac{S_1+S_2-X_2}{\alpha*(V_{12}+V_{22})} + \frac{S_2}{\alpha*(V_{12}+V_{22})} + \frac{S_3}{\alpha*(V_{13}+V_{23})}, TH = \frac{2}{CT}.$$

$$\frac{\partial TH}{\partial S_1} = \frac{2*\left(\frac{1}{\alpha*(V_{12}+V_{22})} - \frac{2}{V_{11}} + \frac{\frac{V_{22}}{V_{11}}+1}{\alpha*(V_{12}+V_{22})} + \frac{V_{23}}{\alpha*V_{11}(V_{13}+V_{23})}\right)}{CT^2},$$

$$\frac{\partial TH}{\partial S_3} = \frac{2*\left(\frac{2}{\alpha*(V_{12}+V_{22})} - \frac{2}{\alpha*(V_{13}+V_{23})}\right)}{CT^2}.$$

For Region 2:

$X_1 = V_{11} * \frac{S_3}{V_{23}}, X_2 = V_{22} * \frac{S_1}{V_{11}} + S_1$

$CT = \frac{S_3}{V_{23}} + \frac{S_1 - X_1}{\alpha*(V_{11}+V_{21})} + \frac{S_1}{V_{11}} + \frac{S_1+S_2-X_2}{\alpha*(V_{12}+V_{22})} + \frac{S_2}{\alpha*(V_{12}+V_{22})} + \frac{S_3}{\alpha*(V_{13}+V_{23})}, TH = \frac{2}{CT}.$

$$\frac{\partial TH}{\partial S_1} = -\frac{2*\left(\frac{1}{\alpha*(V_{11}+V_{21})} - \frac{1}{\alpha*(V_{12}+V_{22})} + \frac{1}{V_{11}} - \frac{\frac{V_{22}}{V_{11}}+1}{\alpha*(V_{12}+V_{22})}\right)}{CT^2},$$

$$\frac{\partial TH}{\partial S_3} = \frac{2*\left(\frac{2}{\alpha*(V_{12}+V_{22})} - \frac{1}{\alpha*(V_{13}+V_{23})} - \frac{1}{v23} + \frac{V_{11}}{\alpha*V_{23}(V_{11}+V_{21})}\right)}{CT^2}.$$

For Region 3:

$X_1 = V_{23} * \frac{S_1}{V_{11}} + S_1 + S_2, X_2 = V_{11} * \frac{S_2}{V_{22}}$

$CT = \frac{S_1}{V_{11}} + \frac{1-X_1}{\alpha*(V_{13}+V_{23})} + \frac{S_2}{V_{22}} + \frac{S_1 - X_2}{\alpha*(V_{11}+V_{21})} + \frac{S_2}{\alpha*(V_{12}+V_{22})} + \frac{S_3}{\alpha*(V_{13}+V_{23})}, TH = \frac{2}{CT}.$

$$\frac{\partial TH}{\partial S_1} = \frac{2*\left(\frac{1}{\alpha*(V_{12}+V_{22})} - \frac{1}{V_{11}} + \frac{1}{V_{22}} - \frac{\frac{V_{11}}{V_{22}}+1}{\alpha*(V_{11}+V_{21})} + \frac{V_{23}}{\alpha*V_{11}(V_{13}+V_{23})}\right)}{CT^2},$$

$$\frac{\partial TH}{\partial S_3} = \frac{2*\left(\frac{1}{\alpha*(V_{12}+V_{22})} - \frac{2}{\alpha*(V_{13}+V_{23})} + \frac{1}{V_{22}} - \frac{V_{11}}{\alpha*V_{22}(V_{11}+V_{21})}\right)}{CT^2}.$$

For Region 4:

$X_1 = V_{11} * \frac{S_3}{V_{23}}, X_2 = V_{11} * \frac{S_2}{V_{22}}$

$CT = \frac{S_3}{V_{23}} + \frac{S_1 - X_1}{\alpha*(V_{11}+V_{21})} + \frac{S_2}{V_{22}} + \frac{S_1 - X_2}{\alpha*(V_{11}+V_{21})} + \frac{S_2}{\alpha*(V_{12}+V_{22})} + \frac{S_3}{\alpha*(V_{13}+V_{23})}, TH = \frac{2}{CT}.$

$$\frac{\partial TH}{\partial S_1} = \frac{2*\left(-\frac{1}{\alpha*(V_{11}+v21)} + \frac{1}{\alpha*(V_{12}+V_{22})} + \frac{1}{V_{22}} - \frac{\frac{V_{11}}{V_{22}}+1}{\alpha*(V_{11}+V_{21})}\right)}{CT^2},$$

$$\frac{\partial TH}{\partial S_3} = \frac{2*\left(\frac{1}{\alpha*(V_{12}+V_{22})} - \frac{1}{\alpha*(V_{13}+V_{23})} + \frac{1}{V_{22}} - \frac{1}{V_{23}}\right)}{CT^2} + \frac{2*\left(-\frac{v11}{\alpha*V_{22}(V_{11}+V_{21})} + \frac{V_{11}}{\alpha*V_{23}(V_{11}+v21)}\right)}{CT^2}.$$

In the four regions, the differentiations of the throughput function TH remain large/less than 0 (or equal to 0) since the denominators are always larger than 0 (it is the square of cycle time) and the numerators are constants. In other words, the throughput functions at the four regions are monotonic with S_1 and S_3. Therefore, the maximum throughput only appears at one of the crossing points.

A.2 The Condition for Model 1 is Better than Worker Collaboration Type 1

$Condition$ 1 is the condition of Model 1's being better than Worker Collaboration Type 1. If $\alpha = 1$, $Condition$ 1 can be simplified as $Condition$ 2.

$Condition\ 1: \frac{V_{22}}{V_{12}+V_{22}} + \frac{V_{13}}{V_{13}+V_{23}} < \alpha$

$Condition\ 2$: $\frac{V_{13}*V_{22}}{V_{12}*V_{23}} < 1$

Proof:

Model 1 and Worker Collaboration Type 1 have the same operating principle from Step 1 to Step 4. In their different parts, Model 1 should take less time than Worker Collaboration Type 1. The behavior of workers in Worker Collaboration Type 1 has two different cases, which depend on who arrives at the end of the stages faster.

In $Case$ 1, W_1 reaches the end of S_3 before W_2 at S_2 as shown in Figure 2-23(b).

***Case* 1:**

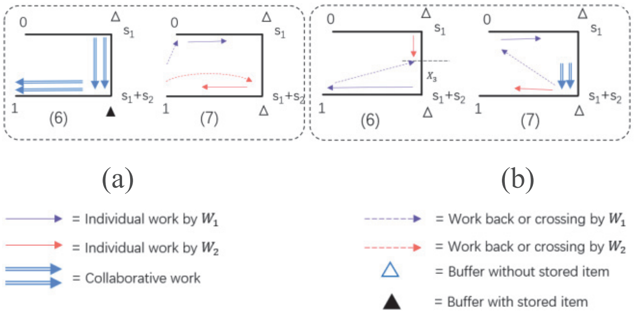

Figure 2-23 Operating principle of Model 1 and Worker Collaboration Type 1 in steps 5 and 6 ($Case$ 1).

$$X_3 = V_{22}\frac{S_3}{V_{13}} + S_1$$

$$\frac{S_2}{\alpha(V_{12}+V_{22})} + \frac{S_3}{\alpha(V_{13}+V_{23})} < \frac{S_3}{V_{13}} + \frac{S_1+S_2-X_3}{\alpha(V_{12}+V_{22})}$$

Simplifying the above inequality, we get Inequality (1):

$$\frac{V_{22}}{V_{12}+V_{22}} + \frac{V_{13}}{V_{13}+V_{23}} < \alpha \qquad (1)$$

***Case* 2:**

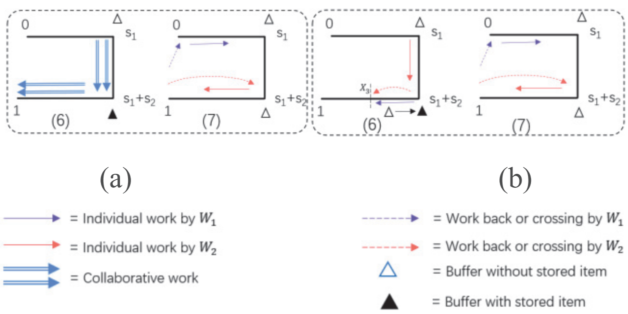

Figure 2-24 Operating principle of Model 1 and Worker Collaboration Type 1 in steps 5 and 6 ($Case$ 2).

In $Case$ 2, W_1 finishes the work contents of S_3 later than W_2 at S_2, as shown in Figure 2-24(b).

$X_3 = V_{13}\frac{S_2}{V_{22}} + S_1 + S_2$

$\frac{S_2}{\alpha(V_{12}+V_{22})} + \frac{S_3}{\alpha(V_{13}+V_{23})} < \frac{S_2}{V_{22}} + \frac{1-X_3}{\alpha(V_{13}+V_{23})}$

Simplifying the above inequality, we get Inequality (2):

$$\frac{V_{22}}{V_{12}+V_{22}} + \frac{V_{13}}{V_{13}+V_{23}} < \alpha \qquad (2)$$

$Inequalities$ 1 and 2 are the same. Therefore, the condition for Model 1 being better than Worker Collaboration Type 1 is $\frac{V_{22}}{V_{12}+V_{22}} + \frac{V_{13}}{V_{13}+V_{23}} < \alpha.$

Let $\alpha = 1$ in $Inequality$ 2; then we can get $Inequality$ 3, which is the condition for Model 1 being better than Worker Collaboration Type 1 when $\alpha = 1$.

$$\frac{V_{13}*V_{22}}{V_{12}*V_{23}} < 1 \qquad (3)$$

A.3 Location of Maximum Throughput Point for Model 2

The maximum throughput only appears at one of the crossing points in the throughput figure.

Proof:

For $Region$ 1:

$S_2 = 1 - S_1 - S_3, X_1 = V_{22}\frac{S_1}{V_{11}} + S_1,$

$CT = \frac{S_1}{V_{11}} + \frac{S_1+S_2-X_1}{\alpha*(V_{12}+V_{22})} + \frac{S_3}{\alpha*(V_{13}+V_{23})}, TH = \frac{1}{CT}.$

$\frac{\partial TH}{\partial S_1} = \frac{\frac{\frac{V_{22}}{V_{11}}+1}{\alpha*(V_{12}+V_{22})} - \frac{1}{V_{11}}}{CT^2}.$

$\frac{\partial TH}{\partial S_3} = \frac{\frac{1}{\alpha*(V_{12}+V_{22})} - \frac{1}{\alpha*(V_{13}+V_{23})}}{CT^2}.$

Because $CT^2 > 0$, $\frac{\frac{V_{22}}{V_{11}}+1}{\alpha*(V_{12}+V_{22})} - \frac{1}{V_{11}}$ and $\frac{1}{\alpha*(\mathrm{v12}+\mathrm{v22})} - \frac{1}{\alpha*(v13+v23)}$ are constants, in $Region$ 1 the function TH is monotonic for S_1 and S_3.

For $Region$ 2:

$S_2 = 1 - S_1 - S_3, X_2 = V_{11}\frac{S_2}{V_{22}},$

$CT = \frac{S_2}{V_{22}} + \frac{S_1-X_2}{\alpha*(V_{11}+V_{21})} + \frac{S_3}{\alpha*(V_{13}+V_{23})}, TH = \frac{1}{CT},$

$$\frac{\partial TH}{\partial S_1} = \frac{\frac{1}{V_{22}} - \frac{\frac{V_{11}}{V_{22}}+1}{\alpha*(V_{11}+V_{21})}}{CT^2}.$$

$$\frac{\partial TH}{\partial S_3} = \frac{\frac{1}{V_{22}} - \frac{1}{\alpha*(V_{13}+V_{23})} - \frac{V_{11}}{\alpha*V_{22}*(V_{11}+V_{21})}}{CT^2}.$$

Since $CT^2 > 0$, $\frac{1}{V_{22}} - \frac{\frac{V_{11}}{V_{22}}+1}{\alpha*(V_{11}+V_{21})}$ and $\frac{1}{V_{22}} - \frac{1}{\alpha*(V_{13}+V_{23})} - \frac{V_{11}}{\alpha*V_{22}*(V_{11}+V_{21})}$ are constants, in $Region\ 2$, the function TH is also monotonic for $S_1\ and\ S_3$.

The throughput functions TH are monotonic for $S_1\ and\ S_3$ in both $Regions\ 1\ and\ 2$. Therefore, the maximum throughput only appears at one of the crossing points.

A.4 Combination of Sequences AB and BA

All the combinations of $Sequences\ AB\ and\ BA$ are $C1C1, C1C2, C2C1\ and\ C2C2$. Some conclusions can be drawn about the combinations:

1. Only one relative difference figure contains three combinations, which are $C1C1, C2C2, and\ C1C2/C2C1$.
2. $C1C2$ can happen with $\frac{V_{a1}}{V_{b2}} > \frac{V_{a1}}{V_{b2}}$.
3. $C2C1$ can happen with $\frac{V_{a1}}{V_{b2}} < \frac{V_{a1}}{V_{b2}}$.
4. The expression of the boundary that distinguishes $C1C1, C1C2,\ or\ C2C1, C2C2$ is $S_1 = \frac{1-S_3}{1+V_{a2}/V_{b1}}$.
5. The expression of the boundary that distinguishes $C1C2, C2C2, or\ C1C1, C2C1$ is $S_1 = \frac{1-S_3}{1+V_{b2}/V_{a1}}$.

Proof:

To make the $Sequences\ AB$ and BA belong to $Case\ 1\ and\ Case\ 2$, respectively, before the first collaboration, W_1 should finish his/her job faster than W_2 for $Sequence\ AB$, while, for $Sequence\ BA$, W_1 should finish his/her job later than W_2. The formula is described as follows:

$$\frac{S_1}{V_{a1}} < \frac{S_2}{V_{b2}}\ and\ \frac{S_1}{V_{b1}} > \frac{S_2}{V_{a2}}$$

Transfer the above inequality to the following:

$$S_1 < \frac{V_{a1}}{V_{b2}} S_2\ and\ S_1 > \frac{V_{b1}}{V_{a2}} S_2$$

The set of S_1 should not be empty. Therefore, we need to let $\frac{V_{a1}}{V_{b2}} > \frac{V_{b1}}{V_{a2}}$.

The case distribution for S_1 is shown in Figure 2-25(a). According to $S_2 = 1 - S_1 - S_3$, Figure 2-25(b) is obtained.

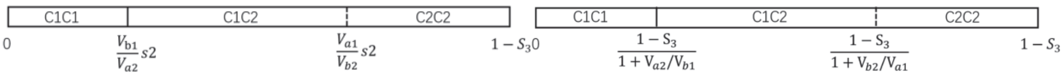

(a) (b)

Figure 2-25 Distribution of cases for S_1 with $C1C2$.

If we let $Sequence\ AB$ belong to $Case$ 2 and BA belong to $Case$ 1, the velocity conditions and case distribution can be obtained as follows:

$\frac{S_1}{V_{a1}} > \frac{S_2}{V_{b2}}$ and $\frac{S_1}{V_{b1}} < \frac{S_2}{V_{a2}}$

Transfer the above inequality to the following:

$S_1 > \frac{V_{a1}}{V_{b2}} S_2$ and $S_1 < \frac{V_{b1}}{V_{a2}} S_2$

The set of S_1 should not be empty.

Then, we get $\frac{V_{a1}}{V_{b2}} < \frac{V_{b1}}{V_{a2}}$.

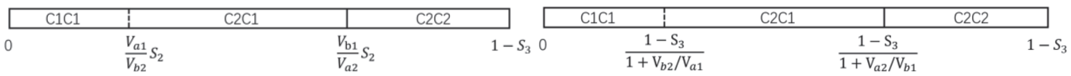

(a) (b)

Figure 2-26 Distribution of cases for S_1 with $C2C1$.

Therefore, only three combinations of cases are shown in the relative difference figure. If $\frac{V_{a1}}{V_{b2}} > \frac{V_{a1}}{V_{b2}}$, $C1C2$ appears; otherwise, $C2C1$ appears. The expressions of the $Solid\ and\ Dashed\ boundaries$ are $S_1 = \frac{1-S_3}{1+V_{a2}/V_{b1}}$ and $S_1 = \frac{1-S_3}{1+V_{b2}/V_{a1}}$, respectively.

A.5 The Best Worker Sequence ($\alpha = 1$)

The condition for the best worker sequence where AB ($\alpha = 1$) is

$$\frac{V_{a1}}{V_{a2}} > \frac{V_{b1}}{V_{b2}}$$

Proof:

Suppose the velocities of $Workers\ A\ and\ B$ are given as $V_{a1}, V_{a2}, V_{a3}, V_{b1}, V_{b2}, and\ V_{b3}$, and the collaborative coefficient $\alpha = 1$.

Since the best sequence is AB, the cycle time of $Sequence\ AB$ should be less than $Sequence\ BA$.

$$CT_{AB} < CT_{BA}$$

There are four different combinations of $Sequences\ AB\ and\ BA$ in Model 2, namely $C1C1, C2C2, C1C2, or\ C2C1$:

(1) $AB\ and\ BA$ both belong to $Case\ 1(C1C1)$

$$\frac{S_1}{V_{a1}} + \frac{1}{\alpha(V_{a2} + V_{b2})}\left(S_2 - \frac{S_1}{V_{a1}}V_{b2}\right) < \frac{S_1}{V_{b1}} + \frac{1}{\alpha(V_{a2} + V_{b2})}\left(S_2 - \frac{S_1}{V_{b1}}V_{a2}\right)$$

Simplifying the above inequality, we get $Inequality\ 4$:

$$\frac{V_{a1}}{V_{a2}} > \frac{V_{b1}}{V_{b2}} \tag{4}$$

(2) $AB\ and\ BA$ both belong to $Case\ 2(C2C2)$

$$\frac{S_2}{V_{b2}} + \frac{1}{\alpha(V_{a1}+V_{b1})}\left(S_1 - \frac{S_2}{V_{b2}}V_{a1}\right) < \frac{S_2}{V_{a2}} + \frac{1}{\alpha(V_{a1}+V_{b1})}\left(S_1 - \frac{S_2}{V_{a2}}V_{b1}\right)$$

Simplifying the above inequality, we get $Inequality\ 5$:

$$\frac{V_{a1}}{V_{a2}} > \frac{V_{b1}}{V_{b2}} \tag{5}$$

(3) AB, BA belong to $Case\ 1\ and\ Case\ 2$, respectively ($C1C2, \frac{V_{a1}}{V_{a2}} > \frac{V_{b1}}{V_{b2}}$)

$$\frac{S_1}{V_{a1}} + \frac{1}{\alpha(V_{a2}+V_{b2})}\left(S_2 - \frac{S_1}{V_{a1}}V_{b2}\right) < \frac{S_2}{V_{a2}} + \frac{1}{\alpha(V_{a1}+V_{b1})}\left(S_1 - \frac{S_2}{V_{a2}}V_{b1}\right)$$

Simplifying the above inequality, we get $Inequality\ 6$:

$$S_1 > -\frac{V_{a1}}{V_{a2}}S_2 \tag{6}$$

(4) AB, BA belong to $Case\ 2\ and\ Case\ 1$, respectively ($C2C1, \frac{V_{a1}}{V_{a2}} > \frac{V_{b1}}{V_{b2}}$)

$$\frac{S_2}{V_{b2}} + \frac{1}{\alpha(V_{a1} + V_{b1})}\left(S_1 - \frac{S_2}{V_{b2}}V_{a1}\right) < \frac{S_1}{V_{b1}} + \frac{1}{\alpha(V_{a2} + V_{b2})}\left(S_2 - \frac{S_1}{V_{b1}}V_{a2}\right)$$

Simplifying the above inequality, we get $Inequality\ 7$:

$$S_1 > -\frac{V_{b1}}{V_{b2}}S_2 \tag{7}$$

In $Inequalities\ 6\ and\ 7$, $Sequence\ AB$ performs better than BA, S_1 should be larger than a negative, and this condition is always satisfied since $0 < S_1 < 1$. Therefore, to get the best sequence for Model 2, we need only compare the ratio of $Worker\ A\ and\ WorkerB$ velocities in Stages 1 and 2.

A.6 Conditions 5, 6, and Red Boundary

Suppose $Sequence\ AB$ is the best worker sequence. Then, the cycle time of $Sequence\ AB$ should be less than $Sequence\ BA$. The formula is expressed as

$$CT_{AB} < CT_{BA}$$

By simplifying the above inequality, the following results are derived.

(1) $Sequences\ AB\ and\ BA$ both belong to $Case\ 1\ (C1C1)$

$\frac{\alpha(V_{a2}+V_{b2})-V_{b2}}{V_{a1}} < \frac{\alpha(V_{a2}+V_{b2})-V_{a2}}{V_{b1}}$ $(Condition\ 5)$

(2) $Sequences\ AB\ and\ BA$ both belong to $Case\ 2\ (C2C2)$

$\frac{\alpha(V_{a1}+V_{b1})-V_{a1}}{V_{b2}} < \frac{\alpha(V_{a1}+V_{b1})-V_{b1}}{V_{a2}}$ $(Condition\ 6)$

(3) $Sequences\ AB\ and\ BA$ belong to $Cases$ 1 and 2, respectively ($C1C2, \frac{V_{b1}}{V_{a2}} < \frac{V_{a1}}{V_{b2}}$)

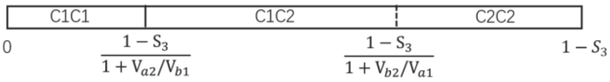

$\frac{S_1(\alpha*V_{a2}+\alpha*V_{b2}-V_{b2})+V_{a1}*S_2}{V_{a1}(V_{a2}+V_{b2})} < \frac{S_2\ (\alpha*V_{a1}+\alpha*V_{b1}-V_{b1})+V_{a2}*S_1}{V_{a2}(V_{a1}+V_{b1})}.$

(4) $Sequences\ AB\ and\ BA$ belong to $Case$ 2 and 1, respectively ($C2C1, \frac{V_{b1}}{V_{a2}} > \frac{V_{a1}}{V_{b2}}$)

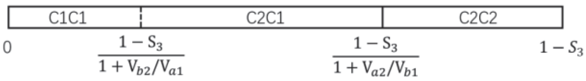

$\frac{S_2(\alpha*V_{a1}+\alpha*V_{b1}-V_{a1})+S_1*V_{b2}}{\alpha*V_{b2}(V_{a1}+V_{b1})} < \frac{S_1(\alpha*V_{a2}+\alpha*V_{b2}-V_{a2})+S_2*V_{b1}}{\alpha*V_{b1}(V_{a2}+V_{b2})}.$

In illustrations (3) and (4), let $CT_{AB} = CT_{BA}$. Then, we have
$Red\ boundary$ 1:

$$S_3 = \left(-\frac{\frac{1}{V_{a1}}-\frac{1}{(V_{a1}+V_{b1})\alpha}-\frac{V_{b2}}{V_{a1}(V_{a2}+V_{b2})\alpha}}{\frac{1}{V_{a2}}-\frac{1}{(V_{a2}+V_{b2})\alpha}-\frac{V_{b1}}{V_{a2}(V_{a1}+V_{b1})\alpha}} - 1\right)S_1 + 1,$$

$Red\ boundary$ 2:

$$S_3 = \left(-\frac{\frac{1}{(V_{a1}+V_{b1})\alpha}-\frac{-V_{a2}+V_{a2}\alpha+V_{b2}\alpha}{V_{b1}(V_{a2}+V_{b2})\alpha}}{\frac{1}{(V_{a2}+V_{b2})\alpha}-\frac{-V_{a1}+V_{a1}\alpha+V_{b1}\alpha}{V_{b2}(V_{a1}+V_{b1})\alpha}} - 1\right)S_1 + 1.$$

A.7 **Lemma 1**

$Lemma$ 1. As S_1 increases, and the absolute value of the relative difference function RD increases in $Region\ C1C1$ and decreases in $Region\ C2C2$. ($\frac{1}{V_{a1}} - \frac{1}{V_{b1}} - \frac{\frac{V_{b2}}{V_{a1}}-\frac{V_{a2}}{V_{b1}}}{\alpha*(V_{a2}+V_{b2})} \neq 0\ and\ \frac{1}{V_{b2}} - \frac{1}{V_{a2}} - \frac{\frac{V_{a1}}{V_{b2}}-\frac{V_{b1}}{V_{a2}}}{\alpha*(V_{a1}+V_{b1})} \neq 0$)

Proof:
For $Region\ C1C1$:

$RD_{C1C1} = \frac{TH_{AB}-TH_{BA}}{TH_{BA}} \times 100\%.$

$Sequence\ AB$:

$X_{1AB} = V_{b2} * \left(\frac{S_1}{V_{a1}}\right) + S_1,$

$CT_{AB} = \frac{S_1}{V_{a1}} + \frac{S_1+S_2-X_{1AB}}{\alpha*(V_{a2}+V_{b2})} + \frac{S_3}{\alpha*(V_{a3}+V_{b3})}, TH_{AB} = \frac{1}{CT_{AB}}$

Sequence BA:

$X_{1BA} = V_{a2} * \left(\frac{S_1}{V_{b1}}\right) + S_1,$

$CT_{BA} = \frac{S_1}{V_{b1}} + \frac{S_1+S_2-X_{1BA}}{\alpha*(V_{a2}+V_{b2})} + \frac{S_3}{\alpha*(V_{a3}+V_{b3})}, TH_{BA} = \frac{1}{CT_{BA}}$

$CT_{AB} - CT_{BA} = S_1\left(\frac{1}{V_{a1}} - \frac{1}{vV_1} - \frac{\frac{V_{b2}}{V_{a1}} - \frac{V_{a2}}{V_{b1}}}{\alpha*(V_{a2}+V_{b2})}\right).$

$\frac{1}{V_{a1}} - \frac{1}{V_1} - \frac{\frac{V_{b2}}{V_{a1}} - \frac{V_{a2}}{V_{b1}}}{\alpha*(V_{a2}+V_{b2})}$ is a constant. Therefore, in $Region\ C1C1$, as S_1 increases ($\frac{1}{V_{a1}} - \frac{1}{V_1} - \frac{\frac{V_{b2}}{V_{a1}} - \frac{V_{a2}}{V_{b1}}}{\alpha*(V_{a2}+V_{b2})} \neq 0$), the absolute value of the relative difference increases.

For $Region\ C2C2$:

$RD_{C2C2} = \frac{TH_{AB}-TH_{BA}}{TH_{BA}} \times 100\%.$

Sequence AB:

$X_{1AB} = V_{a1}\left(\frac{S_2}{V_{b2}}\right),$

$CT_{AB} = \frac{S_2}{V_{b2}} + \frac{S_1-X_{1AB}}{\alpha(V_{a1}+V_{b1})} + \frac{S_3}{\alpha(V_{a3}+V_{b3})}, TH_{AB} = \frac{1}{CT_{AB}}$

Sequence BA:

$X_{2BA} = V_{b1}\left(\frac{S_2}{V_{a2}}\right),$

$CT_{BA} = \frac{S_2}{V_{a2}} + \frac{S_1-X_{2BA}}{\alpha*(V_{a1}+V_{b1})} + \frac{S_3}{\alpha*(V_{a3}+V_{b3})}, TH_{BA} = \frac{1}{CT_{BA}}$

$CT_{AB} - CT_{BA} = (1 - S_1 - S_3)\left(\frac{1}{V_{b2}} - \frac{1}{V_{a2}} - \frac{\frac{V_{a1}}{V_{b2}} - \frac{V_{b1}}{V_{a2}}}{\alpha*(V_{a1}+V_{b1})}\right).$

$\frac{1}{V_{b2}} - \frac{1}{V_{a2}} - \frac{\frac{V_{a1}}{V_{b2}} - \frac{V_{b1}}{V_{a2}}}{\alpha*(V_{a1}+V_{b1})}$ is also a constant. Therefore, in $Region\ C2C2$, as S_1 increases ($\frac{1}{V_{b2}} - \frac{1}{V_{a2}} - \frac{\frac{V_{a1}}{V_{b2}} - \frac{V_{b1}}{V_{a2}}}{\alpha*(V_{a1}+V_{b1})} \neq 0$), the absolute value of the relative difference decreases.

A.8 Lemma 2

Lemma 2. The relative difference function RD is continuous in the relative difference figure.

Proof:

For a throughput figure of Model 2, let positive number ρ be close to 0. Take any point (S_1, S_3, TH) from the boundary $S_1 = \frac{V_{11}}{V_{22}} S_2$. Then, for $Region\ 1$, we have $(S_1 - \rho, S_3, TH_a)$, and $(S_1 + \rho, S_3, TH_b)$ for $Region\ 2$, as shown in Figure 2-27.

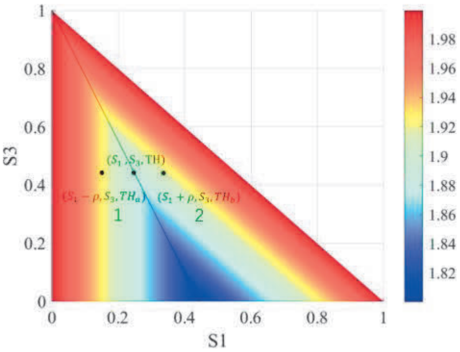

Figure 2-27 Throughput of Model 2.

For TH_a:

$S_{1a} = S_1 - \rho, S_{2a} = S_2 + \rho, X_1 = V_{22}\frac{S_{1a}}{V_{11}} + S_{1a},$

$CT_a = \frac{S_{1a}}{V_{11}} + \frac{S_{1a}+S_{2a}-X_1}{\alpha(V_{12}+V_{22})} + \frac{S_3}{\alpha(V_{13}+V_{23})}, \mathrm{TH_a} = \frac{1}{CT_a}.$

For TH_b:

$S_{1b} = S_1 + \rho, S_{2b} = S_2 - \rho, X_2 = V_{11}\frac{S_{2b}}{V_{22}},$

$CT_b = \frac{S_{2b}}{V_{22}} + \frac{S_{1b}-X_2}{\alpha(V_{11}+V_{21})} + \frac{S_3}{\alpha(V_{13}+V_{23})}, TH_b = \frac{1}{CT_b}.$

Therefore,

$$CT_a - CT_b = \frac{\rho}{V_{22}} - \frac{\rho}{V_{11}} + \frac{\rho + \frac{V_{22}*\rho}{V_{11}}}{\alpha(V_{12}+V_{22})} - \frac{\rho + \frac{V_{11}*\rho}{v22}}{\alpha(V_{11}+V_{21})} = 0.$$

Then, we get $TH_a - TH_b = 0$ since $TH = \frac{1}{CT}$.

For the boundary $S_1 = \frac{V_{11}}{V_{22}}S_2$,

$CT = \frac{S_1}{V_{11}} + \frac{S_3}{\alpha(V_{13}+V_{23})},$

$$CT_a - CT = \frac{S_1-\rho}{V_{11}} + \frac{\rho + S_2 + \frac{V_{22}(\rho - S_1)}{V_{11}}}{\alpha(V_{12}+V_{22})} - \frac{S_1}{V_{11}}.$$

Simplifying the above equality, we get

$$CT_a - CT = -\frac{\rho}{V_{11}} + \frac{\rho + \frac{V_{22}*\rho}{V_{11}}}{\alpha(V_{12}+V_{22})} = 0.$$

Then, we get $TH_a - TH = 0$ since $TH = \frac{1}{CT}$.

Because $\lim_{\rho\to 0} TH(S_1 - \rho) = \lim_{\rho\to 0} TH(S_1 + \rho) = TH(S_1)$, the throughput figure of Model 2 is continuous at the boundary $S_1 = \frac{V_{11}}{V_{22}}S_2$. Therefore, the throughput functions of the proposed model are continuous in the entire throughput figure.

Since all parameters of the relative difference function ($RD = \frac{TH_{AB} - TH_{BA}}{TH_{BA}} * 100\%$) are throughputs, the relative difference function RD is also continuous in the relative difference figure.

A.9 Conclusion 1

When the $Solid\ boundary$ and $Dashed\ boundary$ coincide with each other, the entire relative difference figure shows one kind of area.

Proof:

Suppose $Region\ 1$ is increased in area, and the $Solid\ boundary\ and\ Dashed\ boundary$ coincide with each other, as shown in Figure 2-28.

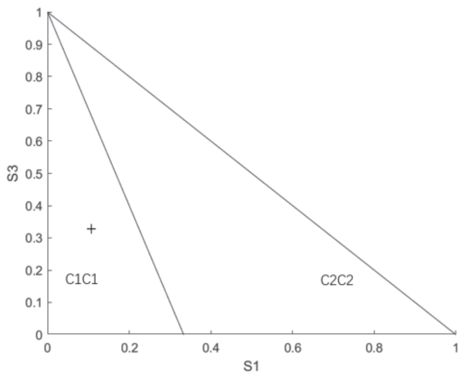

Figure 2-28 Distribution of increased (+) and decreased areas (-) for Conclusion 1.

$Region\ C2C2$ should not be either decreased or a zero area. Since $Region\ C1C1$ is continuous with $Region\ C2C2$ ($Lemma\ 2$) , and as S_1 increases, the absolute value of the relative difference function RD increases in $Region\ C1C1$ ($Lemma\ 1$).

Additionally, if $Region\ 1$ is decreased in area, a similar conclusion is obtained. Therefore, the entire relative difference figure shows only one kind of area.

A.10 Conclusion 2

When the $Red\ boundary$ is located in $Region\ C1C2/C2C1$, the increased/decreased part of $Region\ C1C2/C2C1$ is adjacent to the other region's increased/decreased part.

Proof:

Suppose $Region\ C1C1$ is increased in area, $Region\ C2C2$ is decreased in area, and the $Red\ boundary$ is located in $Region\ C1C2/C2C1$, as shown in Figure 2-29.

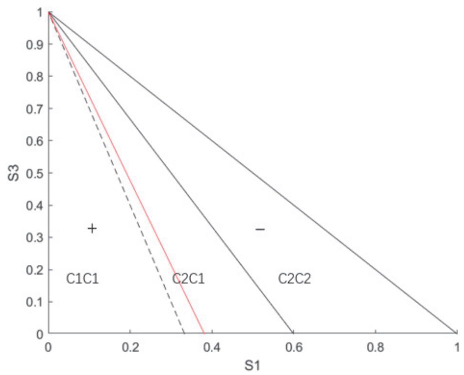

Figure 2-29 Distribution of increased (+) and decreased areas (-) for Conclusion 2.

Then, according to $Lemma$ 1, the relative difference increases as S_1 increases in $Region\ C1C1$. Additionally, the relative difference decreases as S_1 decreases in $Region\ C2C2$. This indicates that the relative difference located at the $Dashed\ boundary$ is a positive value, and the relative difference located at the $Solid\ boundary$ is a negative value.

Next, according to $Lemma$ 2, $Region\ C1C1$ is continuous with $Region\ C2C1$, and $Region\ C2C1$ is continuous with $Region\ C2C2$. Therefore, the left part of the $Red\ boundary$ in $Region\ C2C1$ should be an increased area and the right part should be a decreased area.

If $Region\ C1C1$ is decreased in area and $Region\ C2C2$ is increased in area, a similar conclusion will be obtained.

A.11 Conclusion 3

When the $Red\ boundary$ is beyond $Region\ C1C2/C2C1$, if $Regions\ C1C1\ and\ C2C2$ are the same kind of area, $Region\ C1C2/C2C1$ is the same as other regions. Otherwise, $Region\ C1C2/C2C1$ is the same as the non-zero region.

Proof:

Suppose $Region\ C1C1$ is increased in area, $Region\ C2C2$ is decreased in area, and the $Red\ boundary$ is beyond $Region\ C1C2/C2C1$, as shown in Figure 2-30.

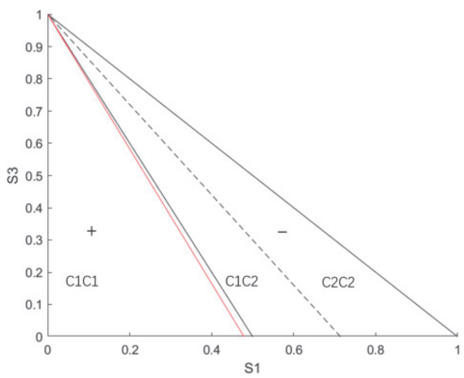

Figure 2-30 Distribution of increased (+) and decreased areas (-) for Conclusion 3.

If $Region\ C1C2$ is increased in area, it is not continuous with $Region\ C2C2$. This situation violates $Lemma\ 2$. If $Region\ C1C2$ is decreased in area, it is not continuous with $Region\ C1C1$. This situation also violates $Lemma\ 2$. Therefore, the increased and decreased areas should not both appear in the same figure. This indicates that $Regions\ C1C1\ and\ C2C2$ should be the same or that one of them is a zero area ($\frac{1}{V_{a1}} - \frac{1}{V_{b1}} - \frac{\frac{V_{b2}}{V_{a1}} - \frac{V_{a2}}{V_{b1}}}{\alpha * (V_{a2} + V_{b2})} = 0\ or\ \frac{1}{V_{b2}} - \frac{1}{V_{a2}} - \frac{\frac{V_{a1}}{V_{b2}} - \frac{V_{b1}}{V_{a2}}}{\alpha * (V_{a1} + V_{b1})} = 0$). In these cases, according to $Lemmas\ 1\ and\ 2$, $Conclusion\ 3$ is obtained.

Chapter 3 Bucket Brigade for Order Picking System with Order Batching

3.1 Introduction

The concept of the *bucket brigade*, inspired by the Toyota Sewn Production Management System (TSS), has found applications in manufacturing and warehousing due to its efficiency in labor-intensive scenarios (Granotto et al., 2019). Bartholdi and Eisenstein were the first to study this concept and found that it dynamically arranges human labor and workload without requiring management intervention. The maximum possible production rate can be achieved by applying this concept compared to various other methods of organizing workers and workstations (Bartholdi & Eisenstein, 1996a). Several examples here demonstrate the improvements when companies implemented the bucket brigade concept: Revco Drug Stores (now CVS) increased pick rates by 34% in their national distribution center, pickers at Anderson Merchandisers increased production rates by 20% and reduced variance in pick rates by 90% in a two-week trial, and, in the Ford Customer Service Division, the most popular products were moved out of carousels and into flow racks, where they were picked by a bucket brigade, resulting in a pick rate increase of over 50% (Bartholdi & Eisenstein, 2006).

Although the bucket brigade concept demonstrates efficiency in manufacturing and warehousing, particularly for OPSs, it still faces some challenges that impede its performance. In this study we discuss two key issues. The first is small orders, which are commonplace in warehousing (Bahrami et al., 2019; Guo et al., 2021; Yu & De Koster, 2009). Small orders are known to significantly impair OPS efficiency because pickers must make many trips within the OPS to fulfill these orders. The second issue is the blocking delay. In a bucket brigade OPS, one picker is not allowed to pass another. If a picker needs to walk forward to pick the next items but the downstream picker is picking items nearby, blocking occurs in the bucket brigade OPS, resulting in a loss of efficiency.

To overcome the small-order problem, researchers have proposed various solution methods. One of the most widely used methods is order batching, which allocates small orders into several batches to fulfill multiple orders as one batch in a single trip (Gademann et al., 2001; Parikh & Meller, 2008; Xie et al., 2023). Hong et al. (2016) were the first to apply the order batching method to bucket brigade OPSs, considering identical pickers to handle situations with many small orders. Building on the work of Hong et al. (2016), Fibrianto and Hong (2019) introduced the Dynamic Indexed Batching Model for Bucket Brigades (DIBMB), which considered non-identical pickers. The DIBMB model batches orders by minimizing batch completion times. Accurately calculating completion times in the presence of non-identical pickers is challenging, however, due to the complexity of bucket brigade OPSs. Therefore, the DIBMB model develops formulas to estimate completion times. Nevertheless, errors between accurate and estimated results persist within the DIBMB model. These errors lead to the occurrence of blocking in bucket brigade OPSs, subsequently reducing operational efficiency.

In this study we propose the Balanced Batching Model for Bucket Brigade (BBMB) to reduce the blocking delay when the bucket brigade OPS with non-identical pickers process batched orders. According to Bartholdi and Eisenstein (1996b), the bucket brigade OPS achieves the highest efficiency when it is in a balance status, and the balanced distribution of work content in the OPS directly contributes to the system's balance. Notably, there is no blocking in a bucket brigade OPS when it is in the balance status. Based on these concepts, the BBMB model batches orders by balancing the work content in the picking line for the non-identical pickers.

Compared to the idea of developing formulas to calculate the completion time of batches, balancing work content for pickers is a simpler approach. Calculating completion times requires evaluating the time pickers spend on picking items, traveling within the OPS, and being blocked by others. In contrast, balancing work content only requires considering the contents of batches and the capabilities of pickers. Moreover, the BBMB model is less affected by errors. The calculation of batch-completion time is based on previous batches. This means that, if an error occurs in a calculation for one batch, it will affect the results of all subsequent batch calculations. Such a chain reaction does not exist in the BBMB model. The simulation experiment demonstrates that the BBMB model enhances the productivity of bucket brigade OPSs when handling a large volume of small orders.

3.2 Bucket Brigade Order Picking System and Order Batching

This section first introduces the layout of a typical bucket brigade OPS and explains the motion of pickers in processing orders within a bucket brigade OPS in Section 3.1. It then discusses the effect of small orders and the order batching method in Section 3.2. Finally, Section 3.3 introduces three types of time costs associated with pickers' motion: picking, walking, and blocking time costs. Particular emphasis is placed on the blocking time cost because it reduces OPS efficiency, and our goal is to propose a model to reduce it.

3.2.1 Bucket Brigade Order Picking Systems

Layout of a Bucket Brigade OPS

We consider the layout of a bucket brigade OPS adapted from Hong et al. (2016), as shown in Figure 3-1. Several items are stored in pick faces, and the different shapes indicate that they are listed in different orders. The number of items in each order and the location of the items follow a uniform distribution. A loading station (L) is located before the head of the pick faces, where empty totes are released. An unloading station (L) is set up behind the end of the pick faces, where the last picker unloads a tote that is full of picked items. These elements make up a picking line. Several pickers travel through the picking line, pick items from the pick faces, and place the picked items into totes. Each pick face allows only one picker to pick items, and pickers cannot pass over other pickers.

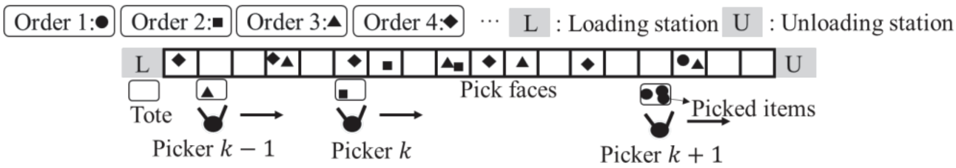

Figure 3-1 Layout of a typical bucket brigade OPS.

Operational Principle of Pickers and Pickers' Non-identical Picking Capability

Figure 3-2 illustrates the motion of pickers processing orders in a bucket brigade OPS. In Figure 3-2(a), two pickers pick items and move forward. Figure 3-2(b) shows Picker 2 walking backward to obtain another tote after unloading the filled tote at the unloading station. In Figure 3-2(c), when the two pickers meet, Picker 1 hands the tote to Picker 2, then walks backward to get another tote. Since there is no picker before Picker 1, instead of receiving a tote from an upstream picker, Picker 1 introduces a new tote into the picking line to process the next order, as shown in Figure 3-2(d). These four steps describe the operational principle of pickers in a typical bucket brigade OPS.

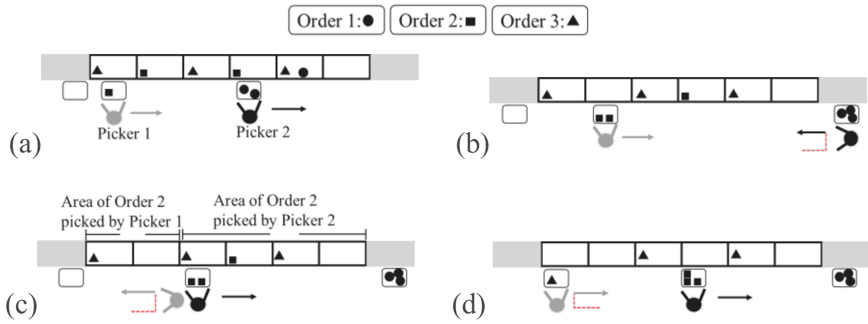

Figure 3-2 Bucket brigade order picking operation.

It is challenging to accurately evaluate the total picking time of orders in a bucket brigade OPS because one order is processed by multiple pickers. Figure 3-2(c) illustrates the areas in which Order 2 is picked by specific pickers. In the first area, from the first pick face to the pick face where the hand-off behavior occurs, Picker 1 is responsible for picking items for Order 2. In the second area, from the pick face where the hand-off occurs to the end of the pick faces, Picker 2 picks items for Order 2. Based on Figure 3-2(c), we can easily calculate the total picking time for Order 2 because we know Picker 1 picks one item in the first area, Picker 2 picks one item in the second area, and we have the unit picking time for each picker. The boundaries of these areas vary among different orders, however, depending on factors like the distribution of items of orders, the unit pick time of pickers, and the walk velocity of pickers. To evaluate the pick time of orders, the areas of orders must be predicted in advance. To our knowledge, no previous study has accurately calculated the total pick time of orders by predicting the areas of all orders.

3.2.2 *Effect of Small Orders and Order-Batching Method*

Small orders have a notable effect on the efficiency of OPSs since pickers must make numerous trips within the OPS to fulfill these orders. The order batching method has proven highly effective, particularly when an OPS is tasked with handling many small orders. To illustrate this, Figure 3 compares order picking processes with and without order batching. In Figure 3-3(a), pickers make four separate trips to fulfill the four individual orders. When the order batching method is applied, as demonstrated in Figure 3-3(b), Orders 1 and 2 are grouped into Batch 1 and Orders 3 and 4 into Batch 2. Pickers complete the order picking in just two trips. This significant reduction in the number of trips directly results in an overall increase in the efficiency of the OPS. It is important to note that the capacity of the totes must be considered when batching orders (this example is limited to six items).

(a) 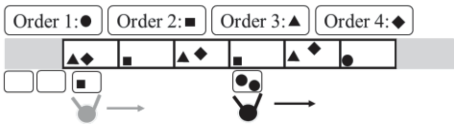

(b) 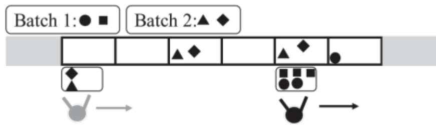

Figure 3-3(a) Picking items without order batching, (b) picking items with order batching.

3.2.3 *Picking, Walking, and Blocking-Delay Behaviors of Pickers*

In a pick face, there are three main types of time costs for a picker: pick time cost, walk time cost, and blocking-delay time cost. The pick time cost occurs when the picker picks items for a batch from a pick face. After picking, the picker must leave the current pick face, resulting in a walk time cost. There are instances where the picker cannot enter the next pick face because it is occupied by a downstream picker, leading to a blocking-delay time cost. In this section, we begin by introducing formulas for calculating the pick and walk time. We then use these formulas to quantify the time cost of blocking delays.

The assumptions and definitions regarding bucket brigade OPSs are adopted from Fibrianto and Hong (2019). The OPS consists of n pick faces, numbered from 1 to n, with the loading station positioned in front of the first pick face (numbered 0) and the unloading station located behind the last pick face (numbered $n + 1$). WT denotes the forward walk time required for a picker to move between two pick faces. In the OPS, there are $|K|$ pickers, numbered from 1 to k, and picker k takes PT_k time to pick an item from a pick face. The pickers are arranged in ascending order based on their picking behavior, from slowest to fastest, as this arrangement has been identified as the most efficient approach in bucket brigade OPSs (Bartholdi & Eisenstein, 1996b). All definitions are summarized as follows:

Definitions.

$F,\ f$: The set of pick faces, and its index $f \in F$.

$K,\ k$: The set of pickers, and its index $k \in K$.

B, i: The set of batches, and its index $i \in B$.

$NB_{i,f}$: The number of items that need to be picked for batch i at pick face f.

ST_i: The starting time of batch i (i.e., the time when batch i is introduced into OPS at the loading station).

PT_k: The unit pick time to pick an item for picker k.

WT: The forward walk time of a picker between two pick faces.

$P_{i,f}$, $CP_{i,f}$: The pick time of batch i at pick face f and its cumulative pick time.

$CW_{i,f}$: The cumulative walk time of batch i at pick face f.

$D_{i,f}$, $CD_{i,f}$: The blocking delay of batch i at pick face f and its cumulative blocking delay time.

Pick and Walk Time

The pick time cost occurs when a picker enters a pick face and starts picking items for a batch. After completing the picking process, the picker must leave the current pick face, resulting in a walk time cost. Figure 3-4 shows three types of time costs in a pick face. Figure 3-4(a) is a time chart that visually illustrates the time costs of the picking and walking behaviors of pickers. The horizontal axis represents the picking line, while the vertical axis represents time. The pick time for batch i and picker k at pick face f is determined by multiplying the unit pick time per item of picker k by the number of items in the batch (Fibrianto & Hong, 2019), and it can be expressed as:

$$P_{i,f} = \begin{cases} 0 & if\ f = 0\ or\ n+1 \\ PT_k \cdot NB_{i,f} & otherwise \end{cases} \quad \forall i \epsilon B, \forall f \epsilon F \cup \{0, n+1\}, \forall k \epsilon K \qquad 3-1$$

The pick time of any batch at the loading or unloading stations is 0, as no items are stored in these two stations. The cumulative pick time of batch i at pick face f is calculated by adding the cumulative pick time of the previous pick face to the pick time of the current pick face (Hong et al., 2016). This can be expressed as:

$$CP_{i,f} = \begin{cases} P_{i,f} & if\ f = 0 \\ P_{i,f} + CP_{i,f-1} & otherwise \end{cases} \quad \forall i \epsilon B, \forall f \epsilon F \cup \{0, n+1\} \qquad 3-2$$

As with Hong et al. (2016), we assume that pickers have the same unit walk time. The walk time of batch i at pick face f is WT, and the cumulative walk time of batch i at pick face f can be expressed as:

$$CW_{i,f} = \begin{cases} WT & if\ f = 0 \\ WT + CW_{i,f-1} & otherwise \end{cases} \quad \forall i \epsilon B, \forall f \epsilon F \cup \{0, n+1\} \qquad 3-3$$

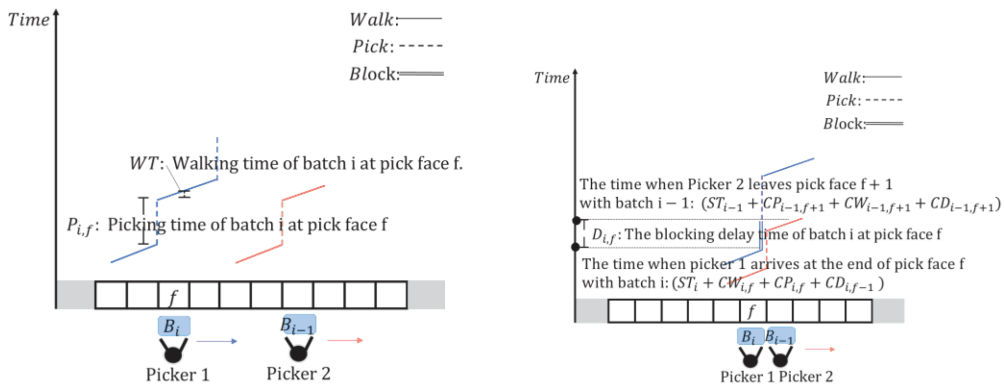

(a) (b)

Figure 3-4 Time cost of pickers' behaviors in a picking line: (a) Picking and walking time; and (b) blocking delay time

Blocking Delay Time

Blocking delay has a significant influence on the efficiency of bucket brigade OPSs. Once a blocking occurs, the blocked picker can do nothing but wait for the downstream picker to leave. In a bucket brigade OPS, pickers are not permitted to pass other pickers (i.e., they should maintain sequence), and one pick face can be occupied by only one picker at a time. Blocking may occur in the picking line if the work content assigned to pickers is inappropriate. For example, when a picker finds that the next items needed to be picked are in a faraway pick face, then he/she walks to that pick face. During the walk, however, a downstream picker appears in front of him/her and is already picking items. Due to the rules governing picker sequence and pick faces, the picker will be blocked by the downstream picker.

Figure 3-4(b) illustrates an example where Picker 1 is blocked at the end of pick face f while attempting to enter pick face $f+1$, as Picker 2 is still occupying pick face $f+1$. The blocking delay time of batch i at pick face f in this example can be calculated as the time when the downstream picker (i.e., Picker 2) leaves pick face $f+1$ minus the time when the upstream picker (i.e., Picker 1) arrives at the end of pick face f. This can be expressed as:

$$D_{i,f} = \begin{cases} max\big((ST_{i-1} + CP_{i-1,f+1} + CW_{i-1,f+1} + CD_{i-1,f+1}) - (ST_i + CW_{i,f}),0\big) & f = 0 \\ 0 & f = n+1 \\ max\big((ST_{i-1} + CP_{i-1,f+1} + CW_{i-1,f+1} + CD_{i-1,f+1}) - (ST_i + CP_{i,f} + CW_{i,f} + CD_{i,f-1}),0\big) & otherwise \end{cases} \tag{3-4}$$

$\forall i \epsilon B, \forall f \epsilon F \cup \{0, n+1\}$.

The blocking-delay time is a value that should be equal to or greater than 0. Hence, the $max()$ function is used in the formula to ensure this. Since there are no items stored in the loading station and blocking does not occur before the loading station (i.e., $f = 0$), the first equation in the formula can be simplified according to the third equation. Additionally, the blocking-delay time at the unloading station (i.e., $f = n+1$) is always 0 since batches are always unloaded by the last picker. Similar to the cumulative pick and walk time, the cumulative blocking delay can be expressed as follows (Hong et al., 2016):

$$CD_{if} = \begin{cases} D_{if} & if\ f = 0 \\ D_{if} + CD_{i,f-1} & otherwise \end{cases} \quad \forall i \epsilon B \cup \{d\},\ \forall f \epsilon F \cup \{0, n+1\} \qquad 3-5$$

Blocking delay is a significant factor that can decrease the productivity of a bucket brigade OPS. In the next section, we will investigate the formula used to calculate the blocking delay to identify the causes of blocking delay and propose a solution to reduce it.

3.2.4 Dynamic Indexed Batching Model for Bucket Brigade (DIBMB)

Fibrianto and Hong (2019) propose the dynamic indexed batching model for bucket brigade (DIBMB) to batch orders. The DIBMB model groups orders into batches to minimize the completion time of all orders. The completion time is the sum of the start time, cumulative pick time, cumulative walk time, and cumulative blocking time of batches at the end of the picking line, which can be expressed as:

$$Min \sum_{i \epsilon B} (ST_i + CP_{i,n} + CW_{i,n} + CD_{i,n}) \qquad 3-6$$

(Although some small revisions have been made to the above formula, the essence of the formula is the same as in the original DIBMB model.)

Due, however, to the complexity of the bucket brigade OPS with non-identical pickers, the DIBMB model cannot accurately calculate the start time (i.e., ST_i) or cumulative pick time (i.e., $CP_{i,n}$), which may cause the system to lose efficiency.

3.3 Balanced Batching Model for Bucket Brigade (BBMB)

This section introduces the proposed BBMB model. It starts by introducing the objective function of the previous model in Section 3.3.1. It then discusses the concept behind the proposed model by analyzing the formula for block-delay calculation and the balance status of a production line in Section 3.3.2. After that, based on the concept, we formulate the BBMB model in Section 3.3.3 and propose a method to arrange the sequence of batches.

3.3.1 Concept Behind the Proposed Model

In this study, our aim is to propose an order batching model with non-identical pickers to reduce the blocking delays of bucket brigade OPSs. The proposed model should demonstrate better performance in improving productivity compared to the DIBMB model. In this section, we first analyze the formula for block delay calculation and find that balancing the work content in the picking line can reduce the blocking delays. Then, to balance the work content, we propose a method of dividing the picking line into several regions. After that, the concept behind the proposed model is derived: bring the bucket brigade OPS closer to a balance status. Lastly, we confirm the effects of the proposed model.

Method of Reducing Blocking Delays

The reduction of blocking delays can be achieved by balancing the work content in the picking line. This conclusion is derived from an analysis of the formula for calculating the blocking delay (Formula 3-4). For ease of explanation, Formula 4 is transformed into Formula 3-7, which calculates the blocking delay of batch i at pick face f. The actual term in Formula 3-7 that determines the blocking delay is $(PT_{k+1} \cdot NB_{i-1,f+1} - PT_k \cdot NB_{i,f})$. Because the terms $(ST_{i-1} + CP_{i-1,f} + CW_{i-1,f+1} + CD_{i-1,f+1})$ and $(ST_i + CP_{i,f-1} + CW_{i,f} + CD_{i,f-1})$ in Formula 3-7 are determined by the previous calculations, to reduce $D_{i,f}$ we need to reduce the value of term $(PT_{k+1} \cdot NB_{i-1,f+1} - PT_k \cdot NB_{i,f})$.

$$
\begin{aligned}
D_{i,f} &= \left(ST_{i-1} + CP_{i-1,f+1} + CW_{i-1,f+1} + CD_{i-1,f+1}\right) - (ST_i + CP_{i,f} + CW_{i,f} + CD_{i,f-1}) \\
&= \left(ST_{i-1} + CP_{i-1,f} + CW_{i-1,f+1} + CD_{i-1,f+1}\right) - (ST_i + CP_{i,f-1} + CW_{i,f} + CD_{i,f-1}) + (PT_{k+1} \\
&\qquad \cdot NB_{i-1,f+1} - PT_k \cdot NB_{i,f}) \qquad 3-7
\end{aligned}
$$

The best way to reduce the value of term $(PT_{k+1} \cdot NB_{i-1,f+1} - PT_k \cdot NB_{i,f})$ is to ensure that batches $i-1$ and i have the same number of items in pick faces f and $f+1$ (i.e., $NB_{i-1,f+1} = NB_{i,f}$). This way, the term $(PT_{k+1} \cdot NB_{i-1,f+1} - PT_k \cdot NB_{i,f})$ will be less than zero for all batches in every pick face because the pickers are arranged in the picking line from slowest to fastest in terms of unit pick time (i.e., $PT_1 > PT_2 > \cdots > PT_{|K|}$).

Method of Dividing Regions

From the previous section, we have learned that minimizing blocking delay is possible if we ensure that every pick face contains the same number of items for each batch. It is, however, common that not all pick faces store items in an OPS. To address this, we can divide the picking line into several regions and ensure that each region contains the same number of items (i.e., balancing the distribution of work content in the picking line). The remaining task is to propose a method for dividing the picking line into regions and determining the number of items in each region.

The regions and the number of items in each region can be determined by referring to the study by Bartholdi and Eisenstein (1996a), which proposed a production line known as the *bucket brigade production line*, which shows a self-balancing feature. If certain conditions are met, a bucket brigade production line spontaneously reaches a balance status after a period of operation. In this balance status, workers work in specific regions of the production line, resulting in the line's achieving maximum productivity, and no blocking occurs. There are two conditions for achieving the balance status. The first one is that workers are sequenced from slowest to fastest at work. The second one is that the work content is evenly distributed in the picking line.

Figure 3-5 shows a time chart of a bucket brigade production line that demonstrates its self-balancing feature. The horizontal axis represents the production line, and the vertical axis represents time. The length of the production line is normalized as one unit, and three workers work in the line. The work velocities (forward velocities) of the three workers are $V_1 = 1, V_2 = 2$, and $V_3 = 3$, and the backward walk time is instantaneous since it is insignificant compared to work time (Bartholdi & Eisenstein, 1996a). The workers' initial positions are 0, 0.5, and 0.75, respectively. Similar to the bucket brigade OPS, the workers walk forward and complete their workloads, then walk backward for new workloads. The workloads are evenly distributed along the production line, and the distance a worker has traveled reflects the amount of work he/she has completed. As shown in Figure 3-5, each worker eventually settles into a particular region, resulting in the balance status. The position of the endpoint of Region r is referred to as Fixed point r, and its location can be calculated as $\sum_{k=1}^{r} V_k \,/\, \sum_{k=1}^{K} V_k$ (where K and k are the number and index of workers, respectively). The bucket brigade OPS can be viewed as a specific case of a bucket brigade production line where workloads are not evenly distributed along the production line.

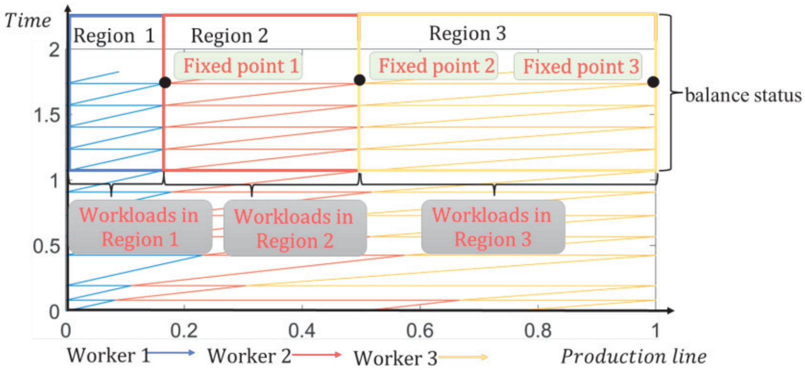

Figure 3-5 Time chart of a bucket brigade production line.

The Concept

The concept of the Balanced Batching Model for Bucket Brigade (BBMB) is to bring the bucket brigade OPS closer to the balance status. This is because maximum productivity with no blocking occurring can be achieved by maintaining the OPS in the balance status (Bartholdi & Eisenstein, 1996b). To achieve this, the BBMB model first divides the picking line into regions based on fixed points. Then, it determines the workloads (items) in each region according to the ideal workloads in the balance status. Lastly, the BBMB model minimizes the difference between the ideal workloads of the balance status and the actual work content assignment by allocating orders into batches.

Confirming the Effects of the BBMB Model

Figure 3-6(a) and 3-6(b) depict the time charts of the DIBMB model (Fibrianto & Hong, 2019) and the BBMB model, respectively, illustrating the effects of the proposed model. (How to draw a time chart for a bucket brigade OPS is explained in Section 5.1). The horizontal axis represents the picking line, which consists of 50 pick faces, one loading station, and one unloading station. The loading station is located at position 0-1, and the unloading station is located at position 51-52. The vertical axis represents time. The different colored lines in the chart represent the behavior of three pickers: red for picker 1 (P 1), green for picker 2 (P 2), and blue for picker 3 (P 3). When a line increases vertically, it means that a picker is picking items at the start of a pick face. When a line grows inclinationally, it means that the picker is walking in the line. When two lines coincide vertically, it means that a blocking delay between pickers is occurring. When the first picker walks back to horizontal position 0, a new batch will be introduced into the picking line. We use both the BBMB and DIBMB models to allocate the same group of randomly generated small orders into batches. The unit pick times of pickers are $PT_1 = 1.2, PT_2 = 1.1, PT_3 = 1.0, PT_4 = 0.9,$ and $PT_5 = 0.8$. “5001” at the top of each figure indicates 50 pick faces and a 0.1 gap among the pickers’ unit pick time.

Compared to the time chart of the DIBMB model, the time chart of the BBMB model shows significantly less blocking. Although the DIBMB model minimizes the total completion time of all batches, the optimized result is based on inaccurate calculation results due to the estimated pick time. The effect of this inaccurate calculation is clearly shown in Figure 3-6(a), where blocking occurs between pickers. On the other hand, the BBMB model avoids the effect of blocking by balancing the work content in the picking line. The time chart of the BBMB model in Figure 3-6(b) shows a close-to-balance status with a very low probability of blocking occurring.

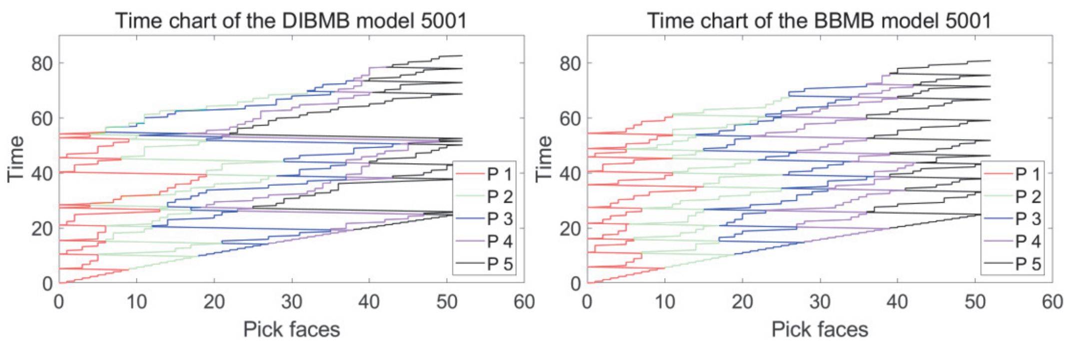

(a) (b)

Figure 3-6 Time charts of the DIBMB model and BBMB model.

3.3.2 BBMB Model Formulation

The BBMB model is proposed to reduce blocking delays in the bucket brigade OPS. To do this, the BBMB model adjusts the conditions of the OPS to be close to the ideal conditions that allow the OPS to remain in a balance status. In the balance status, no blocking occurs, and the OPS can achieve maximum productivity.

The ideal conditions of bucket brigade OPSs can be predicted when the OPS is in a balance status. The ideal fixed point of region k is IFR_k, and the ideal number of items at region k is INR_k. Based on the ideal fixed points, the BBMB model divides the picking line into several regions. According to the ideal number of items in each region, it allocates orders into batches. All the definitions are provided below.

Indices and Parameters.

$O,\ o$: The set of orders, and its index $o \epsilon O$.

K, k: The set of pickers and regions, and its index $k \in K$.

$OP_{o,f}$: The number of picks in order o at pick face f.

OS_o : The number of picks in order o.

$CAPA$: The capacity of a cart (batch size).

PV_k: The picking velocity of picker k, $PV_k = \frac{1}{PT_k}$.

Decision Variables.

$X_{o,i}$: 1 if order o enters the ith batch; 0 otherwise.

$NR_{i,k}$: The number of picks of batch i at region k.

Intermediate and Supplementary Parameters.

IFR_k: The ideal fixed point of region k, $IFR_k = \frac{\sum_{k=1}^{k} PV_k}{\sum_{k \epsilon K} PV_k}$.

NP: The average number of picks of all batches, $NP = \frac{\sum_{o \epsilon O} OS_o}{|B|}$.

INR_k: The ideal number of items at region k, $INR_k = \begin{cases} IFR_k \cdot NP & if\ k = 1 \\ (IFR_k - IFR_{k-1}) \cdot NP & otherwise \end{cases}$.

IFF_k : The pick face includes the ideal ending point of region k , $IFF_k = \begin{cases} 0 & if\ k = 0 \\ \lceil IFR_k \cdot |F| \rceil & otherwise \end{cases}$.

The BBMB model uses two different optimization methods to allocate orders into batches. The first method, called the *BBMB_NB optimization method*, aims to minimize the difference between the ideal and actual number of items assigned to each region for every batch, as indicated by the objective function 2-8.a. The second method, the *BBMB_PT optimization method*, assigns weights to each region by using the picker's unit pick time as a coefficient, as indicated by the objective function 2-8.b. Regions assigned to pickers with longer unit pick times will have a higher weight in the BBMB model. Essentially, the objective function 2-8.b minimizes the pick time of items in each region. The two optimization methods use the same constraints in the model.

BBMB_NB

Objective function

$$min\left(\sum_{i\epsilon B}\sum_{k\epsilon K}\left|NR_{i,k}-INR_k\right|\right) \qquad 2-8.a$$

Subject to

$$\sum_{i\epsilon B} X_{o,i}=1\ \forall o\epsilon O \qquad 2-9$$

$$\sum_{o\epsilon O} OS_o\cdot X_{o,i}\le CAPA\ \forall i\epsilon B \qquad 2-10$$

One order should enter one batch in constraint 2-9, and a batch should not exceed the capacity in constraint 2-10. Constraint 2-11 calculates the number of picks of batch i at region k, which can be considered the actual work content assignment. IFF_k is the pick face that includes the fixed point of region k, like the example in the following Figure 3-7.

$$NR_{i,k}=\sum_{o\epsilon O}\sum_{f=(IFF_{k-1}+1)}^{IFF_k} OP_{o,f}\cdot X_{o,i}\ \ \forall o\epsilon O,\ \forall i\epsilon B, \forall f\epsilon F, \forall k\epsilon K \qquad 2-11$$

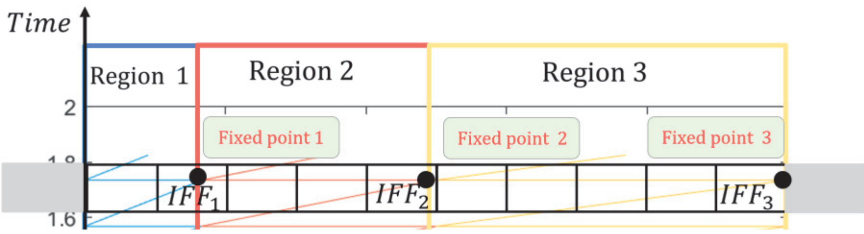

Figure 3-7 Pick faces that include fixed points.

BBMB_PT

Objective function

$$min\left(\sum_{i\epsilon B}\sum_{k\epsilon K}PT_k\cdot\left|NR_{i,k}-INR_k\right|\right) \qquad 2-8.b$$

Subject to constraints 2-9, 2-10, and 2-11.

3.3.3 Batch Sequence Arrangement Method

The formulas of the BBMB model cannot specify the sequence of orders. To determine the optimal batch sequence, we evaluated all 120 possible permutations for five batches within a batch window ($120 = 5!$) and all 14,400 possible permutations for 10 batches across two batch windows ($14{,}400 = 5!\times 5!$) under different conditions. Each evaluation was repeated five times with randomly generated orders. Our findings show that arranging the batches in a descending sequence of workloads (i.e., the number of items in each region multiplied by the unit pick time of each picker) within each batch window produced the most satisfactory results. Specifically, this arrangement produces a completion time for the last batch that is very close to the minimum completion time achievable for the OPS. Therefore, we recommend processing the batches generated by the BBMB model in order of decreasing workload within each batch window.

3.4 Numerical Experiment

This section aims to validate the effectiveness of the BBMB model and compare its performance to the previous DIBMB model. To accomplish this, we first developed a simulation program to analyze the operation of bucket brigade OPS when pickers process batches in Section 3.4.1. Following that, Section 3.4.2 introduces the conditions of the simulation experiments. Finally, in Section 3.4.3, we conduct simulation experiments to validate the BBMB model and compare it with the previous model.

We implemented the order batching procedure using the Python language and Gurobi 9.5.1 and ran the simulation program on Matlab using the obtained batch data from Gurobi. We ran the simulation and optimization program on Windows 11 (Intel Core i5-10210U CPU @1.60GHz, 16 GB memory, x64-based processor).

3.4.1 Simulation Program of Bucket Brigade OPS

Algorithm of the Program

The simulation program we aim to develop can depict the motion of pickers to process orders in a picking line over time, like Figure 3-8: Time charts of the DIBMB model and BBMB model. As the simulation program is quite complex, it involves numerous formulas and algorithms. To ensure the coherence of the content, we provide only a brief overview of the program's basic algorithm in this section and showcase an output result.

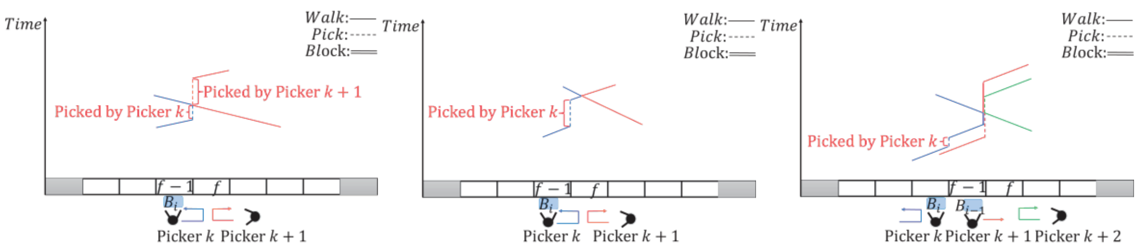

(a) (b) (c)

Figure 3-8 Three different meeting cases: (a) meeting in picking, (b) meeting in walking, (c) meeting in blocking.

Before introducing the program algorithm, some technical details need to be addressed to avoid confusion. When calculating pick time, it is crucial to determine which picker or pickers are responsible for picking items at the current pick face. The hand-off behavior between pickers affects the pick-time calculations. There are three possible cases when hand-off behavior occurs, illustrated in Figure 3-8. In the first case, known as the “meet in picking” case (Figure 3-8(a)), two pickers meet when the upstream picker is in the process of picking items for a batch. The upstream picker picks the initial portion of items, then transfers the tote to the downstream picker to complete the remaining picking task. The meeting point between the pickers is located at the start of pick face f. In the second case, referred to as the “meet in walking” case (Figure 3-8(b)), two pickers meet at pick face f while the upstream picker is walking after completing the picking process. The meeting point occurs within pick face f. In the third case, known as the “meet in blocking” case (Figure 3-8(c)), picker $k+1$ encounters picker k, who is blocked by picker $k+1$. The meeting point is situated at the end of pick face f. For the “meet in walking” and “meet in blocking” cases, the pick time can be calculated by multiplying the number of items by the unit pick time of the picker. Different formulas need to be proposed for the “meet in picking” case, as both pickers are involved in the picking process.

The algorithm for calculating the pick, walk, and blocking-delay times is described as follows. All the formulas with an index of “A” are explained in the appendix. First, we input the necessary parameters in Lines 1-4. Then, for batch i, we calculate its start time in Line 7. After that, the pick, walk, and blocking-delay times of batch i at pick face f are calculated in Lines 9–30. To calculate the pick time, we first need to determine the presence of a hand-off behavior for the current batch in Line 10. Subsequently, we identify specific meeting cases in Lines 12, 15, and 18. In the case of a meeting in picking, the pick time is calculated using Formula A.1 in Line 13. If no hand-off behavior occurs or it occurs in the meet in walking/blocking cases, the pick time is calculated using Formula 1 in Lines 16, 19, and 25. After calculating pick time, we calculate the cumulative pick time, cumulative walk time, blocking delay time, and cumulative blocking delay time in Line 27. Lines 28 and 29 show a special case in which we can calculate pick time directly without identifying the presence of a hand-off behavior for the current batch because no more downstream pickers exist for the last picker.

The algorithm to simulate the hand-off behavior of pickers is described as follows. A batch is always processed by Picker 1 at first in Line 8. If a hand-off behavior is identified at pick face f in Line 11, the batch will be handed to the next picker in line 23. Whenever a hand-off behavior occurs at a pick face, the time and position of a picker walking back after transferring the batch to the downstream picker should be recorded in Lines 14, 17, 20, and 22. The time and position of the pickers, except the first picker, can be used to identify the occurrence of hand-off behavior for the next batch in Line 11 and the specific meeting cases in Lines 12, 15, and 18, while the time and position of the first picker can be used to determine the start time of the next batch in line 7.

Definitions.

BV: The walk-back velocity of the pickers.

$Region_{i,k}$: The region in which batch i is picked by picker k.

$ER_{i,k}$: The endpoint of $Region_{i,k}$.

$LB_{i,k}$: The time when picker k walks back from $ER_{i,k}$.

Algorithm of Pseudo-Code for Pick, Walk, and Blocking Delay Time Calculation

---

Input
Information of pickers.
Set of batches B generated from the BBMB or the DIBMB model.
An initial batch to determine the position and time of pickers walking back for hand-off behavior (i.e., $M_{0,k}$ and $LB_{0,k}$).
Begin
  For each batch i in B do
    Calculate ST_i based on BV, $ER_{i-1,1}$, and $LB_{i-1,1}$, (please refer to Formula A.8 in the Appendix for more details).
    $k = 1$
    For each pick face f in F do
      If $k < K$ (picker k is not the last picker.) then
        If hand-off behavior occurs at pick face f (identified based on $ER_{i-1,k+1}$, $LB_{i-1,k+1}$, and so on, refer to Formula A.5) then
          If pickers meet in the picking progress (identified based on PT_k, $NB_{i,f}$, and so on, refer to the first inequality of Formula A.9) then
            Calculate $P_{i,f}$ (special case where two pickers participate in the picking progress, refer to Formula A.1)
            Calculate $ER_{i,k}$ ($ER_{i,k}$ is located at the start of pick face f, see Figure 3-8(a) for details, refer to the first equation of Formula A.6)
          Elseif pickers meet in during the walking progress (identified based on WT, $ER_{i-1,k+1}$, and so on, refer to the second inequality of Formula A.9) then
            Calculate $P_{i,f}$ (see Section 3.4 for details)
            Calculate $ER_{i,k}$ ($ER_{i,k}$ is located in pick face f, see Figure 3-8(b) for details, refer to the third equation of Formula A.6)
          Else pickers meet in during the blocking progress (refer to the third inequality of Formula A.9) then
            Calculate $P_{i,f}$
            Calculate $ER_{i,k}$ ($ER_{i,k}$ is located at the end of pick face f, see Figure 3-8(c) for details, refer to the fourth equation of Formula A.6)
          End if
          Calculate $LB_{i,k}$ based on $ER_{i,k}$, $ER_{i-1,k+1}$, $LB_{i-1,k+1}$, and BV (refer to the third inequality of Formula A.7)
          $k = k + 1$ (batch i is transferred to picker $k + 1$)
        Else hand-off behavior does not occur at pick face f then
          Calculate $P_{i,f}$
        End if
        Calculate $W_{i,f}$ and $D_{i,f}$
      Else picker k is the last picker then
        Calculate $P_{i,f}$, $W_{i,f}$ and $D_{i,f}$ (see Section 3.4 for details)
      End if
    End for
  End for
End

Time Chart Generated by the Simulation Program

A simulation program was developed in Matlab to simulate the operation of a bucket brigade OPS by following the algorithm. Figure 3-9 shows one of the outputs of the simulation program:

a time chart for describing the behavior of pickers in the picking line. The horizontal axis represents the picking line, which consists of 15 pick faces, one loading station, and one unloading station. The loading station is located at position 0-1, and the unloading station is located at position 16-17. The vertical axis represents time. The different colored lines in the chart represent the behavior of three pickers: red for picker 1 (P 1), green for picker 2 (P 2), and blue for picker 3 (P 3). The unit pick times of the three pickers are $PT_1 = 1.2$, $PT_2 = 1.0$, and $PT_3 = 0.8$. The unit forward walk time of pickers is 0.1, and the unit backward walk time is 0.05.

When a line increases vertically, it means that a picker is picking items at the start of a pick face. When a line grows diagonally, it means that the picker is walking in the line. When two different color lines coincide vertically, it means that a blocking delay between pickers is occurring. When the first picker walks back to horizontal position 0, a new batch is introduced into the picking line. Eleven batches are introduced into the picking line. The first batch, which starts at (0, 0), is an initial batch. We manually set every pick face to store one item in the initial batch to set the starting conditions of the OPS. Picker 1 walks back at (5, 5.3), picker 2 walks back at (9, 9.7), and picker 3 walks back at (17, 16.1) to introduce batch 2. From batch 2 (starting at (0, 0.55)) to batch 6 (starting at (0, 28.5253)), the work content is generated randomly and follows a uniform distribution.

This simulation program could be helpful to analyze the behavior of pickers and evaluate the performance of the OPS. For example, by observing the completion time of the last batch, we could evaluate the efficiency of the OPS. By calculating the blocking time of batches, we could determine whether the work content distribution of batches was appropriate.

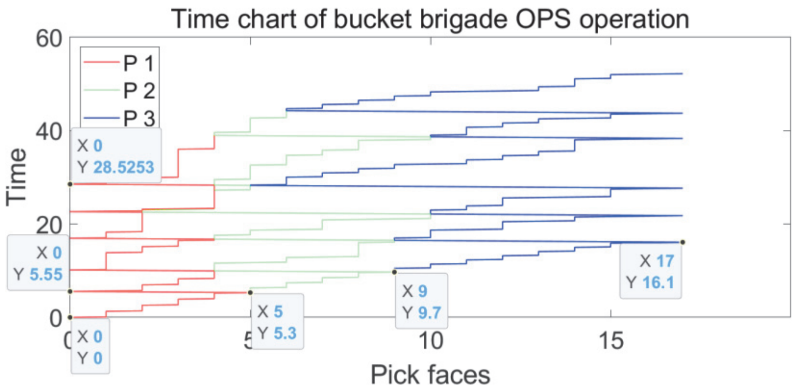

Figure 3-9 Time chart of a bucket brigade OPS with 15 pick faces and three pickers.

3.4.2 *Conditions*

The simulation conditions used in the comparison experiment are summarized in Table 3-1. The conditions in this experiment are mainly adopted from Fibrianto and Hong's 2019 experiment, with some revisions. Because both the BBMB (proposed) and the DIBMB (Fibrianto & Hong,

2019) aim to reduce blocking delays when pickers process batched small orders in bucket brigade OPSs. Three factors (pickers, work content, and picking line) can affect the occurrence of blocking, as blocking occurs when pickers process inappropriately assigned work content in the picking line. Since the work content is already determined by the two models, this experiment focuses on discussing the effect of pickers and the picking line.

The picking line comprises 25 pick faces for the small OPS, 50 pick faces for the standard OPS, and 75 pick faces for the large OPS, along with one loading station and one unloading station. Each pick face has a length of one unit, and there are five pickers involved in the picking line, which is consistent with Fibrianto and Hong (2019). Four different picker capability scenarios are set. The backward walk time is twice as fast as the forward walk time, as pickers walking forward need to carry a tote filled with picked items, while they walk back with empty hands. We randomly selected the size of each order based on a uniform distribution [min, max] = [mean/2, mean*3/2], where mean = 4 (Fibrianto & Hong 2019). The location of items in each order also follows a uniform distribution [min, max] = [the first pick face, the last pick face]. There are 250 orders randomly generated for every run in the experiment. The orders are divided into 10 batch windows evenly. One batch window generates five batches, and each batch contains five orders. Figure 3-10 shows the relationship among orders, batches, and batch windows in this experiment.

Table 3-1 Summary of Simulation Environments.

Configuration	Values
Picker capability scenario	Identical capability [pt1, pt2, pt3, pt4, pt5] = [1.0, 1.0, 1.0, 1.0, 1.0]
	Small-gap (0.05 gap) [pt1, pt2, pt3, pt4, pt5] = [1.1, 1.05, 1.0, 0.95, 0.9]
	Medium-gap (0.1 gap) [pt1, pt2, pt3, pt4, pt5] = [1.2, 1.1, 1.0, 0.9, 0.8]
	Large-gap (0.2 gap) [pt1, pt2, pt3, pt4, pt5] = [1.4, 1.2, 1.0, 0.8, 0.6]
OPS size	Small OPS [25 pick faces]
	Standard OPS [50 pick faces]
	Lage OPS [75 pick faces]
Number of items per order	Uniform distribution [min, max] = [2, 6]
Location of items	Uniform distribution [min, max] = [the first pick face, the last pick face]
Forward walk time	0.1 unit time/pick face
Backward walk time	0.05 unit time/pick face
Performance measure	LCT (last batch's completion time), BTP (blocking time percentage, %), Utilization (%)
Number of batches	25 orders per batch window, 5 batches per batch window, 10 batch windows
Capacity of a batch	25 items
Runs per instance	5 runs with 2,500 orders (25 orders per batch window × 10 batch windows × repeat 5 times) × 2 OPS sizes
Number of items in an initial order	0.25 items/pick face

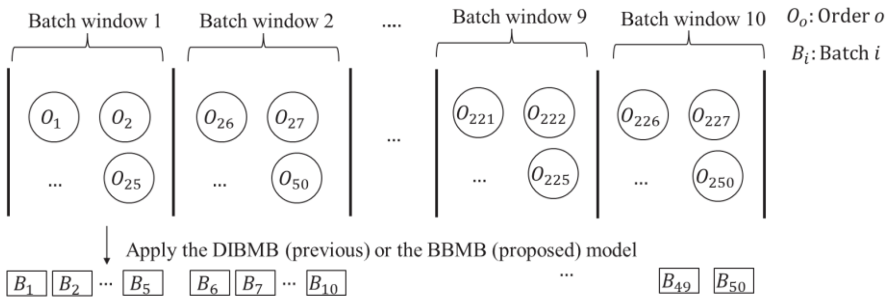

Figure 3-10 Orders, batches, and batch windows.

Our simulations report the picker use percentage, the blocking time percentage (BTP), and the last batch's completion time (LCT). The picker use percentage is the percentage of time spent picking compared to the overall operations. The blocking time percentage (BTP) represents a productivity loss, the percentage of time blocked compared to overall operations. The last batch's completion time (LCT) is the time when all items listed in the last batch have been picked by pickers and the last picker unloads the batch at the unloading station.

Some conditions in this experiment differ from those in the experiment conducted by Fibrianto and Hong (2019). In addition to the standard OPS (50 pick faces) and small OPS (25 pick faces), we included a large OPS (75 pick faces) in the experiment. The inclusion of a large OPS, as opposed the small OPS, enabled us to conduct a deeper analysis of the effect of OPS size on the performance of the two models, resulting in more comprehensive results. Similarly, more picker-capability scenarios were added in this experiment compared to the study of Fibrianto and Hong (2019). We ignored the hand-off delay and assumed the length of the loading and unloading stations to be 1 unit instead of 0.5 units to simplify calculations. The start time calculation algorithm of the DIBMB model assumes that all empty-hand pickers walk back from different positions in the picking line at time zero when the OPS starts. This behavior, however, can significantly increase the likelihood of blocking among pickers at the start of the picking line. To avoid this, we had empty-handed pickers walk back one by one after certain periods.

3.4.3 Results and Analysis

Model Validation: Work Content Distribution in Picking Line

The BBMB model is proposed to balance the distribution of work content in the picking line to reduce blocking. To validate that the BBMB model successfully balances the work content, we investigated the information about the batches optimized by the BBMB model and compared them to the DIBMB model's batches. Table 3 presents the number of items in batches in every region of the picking line. The initial batch is manually set according to Table 2. Batches 1–10 were determined by the BBMB model using the BBMB_NB method and the DIBMB model. Table 3 reveals that, compared to the DIBMB model, the BBMB model has a significantly smaller gap in the number of items between regions, indicating that the work content of the batches in the BBMB model is more balanced and distributed in the picking line. The even distribution of work can reduce blocking time. Therefore, the BBMB model will achieve lower blocking time percentages (BPT) than the DIBMB model.

Table 3-2 Number of Items of Batches in Every Region for the Two Models

	BBMB Model with BBMB_NB method					DIBMB Model				
	Region 1	Region 2	Region 3	Region 4	Region 5	Region 1	Region 2	Region 3	Region 4	Region 5
Initial batch	3.6	3.6	3.6	4.4	4.8	3.6	3.6	3.6	4.4	4.8
Batch 1	6	4	3	4	6	4	5	1	4	2
Batch 2	4	5	4	4	6	5	6	6	3	5
Batch 3	4	7	2	4	5	7	5	2	1	10
Batch 4	4	4	4	4	6	5	3	3	7	7
Batch 5	4	4	3	4	6	1	5	4	5	5
Batch 6	2	4	6	5	4	2	1	3	2	3
Batch 7	3	3	5	5	4	2	5	7	5	3
Batch 8	2	4	5	5	4	2	5	7	6	5
Batch 9	2	3	6	5	4	4	4	4	6	5
Batch 10	3	3	4	5	4	2	2	5	6	4

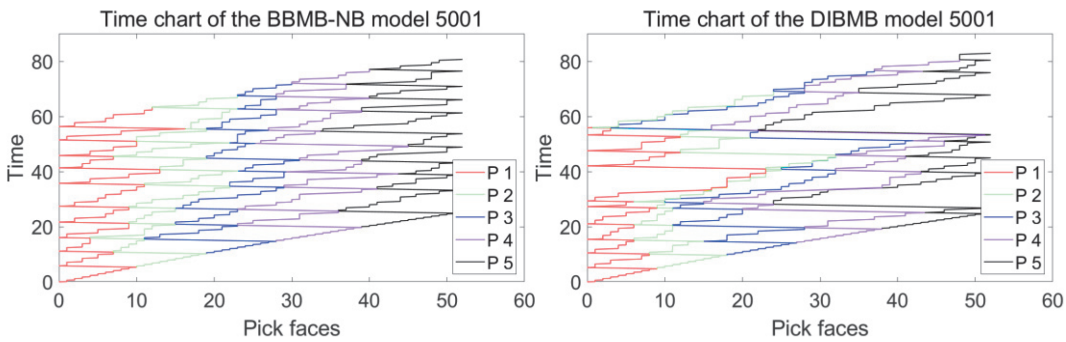

(a) (b)

Figure 3-11 Effect of work-content distribution: (a) time chart of the BBMB_NB model in which no blocking occurs, (b) time chart of the DIBMB model in which blocking occurs.

Based on the data from Table 3-2, the simulation program draws time charts for the two models, as shown in Figure 3-11, to confirm that the BBMB model can achieve a lower BTP. Compared to Figure 3-11(a), blocking occurs more frequently in Figure 3-11(b). So far, we can confirm that the BBMB model successfully balances the distribution of work content in the picking line (see Table 3-2), consequently achieving a lower BTP compared to the DIBMB model (see Figure 3-11).

Performance Comparison: Blocking Time Percentage (BTP)

Table 3-3 presents the BTP (blocking time percentage) of different models for various sizes of OPS and different gaps of unit pick time. BTP represents the percentage of the total blocking time of batches in comparison to the overall operation time. The "D" behind BBMB_NB and BBMB_PT represents the difference in BTP between the previous model and the proposed model. Overall, the BTP decreases as the gap of the unit pick time increases because, based on the blocking delay calculation formula with a small revision $D_{i,f} = \left(CP_{i-1,f+1} - CP_{i,f}\right) + (ST_{i-1} + CW_{i-1,f+1} + CD_{i-1,f+1}) - (ST_i + CW_{i,f} + CD_{i,f-1})$, as the gap increases, the value of term $(CP_{i-1,f+1} - CP_{i,f})$ in the formula decreases. Roughly speaking, BTP decreases as the OPS size increases. This is because pickers have a larger working space when the OPS size increases, reducing the likelihood of one picker's being blocked by another. The effect of OPS size on BTP, however, is not so pronounced in this experiment due to the pickers' fast walking velocity, which allows them to move quickly within the working space. Compared to the DIBMB model, the BBMB model with two methods significantly reduces the BTP from 4.46% to 12.50% down to 0.26% to 5.66%. Overall, the difference (D) in BTP between the previous model and the proposed model decreases as the gap increases because it is challenging to further reduce BTP when it is already at a low value in the DIBMB model. Across all different-sized OPSs, D falls within a similar range, typically between 4% and 7%. This suggests that OPS size does not significantly affect the BBMB model's ability to reduce BTP. In summary, the BBMB model is a more efficient approach for reducing blocking time in bucket brigade OPSs compared to the DIBMB model.

Table 3-3 Blocking Time Percentage Comparison Between the DIBMB Model and BBMB Model with Two Optimization Methods.

Scenario		BTP		
Pick faces	Unit picking time	DIBMB	BBMB_NB (D)	BBMB_PT (D)
25	0 gap: [1.0,1.0,1.0,1.0,1.0]	12.50%	5.16% (-7.34)	5.16% (-7.34)
	Small gap: [1.1, 1.05, 1.0, 0.95, 0.9]	9.32%	3.15% (-6.17)	3.69% (-5.63)
	Medium gap: [1.2, 1.1, 1.0, 0.9, 0.8]	7.28%	1.70% (-5.58)	2.02% (-5.26)
	Large gap: [1.4, 1.2, 1.0, 0.8, 0.6]	5.43%	1.16% (-4.27)	1.24% (-4.19)
50	0 gap: [1.0,1.0,1.0,1.0,1.0]	10.83%	5.66% (-5.17)	5.63% (-5.20)
	Small gap: [1.1, 1.05, 1.0, 0.95, 0.9]	9.15%	2.50% (-6.66)	1.85% (-7.30)
	Medium gap: [1.2, 1.1, 1.0, 0.9, 0.8]	7.54%	1.23% (-6.31)	0.77% (-6.77)
	Large gap: [1.4, 1.2, 1.0, 0.8, 0.6]	4.46%	0.31% (-4.15)	0.29% (-4.17)
75	0 gap: [1.0,1.0,1.0,1.0,1.0]	10.86%	3.31% (-7.55)	3.29% (-7.58)
	Small gap: [1.1, 1.05, 1.0, 0.95, 0.9]	8.32%	0.99% (-7.33)	1.11% (-7.21)
	Medium gap: [1.2, 1.1, 1.0, 0.9, 0.8]	7.36%	0.32% (-7.04)	0.62% (-6.74)
	Large gap: [1.4, 1.2, 1.0, 0.8, 0.6]	4.56%	0.28% (-4.28)	0.26% (-4.30)

Performance Comparison: The Last Batch's Completion Time (LCT)

Table 3-4 displays the last batch's completion time (LCT) results of the models under different scenarios with varying sizes of OPS and gaps of unit pick time. The "RD" behind BBMB_NB and BBMB_PT represents the relative difference in LCT between the previous model and the proposed model. It is observed that, as the gap in the unit pick time widens, LCT decreases. This phenomenon is due to a larger gap leading to a smaller BTP (see Table 3-3), resulting in a shorter LCT. The LCT increases as the OPS size increases because pickers spend more time walking in a larger OPS. Overall, the BBMB model reduces LCT by 3.25% to 8.72% compared to the DIBMB model. We conducted a paired t-test on experiment to verify the effectiveness of the BBMB model in reducing LCT when compared with the DIBMB model. The test resulted in a very small p-value ranging from 1.15×10^{-7} to 2.6×10^{-4}, indicating a statistically significant improvement in the BBMB model over the DIBMB model.

Table 3-4 Last Batch's Completion Time Comparison Between the DIBMB Model and BBMB Model with Two Optimization Methods.

Scenario		LCT		
Pick faces	Unit picking time	DIBMB	BBMB_NB (RD)	BBMB_PT (RD)
25	0 gap: [1.0,1.0,1.0,1.0,1.0]	291.95	268.65 (-7.98%)	268.65 (-7.98%)
	Small gap: [1.1, 1.05, 1.0, 0.95, 0.9]	282.88	264.45 (-6.52%)	264.94 (-6.34%)
	Medium gap: [1.2, 1.1, 1.0, 0.9, 0.8]	271.87	258.40 (-4.96%)	259.30 (-4.62%)
	Large gap: [1.4, 1.2, 1.0, 0.8, 0.6]	255.93	247.42 (-3.33%)	247.60 (-3.25%)
50	0 gap: [1.0,1.0,1.0,1.0,1.0]	331.18	308.74 (-6.78%)	308.30 (-6.91%)
	Small gap: [1.1, 1.05, 1.0, 0.95, 0.9]	321.47	301.09 (-6.34%)	298.57 (-7.12%)
	Medium gap: [1.2, 1.1, 1.0, 0.9, 0.8]	314.92	296.42 (-5.87%)	295.18 (-6.27%)
	Large gap: [1.4, 1.2, 1.0, 0.8, 0.6]	296.01	285.89 (-3.42%)	285.66 (-3.50%)
75	0 gap: [1.0,1.0,1.0,1.0,1.0]	373.84	341.65 (-8.61%)	341.23 (-8.72%)
	Small gap: [1.1, 1.05, 1.0, 0.95, 0.9]	361.76	336.50 (-6.98%)	336.28 (-7.04%)
	Medium gap: [1.2, 1.1, 1.0, 0.9, 0.8]	355.81	334.42 (-6.01%)	334.17 (-6.08%)
	Large gap: [1.4, 1.2, 1.0, 0.8, 0.6]	338.10	326.90 (-3.31%)	326.73 (-3.36%)

Performance Comparison: Utilization

Table 3-5 Utilization Comparison Between the DIBMB Model and BBMB Model with Two Optimization Methods.

Scenario		Utilization		
Pick faces	Unit picking time	DIBMB	BBMB_NB (D)	BBMB_PT (D)
25	0 gap: [1.0,1.0,1.0,1.0,1.0]	77.01%	83.47% (+6.46)	83.47% (+6.46)
	Small gap: [1.1, 1.05, 1.0, 0.95, 0.9]	79.71%	85.19% (+5.48)	84.72% (+5.01)
	Medium gap: [1.2, 1.1, 1.0, 0.9, 0.8]	81.34%	86.34% (+5.00)	86.05% (+4.71)
	Large gap: [1.4, 1.2, 1.0, 0.8, 0.6]	82.36%	86.22% (+3.86)	86.15% (+3.79)
50	0 gap: [1.0,1.0,1.0,1.0,1.0]	70.59%	74.68% (+4.09)	74.70% (+4.12)
	Small gap: [1.1, 1.05, 1.0, 0.95, 0.9]	71.77%	77.12% (+5.35)	77.64% (+5.87)
	Medium gap: [1.2, 1.1, 1.0, 0.9, 0.8]	72.82%	77.96% (+5.14)	78.33% (+5.51)
	Large gap: [1.4, 1.2, 1.0, 0.8, 0.6]	74.47%	77.95% (+3.48)	77.95% (+3.48)
75	0 gap: [1.0,1.0,1.0,1.0,1.0]	64.16%	69.60% (+5.43)	69.62% (+5.45)
	Small gap: [1.1, 1.05, 1.0, 0.95, 0.9]	65.82%	71.22% (+5.40)	71.14% (+5.32)
	Medium gap: [1.2, 1.1, 1.0, 0.9, 0.8]	66.23%	71.52% (+5.28)	71.30% (+5.06)
	Large gap: [1.4, 1.2, 1.0, 0.8, 0.6]	67.36%	70.73% (+3.37)	70.76% (+3.40)

Table 3-5 shows the use of different models under varying scenarios with different sizes of OPS and gaps in unit pick time. *Utilization* is the percentage of time spent picking compared to overall operations. The "D" behind BBMB_NB and BBMB_PT represents the difference in use between the previous model and the proposed model. Utilization increases as the gap increases because a larger gap leads to a smaller BTP (see Table 3-3), and the total walking time is constant (all pickers own the same unit walking time). Therefore, the pickers spend relatively more time on picking behaviors. As the number of pick faces increases, the use decreases, as pickers need to spend more time traveling in the picking line. Overall, the BBMB model increases use from 64.16% to 82.36% up to 69.60% to 86.34% compared to the DIBMB model.

3.5 Summary

The objective of this chapter was to balance the work content in the picking line to reduce blocking delays when pickers process batched small orders in bucket brigade OPSs. Through an analysis of the formulas related to blocking delay calculation, we confirmed that balancing work content in the picking line is a direct way to minimize blocking delays. Therefore, we propose the Balanced Batching Model for Bucket Brigade (BBMB) to balance the work content by allocating orders into batches. To compare the performance of the proposed BBMB model and the previous DIBMB model, we have developed a simulation program. This program can analyze the performance of the models and illustrate the progress of processing batches through time charts.

As the effect of this research, the BBMB model has increased the productivity of bucket brigade OPSs when handling many small orders. The experiments found that the BBMB model balances the distribution of work content in the picking line and reduces blocking delays. Compared to the previous model, the BBMB model significantly reduces the blocking time percentage (BTP) from 4.46–12.5% down to 0.26–5.66%. With the reduction in blocking time, the last batch's completion time (LCT) is also shortened by 3.25–8.72%. Additionally, as blocking time decreases, pickers can allocate more time to picking items, increasing the use of human labor from 64.16–82.36% up to 69.60–86.34%.

Although the BBMB model achieves better performance than the previous model, it still has limitations that need to be addressed in the future. The proposed BBMB model performs well when dealing with bucket brigade OPSs that include many small orders and have work-content distributions following a uniform pattern. When dealing with larger orders or non-uniform work-content distributions, however, the BBMB model may not be suitable for enhancing the efficiency of bucket brigade OPSs. Future research could explore methods for balancing work content in OPSs when it does not follow a uniform distribution, such as in cases where items are distributed according to a standard pattern or when there is an imbalance between the front and back sections of a picking line. Moreover, in real life, human movement is unstable and depends on ergonomics. Changing the assumptions of pickers' movement from stable to unstable could make the research better reflect real life. Future work could discuss the effect of unstable picker movement on bucket brigade OPSs.

Appendix

Definitions

BT: The backward walk time between two pick faces.

$\Delta ER_{i,k}$: The time of the upstream picker k spends at $ER_{i,k}$ when the hand-off process occurs.

$L_{i,f}$: The leaving time of batch i at pick face f along the forward direction.

$MP_{i,f}$: The maximum pick time of batch i at pick face f.

$MD_{i,f}$: The maximum blocking delay time of batch i at pick face f.

Effect of Hand-off Behavior

The transfer of a tote from an upstream picker k to the downstream picker $k+1$ is known as a *hand-off*. To simplify the calculation, we assume that the time cost of hand-off behavior is negligible in this study, as it is much shorter than the time cost of picking an item or walking a pick face. Once the hand-off behavior occurs between two pickers, the upstream picker immediately transfers the tote to the downstream picker. When the downstream picker meets the upstream picker after walking back to take over the tote, the upstream picker may be in one of three different operational statuses, as shown in Figure 3-12: the upstream picker is currently picking items (referred to as the “meet in picking” case), the upstream picker is walking along the pick faces (referred to as the “meet in walking” case), or the upstream picker is blocked by him/her (referred to as the “meet in blocking” case). The analysis of the effect of the hand-off behavior in these three cases is discussed below.

In the “meet in picking” case, as shown in Figure 3-12(a), two pickers meet at the starting point of pick face f, where the upstream picker is picking items. $ER_{i,k}$ is the ending point of $Region_{i,k}$ in which the batch i is picked by picker k ($ER_{i,k} = f$). The pick time of batch i at pick face f cannot simply be calculated as the number of items multiplied by the unit pick time of a picker (i.e., $P_{i,f} = PT_k \cdot NB_{i,f}$). This is because the items listed in batch i at pick face f are picked by two pickers in this case. The upstream picker picks the first part of the items, then transfers the tote to the downstream picker to complete the remaining picking job. The pick time of the upstream picker is $\Delta ER_{i,k}$ (how to calculate $\Delta ER_{i,k}$ will be explained later), and the remaining pick time of the downstream picker is the remaining number of items multiplied by the unit pick time of picker $k+1$, which can be expressed as $PT_{k+1} \cdot \left(NB_{i,f} - \frac{\Delta ER_{i,k}}{PT_k}\right)$. Therefore, the pick time of batch i at pick face f when it is picked by two pickers can be expressed as:

$$P_{i,f} = \Delta ER_{i,k} + PT_{k+1} \cdot \left(NB_{i,f} - \frac{\Delta ER_{i,k}}{PT_k}\right) \ \forall i \epsilon B, \forall f \epsilon F, \forall k \epsilon K \qquad (A.1)$$

It is worth noting that we assume the downstream picker could interrupt the pick progress even if the upstream picker is in the middle of picking an item. Therefore, it is possible that the number of items picked by a picker is not an integer.

In the "meet in walking" case, as shown in Figure 3-12(b), picker k and picker $k+1$ meet at pick face f when the upstream picker is walking after picking items. Since all pickers have the same walk velocity, the "meet in walking" case would not affect the walk time of batch i at pick face f.

The "meet in blocking case" is more complex than the two cases above, as three pickers are involved, as shown in Figure 3-12(c). We will analyze the pickers' behavior one by one. Picker $k+2$ walks back with empty hands to take over a tote from the upstream picker $k+1$. When the two pickers meet, picker $k+1$ is picking items for batch $i-1$ at the start of pick face f. Then picker $k+2$ takes over the tote of batch $i-1$ and continues to pick items. The pick time of batch $i-1$ at pick face f is the pick time of picker $k+1$ for batch $i-1$ plus the pick time of picker $k+2$ for batch $i-1$, which can be expressed as $P_{i-1,f} = \Delta ER_{i-1,k+1} + PT_{k+2} \cdot \left(NB_{i-1,f} - \frac{\Delta ER_{i-1,k+1}}{PT_{k+1}}\right)$. Picker $k+1$, after transferring the tote to picker $k+2$, should walk back for a new tote. Then he/she finds Picker K at the end of pick face $f-1$, just behind him/her. Therefore, picker k transfers the tote to picker $k+1$ instantaneously. The block time of batch i at the end of pick face $f-1$ is the time when batch $i-1$ leaves pick face f minus the time when batch i arrives at the end of pick face $f-1$, which can be expressed as $D_{i,f-1} = (ST_{i-1} + CP_{i-1,f} + CW_{i-1,f} + CD_{i-1,f}) - (ST_i + CW_{i,f-1} + CP_{i,f-1} + CD_{i,f-2})$. Picker k walks back for a new tote after transferring the tote to picker $k+1$. Due to the special situation, $ER_{i-1,k+1}$, and $ER_{i,k}$ overlap at the same place, which is the start of pick face *f* or the end of pick face *f–1*.

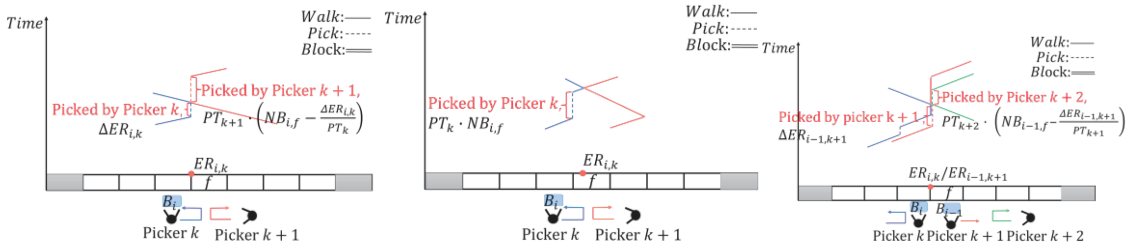

Figure 3-12 Three different meeting cases: (a) meeting in picking, (b) meeting in walking, (c) meeting in blocking.

Hand-off Period

Every batch in every pick face has a hand-off period. If the time when the downstream picker $k+1$ walks back at pick face f is in the hand-off period, two pickers meet in pick face f, as shown in Figure 3-13. The hand-off period of batch i at pick face f starts when batch i leaves pick face $f-1$ (i.e., enters pick face f) which can be expressed as:

$$L_{i,f-1} = ST_i + CP_{i,f-1} + CW_{i,f-1} + CD_{i,f-1} \; \forall i \epsilon B,\ \forall f \epsilon F \cup \{0, n+1\} \qquad (A.2)$$

and ends when batch i leaves pick face f if the two pickers did not meet, which can be expressed as $L_{i,f-1} + MP_{i,f} + WT + MD_{i,f}$. $MP_{i,f}$ is the maximum pick time of batch i at pick face f, which can be thought of as the pick time of batch i at pick face f if two pickers did not meet:

$$MP_{i,f} = \begin{cases} 0 & if\ f = 0\ or\ n+1 \\ PT_k \cdot NB_{i,f} & otherwise \end{cases} \quad \forall i\epsilon B, \forall f\epsilon F \cup \{0, n+1\}, \forall k\epsilon K \qquad (A.3)$$

If the two pickers meet at pick face f, the pick time becomes shorter, since the downstream picker is faster than the upstream picker. Therefore, it is called the *maximum pick time*. $MD_{i,f}$ is the maximum blocking delay time of batch i at pick face f, which can be expressed as the leaving time of batch $i-1$ at pick face $f+1$ minus the time batch i arrives at the end of pick face f if two pickers did not meet:

$$MD_{i,f} = \begin{cases} max\left\{\left(L_{i-1,\,f+1} - \left(ST_i + CW_{i,f}\right)\right), 0\right\} & if\ f = 0 \\ 0 & if\ f = n+1 \\ \max\left\{\left(L_{i-1,\,f+1} - \left(L_{i,\,f-1} + MP_{i,\,f} + FW_{i,f}\right)\right), 0\right\} & otherwise \end{cases} \quad \forall i\epsilon B, \forall f\epsilon F \cup \{0, n+1\} \qquad (A.4)$$

The condition that the time when the downstream picker $k+1$ walks back at pick face f is in the hand-off period of batch i at pick face f can be expressed as:

$$L_{i,f-1} < LB_{i-1,k+1} + \left(ER_{i-1,k+1} - |f|\right) \cdot BT \leq L_{i,f-1} + MP_{i,f} + WT + MD_{i,f} \qquad (A.5)$$

$LB_{i-1,k+1}$ is the time when picker $k+1$ hands-off batch $i-1$ to picker $k+2$ and walks back, and $(ER_{i-1,k+1} - |f|) \cdot BT$ is the walking back time cost from $ER_{i-1,k+1}$ to the start of the pick face f.

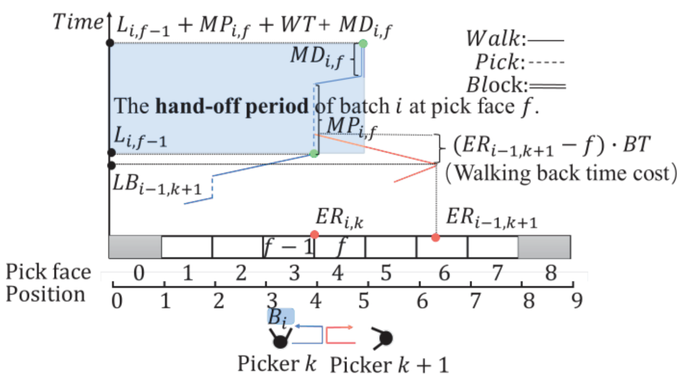

Figure 3-13 Two pickers meet at pick face f in the hand-off period.

Position of Hand-off Process Occurring

The position at which the hand-off process occurs can be calculated based on three different operation statuses of an upstream picker when two pickers meet. In the "meet in picking" case, the upstream picker is picking items for batch i at the start of pick face f when the hand-off process occurs. Therefore, the ending point of $Region_{i,k}$, where batch i is picked by picker k, is $|f|$ (i.e., $ER_{i,k} = |f|$). In the "meet in blocking" case, the upstream picker is blocked at the end of pick face f with batch i when the hand-off process occurs. Therefore, the ending point of $Region_{i,k}$ is $|f| + 1$. In the "meet in walking" case, the upstream picker is walking in pick face f with batch i when the hand-off process occurs. An equation for when the two pickers meet can be formulated. The upstream picker hands off batch i at the time after finishing picking items and walking in the distance $ER_{i,k} - |f|$, which can be expressed as $L_{i,f-1} + P_{i,f} + (ER_{i,k} - |f|) \cdot WT$. The downstream picker takes over batch i at the time after walking back from the place where the previous hand-off process occurred to the position of the upstream picker, which can be expressed as $LB_{i-1,k+1} + \left(ER_{i-1,k+1} - ER_{i,k}\right) \cdot BT$, as shown in Figure 3-14. The equations to calculate $ER_{i,k}$ are summarized as follows:

$$\begin{cases} ER_{i,k} = |f| & \text{meet in picking} \\ ST_i + \left(ER_{i,k} - |f|\right) \cdot WT = LB_{i-1,k+1} + \left(ER_{i-1,k+1} - ER_{i,k}\right) \cdot BT & \text{meet in walking}, \text{if } f = 0 \\ L_{i,f-1} + P_{i,f} + \left(ER_{i,k} - |f|\right) \cdot WT = LB_{i-1,k+1} + \left(ER_{i-1,k+1} - ER_{i,k}\right) \cdot BT & \text{meet in walking}, \text{otherwise} \\ ER_{i,k} = |f| + 1 & \text{meet in blocking} \\ ER_{i,k} = n + 1 & \text{if } k = |K| \end{cases} \quad \forall i \epsilon B, \forall f \epsilon F \cup \{0, n+1\}, \forall k \epsilon K \qquad (A.6)$$

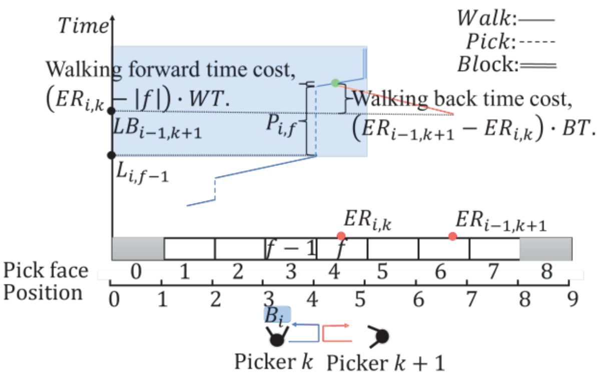

Figure 3-14 Time point of two pickers meeting when the upstream picker is walking.

Walking-back Time and Start Time

After the hand-off process occurs, the upstream picker k should walk back to take over a batch. The time the upstream picker k walks back can be thought of as the time when the downstream picker $k+1$ meets him/her since the time cost of the hand-off process is neglected. This can be expressed as:

$$LB_{i,k} = \begin{cases} ST_i + CP_{i,n+1} + CW_{i,n+1} + CD_{i,n+1} \; if \; k = |K| \\ LB_{i-1,k+1} + \left(ER_{i-1,k+1} - ER_{i,k}\right) \cdot BT \;\; otherwise \end{cases} \forall i \epsilon B, \forall f \epsilon F \cup \{0, n+1\}, \forall k \epsilon K \; (A.7)$$

For the last picker $|K|$, $LB_{i,k}$ represents when batch i is completed at unloading station $n+1$. The start time of batch i can be thought of as the time the first picker walks back from the $ER_{i-1,1}$ (the end point of $Region_{i-1,1}$ in which batch $i-1$ is picked by picker 1) at $LB_{i-1,1}$ (the time when picker 1 walks back), plus the time cost of walking back from $ER_{i-1,1}$ to the loading station, which can be expressed as:

$$ST_i = LB_{i-1,1} + ER_{i-1,1} \cdot BT \quad \forall i \epsilon B \qquad (A.8)$$

Time an Upstream Picker Spends at the Endpoint of a Region

$\Delta ER_{i,k}$ is the time an upstream picker k has spent at $ER_{i,k}$ after entering pick face f when the hand-off process occurs. This value can be used to detect the operation status of the upstream picker. There are three cases when two pickers meet ("meet in picking," "meet in walking," and "meet in blocking"), and each case corresponds to a specific period of the hand-off period, as shown in Figure 3-15. If $\Delta ER_{i,k}$ is smaller than the maximum pick time of batch i at pick face f (i.e., $0 \leq \Delta ER_{i,k} < MP_{i,f}$), two pickers "meet in picking." If $\Delta ER_{i,k}$ is larger than $MP_{i,f}$ but smaller than the time the upstream picker reaches the end of pick face f (i.e., $MP_{i,f} \leq \Delta ER_{i,k} < MP_{i,f}$ +WT), the two pickers "meet in walking". If $\Delta ER_{i,k}$ is larger than the time the upstream picker reaches the end of pick face f but smaller than the time when picker k leaves pick face f (i.e., $MP_{i,f}$+WT $\leq \Delta ER_{i,k} <$ $MP_{i,f}$+WT+$MD_{i,f}$), the two pickers "meet in blocking." The relationships can be summarized as follows:

$$\begin{cases} 0 \leq \Delta ER_{i,k} < MP_{i,f} & \rightarrow \text{ meet in picking} \\ MP_{i,f} \leq \Delta ER_{i,k} < MP_{i,f} + \text{WT} & \rightarrow \text{ meet in walking} \\ MP_{i,f} + \text{WT} \leq \Delta ER_{i,k} < MP_{i,f} + \text{WT} + MD_{i,f} & \rightarrow \text{ meet in blocking} \end{cases} \qquad (A.9)$$

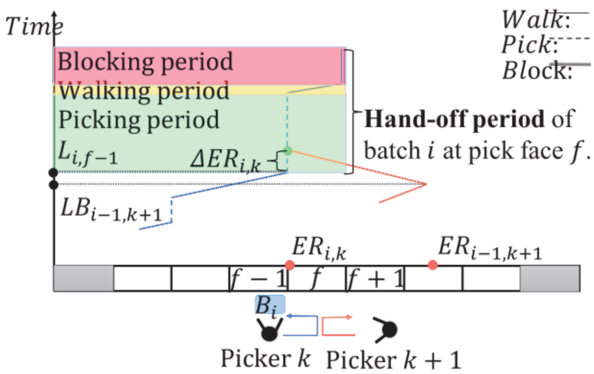

Figure 3-15 Three time periods of the hand-off period.

The time the upstream picker meets the downstream picker is the time picker k with batch i enters pick face f plus $\Delta ER_{i,k}$, which can be expressed as $L_{i,f-1} + \Delta ER_{i,k}$. The time the downstream picker meets the upstream picker is the time picker $k+1$ walks back from $ER_{i-1,k+1}$ plus the walk-back time cost$(ER_{i-1,k+1} - ER_{i,k}) \cdot BT$, which can be expressed as $LB_{i-1,k+1} + (ER_{i-1,k+1} - ER_{i,k}) \cdot BT$. Since these two time points should be equal, an equation can be derived to calculate $\Delta ER_{i,k}$, as follows:

$$L_{i,f-1} + \Delta ER_{i,k} = LB_{i-1,k+1} + \left(ER_{i-1,k+1} - ER_{i,k}\right) \cdot BT$$

$$\Delta ER_{i,k} = LB_{i-1,k+1} + \left(ER_{i-1,k+1} - ER_{i,k}\right) \cdot BT - L_{i,f-1} \quad \forall i \epsilon B, \forall f \epsilon F \cup \{0, n+1\}, \forall k \epsilon K \ (A.10)$$

Chapter 4 An Enhanced Bucket Brigade Order Picking System with a Conveyor

4.1 Introduction

Order picking is a process wherein pickers retrieve items listed in orders from a warehouse (Bansal & Roy, 2021). Bucket brigade OPSs exhibit high efficiency due to the bucket brigade concept's dynamically arranging human labor and workload without requiring management intervention (Fibrianto & Hong, 2019). This concept enables the attainment of the maximum possible production rate when compared to various other methods of organizing workers and workstations for typical production lines (Bartholdi & Eisenstein, 1996a).

The efficiency of bucket brigade OPSs, however, could still be further improved. In the context of bucket brigade OPSs, pickers expend a significant amount of time walking to the unloading station to unload totes containing completed order items and to the loading station to load new totes for upcoming orders (Fontana et al., 2019). To mitigate these costs, we propose the incorporation of a conveyor into bucket brigade OPSs.

The use of conveyors is commonplace in the warehousing industry (Füßler & Boysen, 2017; Yang et al., 2022). Conveyors play a vital role in enhancing the productivity of OPSs by facilitating the efficient transportation of totes from one picking zone to another (Wu et al., 2016) and between different pickers (Ho et al., 2023). In our proposed OPS, a conveyor is introduced and designed to transport totes to the unloading station and introduce new totes to pickers, thereby optimizing the overall process and reducing operational expenses.

4.2 Bucket Brigade Order Picking Systems

This section elucidates the operational principles of bucket brigade OPSs and analyzes the issues that affect the productivity of the OPSs.

4.2.1 Operational Principles of Bucket Brigade OPSs

The operation of the bucket brigade OPS we are examining is adapted from a previous study by Hong et al. (2016), as shown in Figure 4-1, where K pickers work in a linear picking line with a set of pick faces F to process a set of orders O. A picker picks $OP_{o,f}$ items for order o at pick face f and puts the items into a tote. Several items are stored in pick faces, and the different shapes indicate that they are listed in different orders. The number of items in each order and the location of the items follow a uniform distribution. A loading station (L) is positioned at the outset of the pick faces, facilitating the release of empty totes. An unloading station (U) is established at the opposite end, where the last picker unloads totes laden with picked items. These components collectively constitute a picking line, along which K pickers traverse, picking items from the pick faces and depositing them into totes. Each picker possesses an individual unit pick time PT_k and the same unit walking time WT. Each pick face allows only one picker to pick items, and pickers cannot pass over other pickers.

In Bucket Brigade OPSs, pickers adhere to the following rules for order picking:

Forward Rules. A picker moves forward along the picking line, picking items and placing them into a tote until either the tote is taken by his/her successor or the order picking for the current order is completed.

(a) If the tote is taken by his/her successor, the picker switches to following the backward rules.

(b) If the order picking is completed, the picker walks to the unloading station to unload the tote and then follows the backward rules.

Backward Rules. The picker walks backward along the line, taking over a tote from his/her predecessor (or the first picker picks up a new tote at the loading station to start a new order picking). Then the picker starts to follow the forward rules.

4.2.2 Unproductive Walking Behavior for Unloading and Introducing Totes

Figure 4-1 is an operational example of a bucket brigade OPS. Figure 4-1(a) depicts a situation in which pickers pick items and move forward. In Figure 4-1(b), Picker 3 walks backward to take over a tote after unloading the filled tote at the unloading station. Figure 4-1(c) shows that, when the two pickers meet, the upstream picker hands the tote to the downstream picker and walks back for a new tote. In Figure 4-1(d), the first picker introduces a new tote at the loading station and starts picking items. These four steps describe the operational principle of a typical bucket brigade OPS.

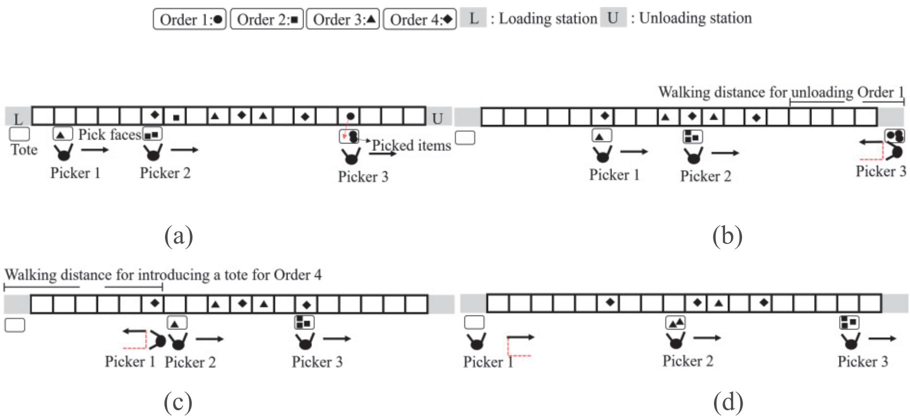

Figure 4-1 Operational example of a bucket brigade OPS.

Specific unproductive walking behaviors during operations, however, can significantly undermine the efficiency of the OPS. In Figure 4-1(b), even after Picker 3 has completed picking all items for Order 1, he/she is still required to walk to the unloading station to unload the totes related to that order. In Figure 4-1(c), upon handing over the tote to Picker 2, Picker 1 must traverse a considerable distance back to introduce a new tote for Order 4. The unproductive walking behavior illustrated in Figure 4-1(b) and Figure 4-1(c) profoundly impairs the overall efficiency of the OPS.

4.3 Proposed Order Picking System

To mitigate the pickers' unnecessary walking behaviors in bucket brigade OPSs, we introduced an enhanced bucket brigade OPS that incorporates a conveyor. The functions of the conveyor are adopted from the study of Zivanic et al. (2019) and enable it to transport totes along a picking line, make a tote stop at any place, and introduce totes into the picking line. Pickers adhere to the subsequent rules for order picking, and the conveyor fulfils the following functions.

4.3.1 Conveyor Functions

(a) The conveyor can transport totes from the upstream to the downstream of the picking line.
(b) The conveyor can automatically unload totes at any position along the pick line.
(c) The conveyor transports a new tote from the loading station to the first picker's position or the pick face storing the first item listed in the order, when the first picker commences moving backward.

4.3.2 Forward Rules

(a) The forward rules of the proposed OPS are the same as the forward rules of the bucket brigade OPSs, except for case (b), which is revised as follows:
(b) If the order picking is completed, the picker places the tote on the conveyor, then follows the backward rules.

4.3.3 Backward Rules

The picker walks backward along the line, taking over a tote from his/her predecessor (except for the first picker). The picker then begins to follow the forward rules. The first picker adheres to one of the following possible backward rules based on the position from which he/she starts walking backward and the position of the pick face that stores the first item listed in the next order:

(a) If the pick face is between the unloading station and the current position of Picker 1, Picker 1 walks backward to the pick face to take a new tote.
(b) If the pick face is not situated between the unloading station and the current position of Picker 1, Picker 1 does not move but waits for the conveyor to transport the tote to him/her.

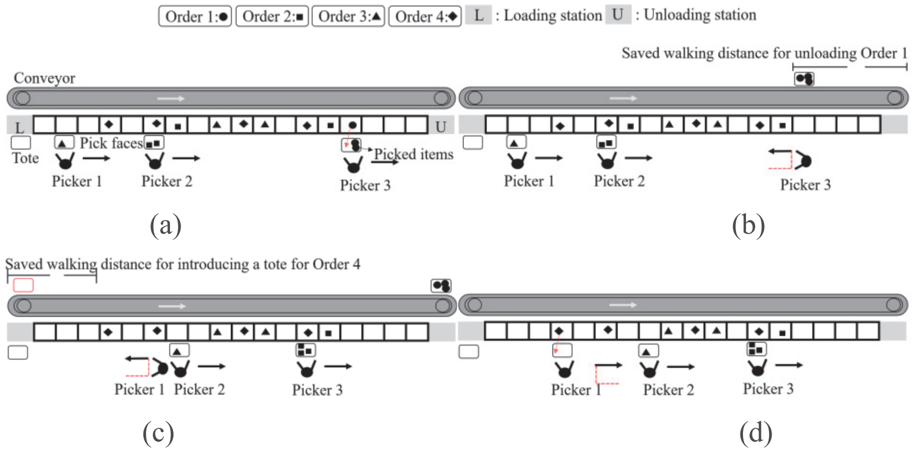

Figure 4-2 Operational example of a proposed order picking system.

Figure 4-2 illustrates an operational example of the proposed OPS. Apart from the placement of a conveyor near the picking line, the remaining components are consistent with the original bucket brigade OPS. Figure 4-2(a) portrays a scenario where pickers are actively engaged in picking items and moving forward. In Figure 4-2(b), Picker 3 completes picking the last item in Order 1, places the tote on the conveyor, and proceeds to walk back in order to acquire a tote. Figure 4-2(c) depicts the conveyor transporting a new tote to Picker 1 as he/she walks back after passing the tote to the downstream picker. Figure 4-2(d) illustrates Picker 1 retrieving the tote and commencing the item-picking process. These four steps succinctly elucidate the operational principle of the proposed OPS.

There are three potential scenarios when Picker 1 introduces a new tote. The first scenario occurs when the tote arrives at the pick face containing the first item listed in the subsequent order. In this case, the tote is unloaded at the pick face and awaits Picker 1 to retrieve it. In the second scenario, Picker 1 reaches the pick face before the tote, resulting in the picker's waiting at the pick face for the tote's arrival. The third scenario involves the pick face's not being positioned between the unloading station and Picker 1's current location. Consequently, Picker 1 remains stationary, waiting on the conveyor to transport the tote to his/her position.

4.4 Simulation Experiment

4.4.1 Conditions

Table 4-1 Conditions of the Simulation Experiment.provides an overview of the simulation environments employed in the experimental simulations. The picking line encompasses 20 pick faces, along with loading and unloading stations. Each pick face spans one unit in length, and the picking process involves three pickers. The time taken by picker k to pick an individual item is denoted as PT_k. Notably, backward walking time is set at twice the rate of forward walking time, as forward movement involves carrying a tote laden with items, whereas backtracking is done empty-handed.

Table 4-1 Conditions of the Simulation Experiment.

Configuration	Values
Picker capability	$[PT_1, PT_2, PT_3]$ = [1.1, 1.0, 0.9]
OPS sizes	20 pick faces
Number of items per order	Uniform distribution [min, max] = [4, 6]
Location of items	Uniform distribution [starting position, ending position] = [pick face 1, pick face 20]
Forward walk time	0.1 unit time/pick face
Backward walk time	0.05 unit time/pick face
Conveyor's velocity	20 pick faces/unit time
Performance measure	TWT (total walking time), Utilization, Y, LCT (the last order's completion time)
Number of orders	15
Initial positions of pickers	Picker 1: 0, Picker 2: 8, Picker 3: 14
Number of items in the initial order	0.25 items/pick face

The size of each order is randomly chosen from a uniform distribution [min, max] = [4, 6]. Additionally, the allocation of items within each order follows a uniform distribution [starting position, ending position] = [pick face 1, pick face 20]. Each experimental run comprises a set of 15 randomly generated orders, and the entire experiment is replicated five times. In each run, the orders are generated anew in a random manner, as shown in Table 4-1.

The performance evaluation of the OPSs encompasses four dimensions: the last Order's Completion Time (LCT), Utilization as the picking time percentage over total operation time, and Total Walking Time (TWT), encompassing both forward and backward walking durations.

In the simulation experiments, the initial status of the OPS is manually configured. This is done to prevent pickers from walking backward simultaneously, which could cause blockages. To address this, an initial order is assumed to exist in the OPS. Within the initial order, each pick face stores 0.25 items. Pickers are allowed to walk back after picking items for the initial order. The starting positions of the pickers are set at 0, 8, and 14. It is worth noting that the initial order does not exist in the real picking line; it is only set to determine the time and position at which pickers walk back.

4.4.2 Results and Discussion

Describing the Behaviors of Pickers

Figure 4-3 illustrates the time charts generated by our simulation programs (details of the simulation program's development are omitted). These time charts provide insights into the actions of pickers and the conveyor within the picking line. The horizontal axis represents the picking line, which comprises 20 pick faces, a loading station (located at positions 0–1), and an unloading station (located at positions 21–22). The vertical axis corresponds to time. Various colored lines on the chart depict the actions of three pickers and the conveyor: red for Picker 1 (P 1), green for Picker 2 (P 2), blue for Picker 3 (P 3), and black for the Conveyor (C).

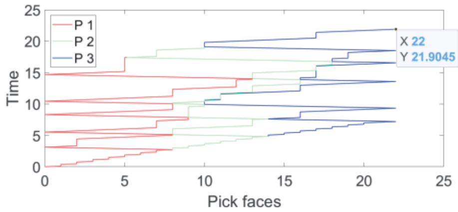

(a) Bucket Brigade OPS

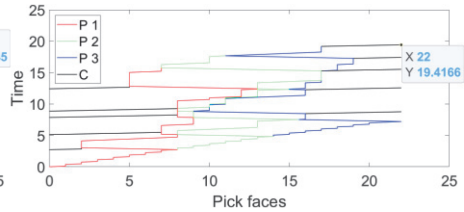

(b) Proposed OPS

Figure 4-3 Time charts generated by the simulation program.

When a line increases vertically, it indicates that a picker is picking items at the start of a pick face. When a line grows inclinationally, it signifies that the picker is walking along the picking line. When two different color lines coincide vertically, it means that a blocking delay between pickers is occurring. When two lines of different colors intersect, it signifies that the upstream picker is passing a tote to the downstream picker or that the first picker is taking a new tote from the conveyor.

Sixteen orders are introduced into the picking line, with the initial order starting at (0, 0). To simplify the time charts, we show only the operations of the picker processing the first six orders (five randomly generated orders and one initial order). The initial order's work content is manually set to store 0.25 items at each pick face, establishing the OPS's initial conditions. For orders 2–16, work content follows a random generation process conforming to the uniform distribution outlined in Table 1.

In Figure 4-3(a), which represents the time chart for the bucket brigade OPS, when the last picker walks forward to horizontal position 22, a tote with the completed order's items is unloaded at the unloading station, signifying the completion of the order processing. Subsequently, as the first picker walks back to horizontal position 0, a new tote for the next order is introduced into the picking line.

In Figure 4-3(b), illustrating the time chart for the proposed OPS, the conveyor operates by transporting totes with completed order items to the unloading station (shown as black lines on the right side of the figure) and new totes for the next orders to the first picker (shown as black lines on the left side of the figure). The walking time of pickers is reduced because the conveyor assists them in loading and unloading totes, thereby improving the OPS's productivity.
By analyzing the last order's completion times for both OPSs within the time charts, the degree of improvement can be computed using the formula $|(19.4166 - 21.9045)/21.9045| \times 100\%$, resulting in a 11.36% enhancement of productivity.

Performance Comparison

The performance of the OPSs was assessed and compared using a simulation program. Fifteen orders, as specified in Table 1, were randomly generated, with an initial order manually set. The simulation program was employed to model order processing in both the bucket brigade OPS and the proposed OPS, and the results are summarized in Table 2. These experiments were conducted over five repeated runs.

Table 4-2 presents the following metrics for both OPSs after processing all 15 randomly generated orders: total walking time (TWT), picking time percentage over the total operation time (Utilization), and the last order's completion time (LCT). In the Proposed OPS section of Table 2, RD represents the relative difference in TWT and LCT between the bucket brigade OPS and the proposed OPS, while D indicates the difference in Utilization between the bucket brigade OPS and the proposed OPS. The first column lists the repeated cases, and the "Average" row presents the average results from these five repeated cases.

In the bucket brigade OPS, the total walking time (TWT) for 15 orders remains constant. This is because, during forward picking operations, orders are consistently moved from the loading station to the unloading station (i.e., from horizontal position 0 to 22). Similarly, during backward order introduction operations, the pickers always walk back from the unloading station to the loading station (i.e., from horizontal position 22 to 0), except for Orders 1 and , for which pickers need only walk back from horizontal positions 8 and 14, respectively, after picking items for the initial order.

Table 4-2 Performance Comparison Between the Bucket Brigade OPS and the Proposed OPS.

	Bucket Brigade OPS			Proposed OPS		
	TWT	Utilization	LCT	TWT (RD)	Utilization (D)	LCT (RD)
Case 1	48.4	59.46%	51.11	32.15 (-33.57%)	67.81% (+8.35)	46.42 (-9.18%)
Case 2	48.4	57.19%	51.36	27.40 (-43.39%)	67.57% (+10.38)	45.53 (-11.36%)
Case 3	48.4	60.48%	50.43	32.45 (-32.95%)	68.01% (+7.53)	46.00 (-8.79%)
Case 4	48.4	59.90%	49.5	31.37 (-35.18%)	67.47% (+7.57)	44.72 (-9.65%)
Case 5	48.4	58.99%	53.03	29.95 (-38.12%)	67.88% (+8.90)	48.12 (-9.26%)
Average	48.4	59.20%	51.09	29.95 (-36.64%)	67.75% (+8.55)	46.16 (-9.65%)

Notes.

TWT: The total walking time required by pickers to complete order picking for the randomly generated orders.

Utilization: The total picking time over the total operation time.

LCT: The time the last order is completed.

RD: The relative difference between the bucket brigade OPS and proposed OPS, calculated by the following formula:

$$\frac{result\ of\ proposed\ OPS - result\ of\ bucket\ brigade\ OPS}{result\ of\ bucket\ brigade\ OPS} \times 100\% .$$

D: The difference between the bucket brigade OPS and proposed OPS, calculated by the following formula:
$result\ of\ proposed\ OPS - result\ of\ bucket\ brigade\ OPS$.

In the proposed OPS, however, TWT exhibits variability due to differing work-content distribution among various orders. During forward picking operations, pickers have the option to place a tote on the conveyor once all items for an order are picked. Subsequently, the conveyor transports the tote to the unloading station. In the context of backward order introduction operations, the conveyor facilitates the delivery of a new tote to the pick face of the first item or to the position of the first picker as soon as the first picker hands off the tote to the downstream picker. This leads to a range of TWT reductions, varying from 32.95% to 43.39%, with an average reduction of -36.64%, expressed as the relative difference (RD). Notably, instances where the last item of an order is positioned far from the end of the picking line or the first item is situated far from the start of the line demonstrate greater TWT reduction potential.

The reduction in walking behavior leads to a relative increase in pickers' time for picking tasks over total operation time, thus boosting use by 7.53% to 10.38%, with an average increase of 8.55% as the difference (D). Moreover, the LCT witnesses a reduction ranging from 8.79% to 11.36%, with an average reduction of 9.65% as the relative difference. This improvement can be attributed to the conveyor system's support in loading and unloading totes. By streamlining these processes, the time required to complete order picking is reduced.

Sensitivity Analysis

Order Size

Among these conditions, order size has the most significant effect on the performance of the proposed OPS. The main objective of the proposed OPS is to reduce the walking distance of pickers during the loading and unloading of orders by using the conveyor. When the number of items in an order increases, the probability that these items are located at the beginning and end of the picking line also increases. As a result, the distance over which the conveyor can be used during the loading and unloading process decreases.

Figure 4-4 illustrates the effect of order size on walking time for both the proposed and bucket brigade OPSs. The horizontal axis represents the mean order size, while the vertical axis represents the total walking time. We calculated the total walking time required by pickers to complete order picking for 15 randomly generated orders in both the bucket brigade OPS and the proposed OPS. The orders' sizes were generated using a uniform distribution with a range of $\left[\frac{mean}{2}, mean \cdot \frac{3}{2}\right]$ (Fibrianto & Hong, 2019), and the mean value varied from 4 to 24.

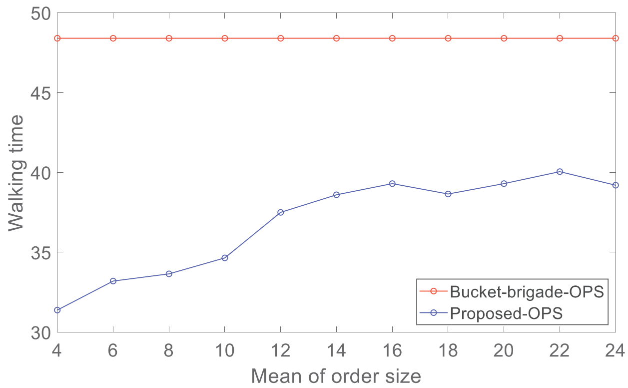

Figure 4-4 Total walking time of bucket brigade OPS and proposed OPS with various order sizes.

In Figure 4-4, we notice that, as the mean value increases from 4 to 16, the total walking time in the proposed OPS also increases. This is due to the reduced use of the conveyor over shorter distances for loading and unloading orders. When the mean value continues to increase from 16 to 24, however, the total walking time is not significantly affected by order size because the items in orders are already distributed along the entire picking line. Nevertheless, the total walking time of the proposed OPS remains shorter than that of the bucket brigade OPS. This is because the conveyor in the proposed OPS saves, at a minimum, the walking distance for pickers in the loading and unloading stations, as well as the last pick face.

Walking Velocity, OPS Size, and Conveyor Velocity

Aside from order size, several other factors that may influence the performance of the proposed OPS are discussed, including picker walking velocity, OPS size, and conveyor velocity.

To simplify the process of setting conditions for different scenarios, the conditions in the simulation experiment are considered as a standard scenario and are summarized as follows: Walking velocity (medium): Forward: 10 pick faces/unit time, backward: 20 pick faces/unit time. Conveyor's velocity (medium): 20 pick faces/unit time. OPS size (medium): 20 pick faces. The following scenarios were derived from the standard scenario by adjusting specific conditions to either smaller or larger values:

Slow walking scenario: Forward: 5 pick faces/unit time, backward: 10 pick faces/unit time.

Fast walking scenario: Forward: 20 pick faces/unit time, backward: 40 pick faces/unit time.

Slow conveyor scenario: 10 pick faces/unit time.

Fast conveyor scenario: 40 pick faces/unit time.

Small OPS size scenario: 10 pick faces.

Large OPS size scenarios: 40 pick faces

The effect of the conditions related to the pickers, the picking line, and the conveyor can be observed in Table 4-3. As the walking velocity of pickers increases, both TWT and LCT decrease, while use increases in both the bucket brigade OPS and the proposed OPS. Notably, the relative difference (RD) of TWT is not influenced by changes in walking velocity. We can infer this based on the formula for calculating the RD of TWT, which can be expressed as $\frac{-\text{saved walking distance} \times (\text{forward walking velocity} + \text{backward walking velocity})}{\text{total walking distance in bucket brigade OPS} \times (\text{forward walking velocity} + \text{backward walking velocity})} \times 100\%$. This formula indicates that the RD of TWT remains constant regardless of walking velocity changes.

Table 4-3 Performance Comparison Across Varied Walking Velocity, Conveyor Velocity, and OPS Size.

	Bucket Brigade OPS			Proposed OPS		
Scenario	TWT	Utilization	LCT	TWT (RD)	Utilization (D)	LCT (RD)
Standard	48.40	59.46%	51.11	32.15 (-33.57%)	67.81% (+8.35)	46.42 (-9.18%)
Slow walking	96.80	44.13%	68.14	64.40 (-33.47%)	53.21% (+9.08)	58.89 (-13.57%)
Fast walking	24.20	71.83%	42.41	16.14 (-33.32%)	78.59% (+6.76)	40.24 (-5.12%)
Slow conveyor	48.40	59.46%	51.11	32.15 (-33.57%)	68.17% (+8.71)	46.92 (-8.19%)
Fast conveyor	48.40	59.46%	51.11	32.15 (-33.57%)	67.62% (+8.16)	46.23 (-9.54%)
Small OPS size	26.45	66.11%	44.44	13.90 (-47.45%)	73.80% (+7.69)	41.94 (-5.62%)
Large OPS size	92.35	45.41%	67.08	65.87 (-28.67%)	53.16% (+7.75)	58.97 (-12.10%)

The velocity of the conveyor does not significantly affect the performance of the proposed OPS because the TWT, use, and LCT of the proposed OPS have only a minor likelihood of being affected by the conveyor's speed. The use and LCT of the proposed OPS are related to TWT. Conveyor velocity can affect TWT only in cases where the first picker must wait for the conveyor to transport a new tote to him/her. In most situations, however, the tote waits for the first picker to pick it up. The first situation occurs only when the first item is located far from the start of the picking line.

As the OPS size increases, both TWT and LCT increase, while use decreases in both the bucket brigade and proposed OPSs. This happens because pickers need more time to travel within the larger picking line. The increasing RD of the TWT indicates that the proposed OPS achieves better improvements in smaller OPS sizes. The formula for calculating the RD of the TWT can be further translated as $\frac{-\text{saved walking distance}}{\text{total walking distance in bucket brigade OPS}} \times 100\%$. The saved walking distance does not increase as rapidly as the total walking distance in the bucket brigade OPS.

This is because the saved walking distance always includes the last pick face, as well as the loading and unloading stations. Even as the OPS size increases, the length of these stations and pick faces remains constant at 1 unit. Therefore, the improvement initially decreases as the OPS size increases. It eventually stabilizes within a certain range, however, because the effect of the last pick face and loading and unloading stations on the saved walking distance becomes negligible in larger OPS sizes. This conclusion is confirmed by the following Figure 4-5, which illustrates the effect of OPS size on TWT. Figure 4-5(a) shows the TWT for various OPS sizes, ranging from 10 pick faces to 60 pick faces. In both OPS types, TWT increases as the OPS size increases. The RD of TWT initially increases, then stabilizes at a value close to -35%, as shown in Figure 4-5(b).

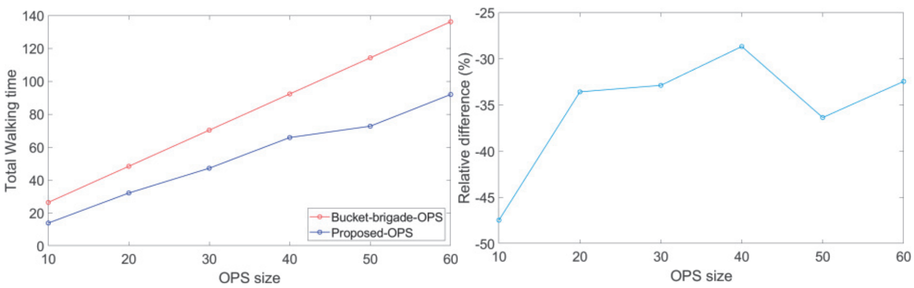

(a) (b)

Figure 4-5 Effect of OPS size on total walking time, (a) total walking time with various OPS sizes, (b) relative difference of total walking time with various OPS sizes.

4.5 Summary

In this chapter, we developed an enhanced bucket brigade OPS with a conveyor, aimed at mitigating unproductive walking behaviors among pickers within bucket brigade OPSs. The comparative experiment yielded compelling results: when contrasted with the traditional bucket brigade OPS, the proposed system achieved a remarkable 36.64% reduction in pickers' walking time cost and a notable 9.65% enhancement in productivity. In our further work, we will introduce operational rules designed for the middle-section pickers to effectively reduce walking time costs by using the conveyor.

Chapter 5 Conclusions and Future Research

5.1 Conclusions

The main purpose of this dissertation was to study systems that have adopted the bucket brigade concept in production and order picking and to enhance the efficiency of these systems. By reproducing models from previous literature through programming, the advantages and disadvantages of these models have been identified. To address the disadvantages, this dissertation proposes several new models in chapters 2, 3, and 4.

In chapter 2, a cellular bucket brigade production system with collaboration models was studied and two collaboration models proposed to enhance production efficiency. These models aim to address two specific problems identified in the existing models. One problem is the underperformance of existing collaborative models in achieving higher throughput in certain scenarios due to design limitations. Another issue is the complexity of worker-operation principles and the occurrence of many unproductive movements. Through numerical experiments, the proposed models demonstrate significant improvements in throughput figures compared to the previous model.

In chapter 3, bucket brigade OPSs with order batching were studied. An algorithm was proposed to simulate the operation of the bucket brigade OPS, along with an order batching model aimed at reducing the blocking time in these systems. The Balanced Batching Model for Bucket Brigade (BBMB) demonstrated increased productivity in bucket brigade OPSs, particularly when handling many small orders. Compared to the previous model, the BBMB model reduces the blocking-time percentage from 4.46–12.5% to 0.26–5.66% across various simulation experiment scenarios.

In chapter 4, the operation of bucket brigade OPSs was studied. An enhanced bucket brigade OPS with a conveyor was proposed to reduce the walking distance of pickers during the loading and unloading of orders. The proposed system demonstrates significant improvements. Specifically, it reduces the average total walking time cost by 36.64% and increases productivity by 9.65%.

Chapters 2, 3, and 4 study systems that apply the bucket brigade concept and provide methods to solve unproductive issues in these systems. By investigating the contents of these three chapters, a conclusion was derived: these systems consistently exhibit unproductive issues. The issues can be blocking, halting, long travel distances, and more. They occur due to the gap between the ideal and real conditions in the systems and can be solved in the following ways:

The first way is to bring the real conditions closer to the ideal conditions. For example, ideally, the work content should be evenly distributed in a bucket brigade OPS. In a real system, however, the work content is randomly distributed. Therefore, Chapter 3 proposed an order batching model to balance the work content.

The second way is to introduce new tools and devices to reduce unproductive behavior. For instance, Chapter 2 introduced collaborative workstations and buffers to eliminate blocking and halting problems. Chapter 4 introduced conveyors to reduce pickers' travel distance.

This research offers several practical implications for both the production system and the OPS. These implications can contribute to optimizing the assignment of labor and workloads, thus enhancing the efficiency of the systems. The proposed study, however, still has some weaknesses, such as neglecting certain factors in the systems to simplify calculations. When these factors are considered, the proposed models may not be suitable for application, potentially affecting system performance. Therefore, this study can be extended in the future to make the models applicable to a wider range of scenarios.

5.2 Future Research

Considering some weaknesses in the current proposed study, some future research will be considered. For production systems, relaxing the assumptions that the time cost of handover and walking back is zero in the proposed collaboration models would bring the proposed models closer to real life. In actual production environments, these time costs can have a significant effect on overall efficiency and throughput. Therefore, future research should aim to incorporate realistic time costs associated with handovers and walking back into the models. This could involve detailed time-motion studies to quantify these costs and integrate them into the simulation models to better predict the performance and identify potential bottlenecks in the system.

Additionally, exploring the effect of varying these time costs under different operational conditions and worker behaviors would provide deeper insights. For instance, examining how different layouts, worker fatigue, and varying levels of task complexity influence these time costs could lead to more robust and adaptable production systems. Future studies might also investigate the use of automation and technological aids, such as conveyor belts, automated guided vehicles, or collaborative robots, to minimize these time costs.

For OPSs, exploring more methods for batching orders when work-content distributions follow different patterns is crucial. Different patterns, such as uniform, normal, or skewed distributions, can significantly affect the efficiency of order batching and the overall performance of the OPS. Future research should develop and test new batching algorithms that are adaptive to various distribution patterns. This could involve machine-learning techniques to dynamically adjust batching strategies based on real-time data and historical trends.

Discussing the effect of unstable human movements could be a focus of future work because changing the assumptions about human behavior from stable to unstable can make the research more realistic and applicable to real-life scenarios. This research investigated the production system and order picking system that apply the bucket brigade concept. Human labor plays an important role in both systems. To simplify the calculations, the behavior of humans was assumed to be stable. For example, the walking velocity of workers was assumed to be constant. In real life, however, workers' behavior can be affected by fatigue, learning curves, and other factors.

This study primarily focused on improving the throughput of the bucket brigade production system and the bucket brigade order picking system. A truly effective system, however, is not solely dependent on its productivity. Other critical factors, such as quality, cost, delivery, safety, morale, and environment (QCDSME), also play a significant role in evaluating a system's overall performance. Investigating the QCDSME aspects of these systems could be an intriguing direction for future research.

References

Armbruster, D., & Gel, E. S. (2006). Bucket brigades revisited: Are they always effective? *European Journal of Operational Research*, *172*(1), 213–229.

Bahrami, B., Aghezzaf, E. H., & Limère, V. (2019). Enhancing the order picking process through a new storage assignment strategy in forward-reserve area. *International Journal of Production Research*, *57*(21), 6593–6614.

Bansal, V., & Roy, D. (2021) Stochastic modeling of multiline orders in integrated storage-order picking system. *Naval Research Logistics*, *68*(6), 810–836.

Bartholdi, J. J., III, Bunimovich, L. A., & Eisenstein, D. D. (1999). Dynamics of two-and three-worker "bucket brigade" production lines. *Operations Research*, *47*(3), 488–491.

Bartholdi, J. J., III, & Eisenstein, D. D. (1996a). A production line that balances itself. *Operations Research*, *44*(1), 21–34.

Bartholdi, J. J., III, & Eisenstein, D. D. (1996b). Bucket brigades: A self-organizing order picking system for a warehouse. Report, School of Industrial Engineering, Georgia Tech, Atlanta, USA.

Bartholdi, J. J., III, Eisenstein, D. D., & Foley, R. D. (2001). Performance of bucket brigades when work is stochastic. *Operations Research*, *49*(5), 710–719.

Bartholdi III, J. J., & Eisenstein, D. D. (2005). Using bucket brigades to migrate from craft manufacturing to assembly lines. Manufacturing & Service Operations Management, 7(2), 121-129.

Bartholdi, J. J., III, & Eisenstein, D. D. (2006a). Bucket brigade assembly lines. www.bucketbrigades.com

Bartholdi, J. J., III, Eisenstein, D. D., &Lim, Y. F. (2006b). Bucket brigades on in-tree assembly networks[J]. European Journal of Operational Research, 168(3): 870-879.

Bratcu, A. I., & Dolgui, A. (2009). Some new results on the analysis and simulation of bucket brigades (self-balancing production lines). *International Journal of Production Research*, *47*(2), 369–387.

Bukchin, Y., Hanany, E., & Khmelnitsky, E. (2024). Sequencing heterogeneous orders in Bucket Brigade order picking lines. *IISE Transactions*, 1–17.

Casella, G., Volpi, A., Montanari, R., Tebaldi, L., & Bottani, E. (2023). Trends in order picking: A 2007–2022 review of the literature. *Production & Manufacturing Research*, *11*(1), 2191115.

De Carlo, F., Borgia, O., & Tucci, M. (2013). Bucket brigades to increase productivity in a luxury assembly line. *International Journal of Engineering Business Management*, *5*, 28.

Fibrianto, H. Y., & Hong, S. (2019). Dynamic order batching in bucket brigade order picking systems with consecutive batch windows and non-identical pickers. *International Journal of Production Research*, *57*(20), 6552–6568.

Fontana, G. G., Sgarbossa, F., Glock, C. H., & Grosse, E. H. (2019). The effect of worker fatigue on the performance of a bucket brigade order picking system. *IFAC-PapersOnLine*, *52*(13), 2195–2200.

Füßler, D., & Boysen, N. (2017). Efficient order processing in an inverse order picking system. *Computers & Operations Research*, *88*, 150–160.

Gademann, A., Van Den Berg, J. P., & Van Der Hoff, H. H. (2001). An order batching algorithm for wave picking in a parallel-aisle warehouse. *IIE Transactions*, *33*(5), 385–398.

Granotto, G. F., Sgarbossa, F., Glock, C. H., & Grosse, E. H. (2019). The effect of worker fatigue on the performance of a bucket brigade order picking system. *IFAC-PapersOnLine*, *52*(13), 2195–2200.

Guo, X., Chen, R., Du, S., & Yu, Y. (2021). Storage assignment for newly arrived items in forward picking areas with limited open locations. *Transportation Research Part E: Logistics and Transportation Review*, *151*, 102359.

Hirotani, D., Morikawa, K., & Takahashi, K. (2006). Analysis and design of self-balancing production line. *Computers & Industrial Engineering*, *50*(4), 488–502.

Ho, Y.-C., Chen, J.-C., & Kao, S.-C. (2023). The design of a parallel zone-picking system with cooperation area between neighboring zones and its cooperation methods. *International Journal of Production Research*, 1–23. 10.1080/00207543.2023.2217946

Holstein, W. K., & Tanenbaum, M. (2024, March 15). Production system. *Encyclopedia Britannica*. Retrieved June 28, 2024, from https://www.britannica.com/money/production-system

Hong, S. (2018). The effects of picker-oriented operational factors on hand-off delay in a bucket brigade order picking system. *OR Spectrum*, *40*(3), 781–808.

Hong, S., Johnson, A. L., & Peters, B. A. (2012). Batch picking in narrow-aisle order picking systems with consideration for picker blocking. *European Journal of Operational Research*, *221*(3), 557–570.

Hong, S., Johnson, A. L., & Peters, B. A. (2015). Quantifying picker blocking in a bucket brigade order picking system. *International Journal of Production Economics*, *170*, 862–873.

Hong, S., Johnson, A. L., & Peters, B. A. (2016). Order batching in a bucket brigade order picking system considering picker blocking. *Flexible Services and Manufacturing Journal*, *28*(3), 425–441.

Hong, S., & Kim, Y. (2018). The effects of loosely coupled hand-off operations on bucket brigade order picking system. *Industrial Engineering & Management Systems*, *17*(4), 745–756.

Koo, P. H. (2009). The use of bucket brigades in zone order picking systems. OR spectrum, 31(4), 759–774.

Lim, Y. F. (2011). Cellular bucket brigades. *Operations Research*, *59*(6), 1539–1545.

Lim, Y. F. (2017). Performance of cellular bucket brigades with hand-off times. *Production and Operations Management*, *26*(10), 1915–1923.

Lim, Y. F., & Wu, Y. (2014). Cellular bucket brigades on U-lines with discrete work stations. *Production and Operations Management*, *23*(7), 1113–1128.

Lim, Y. F., & Yang, K. K. (2009). Maximizing throughput of bucket brigades on discrete work stations. *Production and Operations Management*, *18*(1), 48–59.

Matusiak, M., De Koster, R., Kroon, L., & Saarinen, J. (2014). A fast simulated annealing method for batching precedence-constrained customer orders in a warehouse. *European Journal of Operational Research*, *236*(3), 968–977.

Muter, İ., & Öncan, T. (2022). Order batching and picker scheduling in warehouse order picking. *LISE Transactions*, *54*(5), 435–447.

Pan, J. C. H., Shih, P. H., & Wu, M. H. (2015). Order batching in a pick-and-pass warehousing system with group genetic algorithm. *Omega*, *57*, 238–248.

Parikh, P. J. (2006). *Designing order picking systems for distribution centers* [Unpublished doctoral dissertation]. Virginia Tech.

Parikh, P. J., & Meller, R. D. (2008). Selecting between batch and zone order picking strategies in a distribution center. *Transportation Research Part E: Logistics and Transportation Review*, *44*(5), 696–719.

Pratama, A. T., Takahashi, K., Morikawa, K., Nagasawa, K., & Hirotani, D. (2018a). Cellular bucket brigades with worker collaboration on U-lines with discrete workstations. *Industrial Engineering & Management Systems*, *17*(3), 531–549.

Pratama, A. T., Takahashi, K., Morikawa, K., Nagasawa, K., & Hirotani, D. (2018b). Integration of bucket brigades and worker collaboration on a production line with discrete workstations. *Industrial Engineering & Management Systems*, *17*(3), 514–530.

Scholz, A., & Wäscher, G. (2017). Order batching and picker routing in manual order picking systems: The benefits of integrated routing. *Central European Journal of Operations Research*, *25*(2), 491–520.

Wang, P., Pan, K., Yan, Z., & Lim, Y. F. (2022). Managing stochastic bucket brigades on discrete work stations. *Production and Operations Management*, 31(1), 358-373.

Wu, Y., Zhou, C., Wu, Y., & Kong, X. T. R. (2016). Zone merge sequencing in an automated order picking system. *International Journal of Production Research*, *55*(21), 6500–6515.

Xie, L., Li, H., & Luttmann, L. (2023). Formulating and solving integrated order batching and routing in multi-depot AGV-assisted mixed-shelves warehouses. *European Journal of Operational Research*, *307*(2), 713–730.

Yang, D., Liu, S., & Zhang, Z. (2022). An asymmetric polling-based optimization model in a dynamic order picking system. *Symmetry*, *14*(11), 2283.

Yu, M., & De Koster, R. B. (2009). The impact of order batching and picking area zoning on order picking system performance. *European Journal of Operational Research*, *198*(2), 480–490.

Zivanic, D., Zelic, A., Lalic, B., Simeunovic, N., & Szabo, L. (2019). Improving the order picking efficiency by optimising the orders' sequence. *International Journal of Simulation Modelling*, *18*(1), 125–137.

List of Publications

1. Journal Papers
   a. Xin Zhou, Daisuke Hirotani, "Revised worker collaboration models for cellular bucket brigades with discrete workstations," *Journal of Japan Industrial Management Association*, Vol. 73, No. 2E, July 2022, pp. 104–123. DOI:10.11221/jima.73.104
   b. Xin Zhou, Keisuke Nagasawa, Katsumi Morikawa, Katsuhiko Takahashi, Daisuke Hirotani, "Balanced order batching in bucket brigade order picking systems with non-identical pickers," *Industrial Engineering & Management Systems*, Vol. 23, No. 1, March 2024, pp.34–55. DOI:10.7232/iems.2024.23.1.034

2. Conference Papers
   a. Xin Zhou, Keisuke Nagasawa, Katsumi Morikawa, Katsuhiko Takahashi, Daisuke Hirotani, "An enhanced bucket brigade order picking system with a conveyor," *Proceedings of Industrial Engineering and Management, Asian Conference of Management Science and Applications*, December 2023, Springer Nature Singapore, pp. 341–353. DOI:10.1007/978-981-97-0194-0_35

Research and Publication Relations

Chapter	Title	Main Reference
1	Introduction	1a, 1b 2a
2	Bucket Brigade for a Cellular Production System with Worker Collaboration	1a
3	Bucket Brigade for an Order Picking System with Order Batching	1b
4	An Enhanced Bucket Brigade Order Picking System with a Conveyor	2a
5	Conclusions	1a, 1b 2a